

# Electrospun Nanofibers: Materials, Synthesis Parameters, and Their Role in Sensing Applications

Saraswathi Kailasa, M. Sai Bhargava Reddy, Muni Raj Maurya, B. Geeta Rani, K. Venkateswara Rao,\* and Kishor Kumar Sadasivuni\*

Since the last decade, electrospinning is garnering more attention in the scientific research community, industries, applications like sensing (glucose, H<sub>2</sub>O<sub>2</sub>, dopamine, ascorbic acid, uric acid, neurotransmitter, etc.), biomedical applications (wound dressing, wound healing, skin, nerve, bone tissue engineering, and drug delivery systems), water treatment, energy harvesting, and storage applications. This review paper provides a brief overview of the electrospinning method, history of the electrospinning, factors affecting the electrospun nanofibers, and their morphology with different materials and composites (metals, metal oxides, 2D material, polymers and copolymers, carbon-based materials, etc.) used in the electrospinning technique with optical spinning parameters. Moreover, this paper deliberates the application of electrospun nanofibers and fibrous mats for sensing (electrochemical, optical, fluorescence, colorimetric, mechanical, photoelectric, mass sensitive change, resistive, ultrasensitive, etc.) in most illustrative representations. In the end, the challenges, opportunities of the electrospun nanofibers, and new direction for future progress are also discussed.

## 1. Introduction

Sensors are playing a significant role in modern human life. Sensors are the platform, which is used in many applications including, traffic lights washing mechanics, shopping mass, biosensing chemical sensing, environmental sensing application which leads to biomedical applications, and even in the food industry, which is one of the major pillars of our economy.<sup>[1,2]</sup> It is the conversion of a physical phenomenon into a measurable signal that is then converted into a human-readable display or reading. The main static and dynamic parameters of sensors are sensitivity, the limit of detection, stability, reproducibility, selectivity, repeatability, linear range, response, and recovery time, etc.<sup>[3,4]</sup> The power strategy to improve those parameters is to increase the specific surface of the interfering material. The surface parameters lead to the sensor's ability to interact fully with the target analyte. It has particular prominence for heterogeneous catalysis, adsorption, and reaction.


Moreover, the better ability of the material interaction with medium mainly depends on the large surface area of the material. In this scenario, materials at the nanoscale level play the most crucial role due to the unique feature of tailoring the material's size and surface functionalities.<sup>[5–8]</sup> Consequently, many routes have been approached to augment the surface of sensing with different controlled nanostructures. Recently, electrospinning has become one of the most attractive candidates among the different technologies at nanoscale to design and develop intelligent, easy, and low-cost sensing systems.<sup>[9]</sup>

Electrospinning is an electrostatic process that produces elongated fibers with micro and nanoscale diameters. This electrostatic process results in the movement of liquid or polymer solution.<sup>[10]</sup> This route covers the easy tuning of fiber's assembly in size and shape. The morphology of these spun fibers depends on the process conditions, solution parameters, and environmental conditions.<sup>[11]</sup> The development of electrospun nanofibers has allowed the chance to fabricate more efficient interfaces with different electronic components based on their computability. Moreover, the electrospinning method is a noninterrupted process of creating polymeric fibers.<sup>[12]</sup> The various application of electrospinning is shown in Scheme 1.<sup>[10]</sup>

S. Kailasa, M. S. B. Reddy, B. G. Rani, K. V. Rao  
 Center for Nanoscience and Technology  
 Institute of Science and Technology  
 Jawaharlal Nehru Technological University  
 Hyderabad 500085, India  
 E-mail: kalagadda2003@jntuh.ac.in

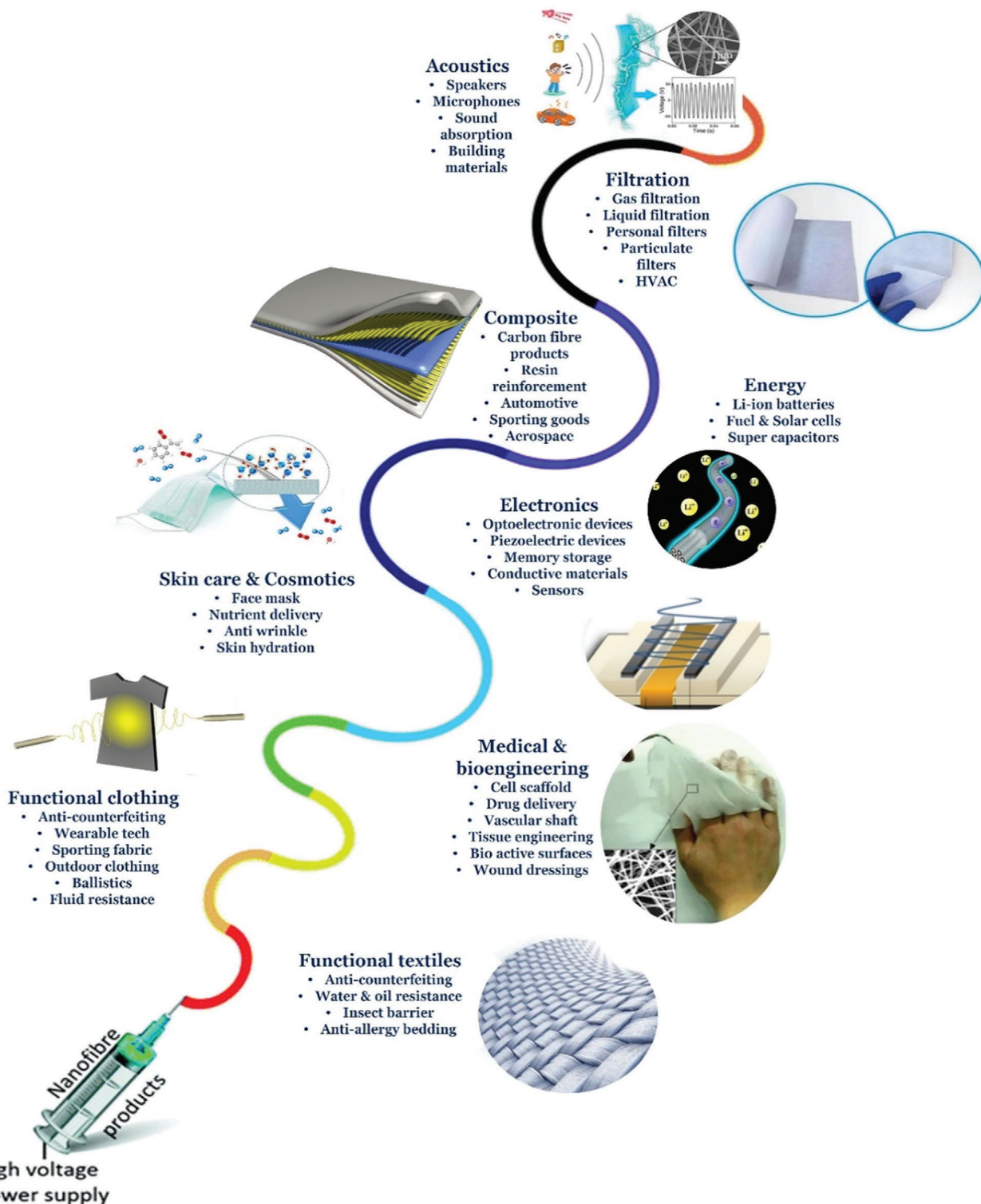
M. R. Maurya, K. K. Sadasivuni  
 Center for Advanced Materials  
 Qatar University  
 PO Box 2713, Doha, Qatar  
 E-mail: kishor\_kumars@qu.edu.qa

M. R. Maurya  
 Department of Mechanical and Industrial Engineering  
 Qatar University  
 PO Box 2713, Doha, Qatar

 The ORCID identification number(s) for the author(s) of this article can be found under <https://doi.org/10.1002/mame.202100410>

© 2021 The Authors. Macromolecular Materials and Engineering published by Wiley-VCH GmbH. This is an open access article under the terms of the Creative Commons Attribution License, which permits use, distribution and reproduction in any medium, provided the original work is properly cited.

DOI: 10.1002/mame.202100410



**Scheme 1.** Electrospun nanofibers in various Applications. Reproduced with permission.<sup>[10]</sup> Copyright 2016, Springer International Publishing Switzerland.

## 2. Historical Background

Since the beginning of civilization, fibers have been a part of human life, the production of fibers have been started in prehistoric times, and the example is the production of silk fibers and textiles using silkworms in 2700 BC. Silkworms are one of the natural sources that produce silk filaments for the construction of cocoons. Moreover, for more than 140 million years, spiders have depended on webs of fibers to capture prey.<sup>[13–15]</sup> Many routes have been opted to produce synthetic polymer-based fibers derived from a gel, dry, wet, and melt spinning. However, these methods are limited to solidification, hearing forces, and jets stretchable to a limited extent, with a high diameter range.<sup>[16,17]</sup> William Gilbert was the first person to observe the electrostatic movement of liquid in 1600. After a considerable gap, Charles Vernon and the team reported drawing fibers from the liquid under the external electric condition in 1887. The first patent was filed in electrospinning by John Francis in 1900. The year-wise progress of the electrospinning procedure is mentioned in **Scheme 2**.<sup>[18–69]</sup> The extensive research has continued till now, and the exponential growth of nanofibers has enhanced year by year with the addition of various new applications like biosensing, biomedical applications, water treatment, energy harvesting, conversion and storage applications, catalysis, etc.<sup>[70–74]</sup>

### 2.1. Principle of Electrospinning

Electrospinning is the formation of nanofibers when the liquid droplet is electrified based on uniaxial stretching and elongation to create the fibers from a polymer solution or melt.<sup>[75,76]</sup> Making of laboratory-based electrospinning setup is easy and more accessible; the typical electrospinning setup consists of components like a high voltage power supply, a hypodermic needle spinneret with blunt tip, a grounded conductive collector.<sup>[77]</sup> During the electrospinning procedure, in the presence of high voltage conditions, the polymer liquid droplet extruded at the needle tip deform into a cone shape known as a Taylor cone under the electrostatic process. These strong electrostatic forces take the initiation for the electrospinning process; under the high electrification, a strong electrostatic repulsion among the induction charges on surfaces produces the shear stress. These repulsive forces act in opposite directions to the surface tension, which leads to the extension of the polymer solution drop in the Taylor cone and plays a crucial part in initiating the surface.<sup>[78]</sup> At the critical voltage  $V_c$ , the repulsive force on the surface gets unbalanced or broken, and thus, a charged jet ejects from the blunt tip of the conical drop. The electrospinning expression based on the Taylor method is mentioned below<sup>[59]</sup>

$$V_c^2 = 4 \frac{H^2}{h^2} \left( \ln \left( \frac{2h}{R} \right) - 1.5 \right) (1.3\pi R\gamma) (0.09) \quad (1)$$

$V_c$  is critical voltage,  $h$  denotes liquid column length,  $H$  is the distance between the spinneret blunt tip and collector,  $\gamma$  is the surface tension of the spinning solution,  $R$  is the spinneret inner radius. Despite electrospinning being a low-cost and easy way of synthesis, there are still few obstacles that could influence the fiber's generation, quality, and nanostructure.<sup>[79,80]</sup> **Scheme 3** rep-

resents the basic spinning setup, operation condition, and electrospinning procedure parameter.

## 3. Experimental Parameters

### 3.1. Factors Affecting the Production and Morphology of Electrospun Nanofibers

Since the 20th-century, electrospinning is one of the most eye-catching routes in the scientific community, and it is considered a commercial and scientific venture with economic benefits (global).<sup>[81]</sup> Many methods have been explored to synthesize nanomaterials, including solvent casting, self-assembly, coprecipitation, template-assisted synthesis, drawing processing, and electrospinning route. Nanotechnology mainly focuses on the size and shape, i.e., mainly related to nanostructures, and in this regard, electrospinning has become the most frequently used method to prepare nanofibers.<sup>[82]</sup> Furthermore, the nanofibers produced through this method possess the advantages of large surface area to volume ratio, high porosity, a large number of fiber pores. According to the literature review, electrospinning nanofiber opened a new platform for many applications including, sensing, water treatment membrane, energy catalysis, and biomedical applications.<sup>[83]</sup>

The electrospinning technique route showed the ability to prepare the nanostructures from various materials ranging from polymers, copolymers, and synthetic polymers and their composites, as shown in **Scheme 4**. Moreover, electrospun nanofibers play a pivotal role in the sensing and biomedical field.<sup>[84]</sup> The biomedical engineering field mainly uses biodegradable and biocompatible synthetic or natural polymers. The electrospun scaffolds are among the essential candidates due to their nature under desire usages, such as growing artificial cells, proliferation, and differentiation.<sup>[85]</sup> Electrospun nanofibers also have massive demand in sensors for detecting various chemical compounds, such as microcompounds in the form of copper, nickel, ferric ions for environmental protection. These nanofibers also actively participate in the optical sensors (with the help of fluorescence and colorimetric sensing), and ultrafine electrospun nanofibers or scaffolds used to make nanotubes for industrial purposes.<sup>[67]</sup> Practically more than 100 natural and synthetic polymers have been in use for the synthesis of electrospun nanofibers. However, the electrospun nanofibers have benefits and an easy setup. However, their morphology is limited by specific parameters such as high voltage, the spinning distance between the needle tip and the collector, control of flow rate concerning time, solution parameters (solubility, polymer type, viscosity, choice of the solvent, conductivity, etc.) and the environmental parameters (temperature, humidity, and atmosphere). All these parameters mentioned above affect the production, breed free, and smoothness of the electrospun nanofibers.<sup>[86]</sup>

### 3.2. Effect of Applied Voltage

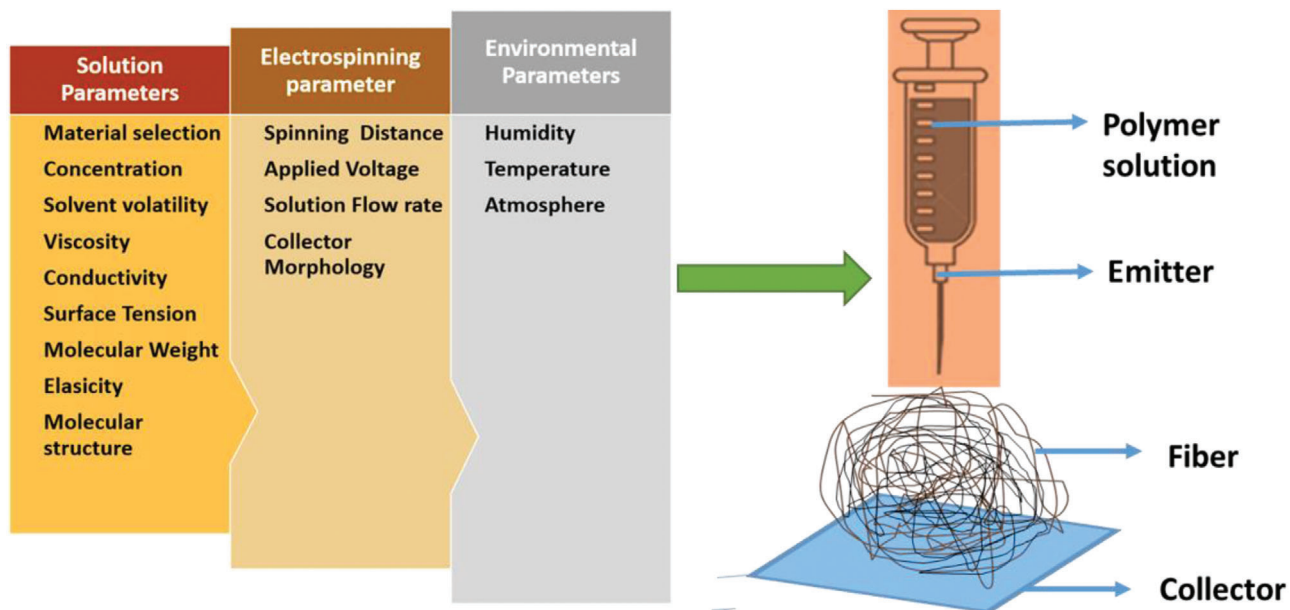
The applied voltage is one of the lead influences for the formation of electrospun nanofibers. The electrospinning happens only when electric potential energy is higher than the surface



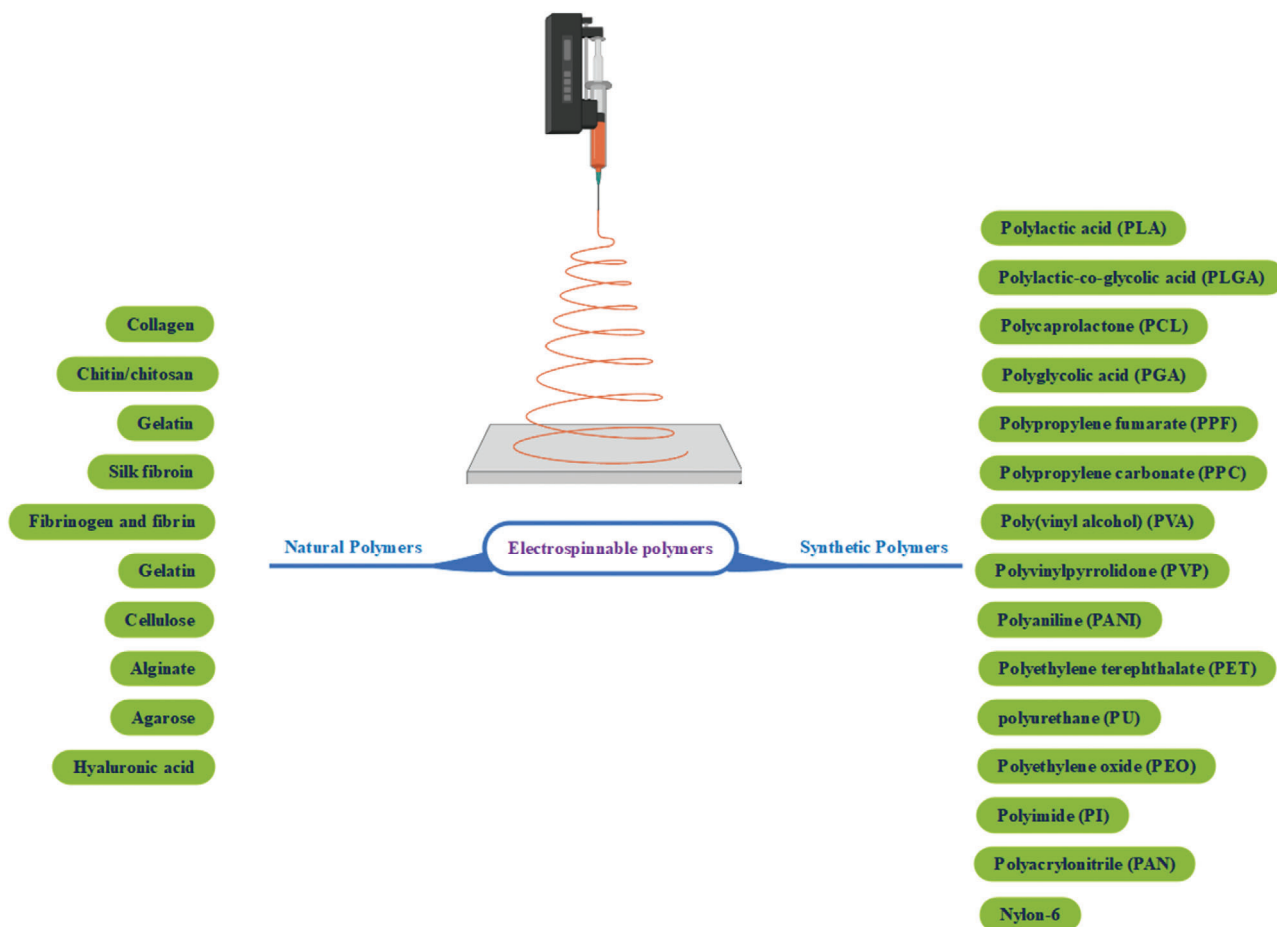
**Scheme 2.** History of electrospinning technique.

energy of the chosen polymer solution with ejection of equal mass. When an appropriate voltage approaches the surface energy quantity, the droplet shape is distorted to form a Tylor cone.<sup>[87]</sup> The critical value of applied voltage varies for different polymer solutions. At higher applied voltages, the thinner and smaller fiber will form due to the stretching of the polymer solution. However, the enhancement in the applied voltage beyond the surface energy will result in the bead or beaded nanofiber formation. Even increases in voltage are recognized to decrease

the size of the Tylor cone and expand the jet velocity with a similar flow rate. Deizel et al. reported the formation of the electrospun formation using polyethylene oxide (PEO) polymer solution. Deizel et al. started the electrospinning process with a slow 7 kV voltage noted few bead formations as the voltage increased from 7 to 9 kV, the increment in the bead formation.<sup>[88]</sup> Similarly, Mazoochi et al. reported the synthesis of PSF nanofibers by varying the voltages 10–25 kV with a distance gap of 15 cm and maintained flow rate at 1 mL h<sup>-1</sup>. He also mentioned that



Scheme 3. Electrospinning parameters.



Scheme 4. Natural and synthetic polymer for the electrospinning technique.

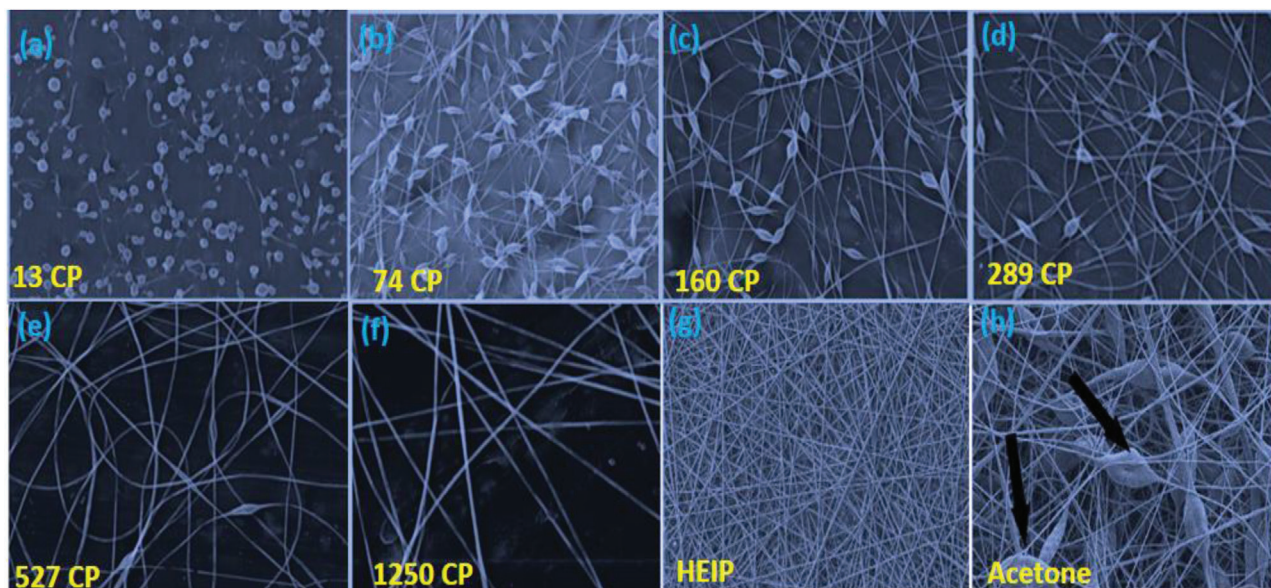


**Figure 1.** SEM images of a–f) PEO nanofibers with different viscosity showed that as the centipoise value (CP) increasing there was a reduction in the bead formation. Reproduced with permission.<sup>[98]</sup> Copyright 1999, Elsevier Science Ltd., g) PCL nanofibers with HEIP solvent with parameters of 20 cm distance and 25 kV, and h) PCL nanofibers with bead formation using acetone solvent with parameters of 20 cm distance and 25 kV. Reproduced with permission.<sup>[92]</sup> Copyright 2011, Woodhead Publishing Limited.

fiber diameter would increase at 20 kV high applied voltages at the starting, but as the voltage has increased to 25 kV, the fiber diameter starts to reduce.<sup>[89]</sup>

### 3.3. Distance between the Tip and Collector

The distance between the spinneret and the collector is a key factor responsible for the morphology of electrospun nanofiber. Once the applied voltage is fixed and kept constant, the electric field strength is inversely proportional to distance.<sup>[90]</sup> Matabola et al. reported the effect of distance variation for the synthesis of polyvinylidene fluoride (PVDF) electrospun nanofibers with 15–16 cm, voltage range 12–18 kV, and the flow rate of 0.050 mm min<sup>-1</sup>. He observed that 15 cm is the most commonly used distance according to literature, but the enhancement in the distance reduces the fiber diameter.<sup>[90]</sup> Furthermore, the electric fields should be enough to accelerate the polymer solution jet over the total distance. However, sometimes the increasing distance beyond a certain level can increase the diameter of the fibers but significantly weakens the field strength. For example, Bosworth et al. reported the synthesis of polycaprolactone (PCL) nanofibers by keeping the distance of 5–10 cm with a 10–25 kV voltage variation. The diameter of the nanofibers significantly decreased with the distance increment alone.<sup>[91]</sup>

### 3.4. Flow Rate

The flow rate of electrospinning polymer solution is typically from the needle and governed by the hydrostatic pressure using a syringe pump. Moreover, the morphology of electrospun nanofibers also depends on the flow of the polymer solution coming from the needle tip. Sometimes the high flow rates can lead to

the formation of beads. Megelski et al. reported how the flow rate influences the electrospun fiber formation, initially, he started with a flow rate of 0.10 mL min<sup>-1</sup> observed the ribbon shaped polystyrene (PS) fibers with a pore diameter of 50–250 nm. It noted that that increasing flow rate allows the formation of beads and increases the pore size and diameter of fiber because a fast flow rate sometimes will not allow the drying of the jet during the flight between the syringe tip and the collector.<sup>[92]</sup>

### 3.5. Collectors Morphology

The electrospinning nanofiber morphology depends on the type of collector fibers. A random orientated unwoven mat of fibers will be obtained from the simple collector plate, whereas aligned fibers are obtained through specially specified collectors.<sup>[93,92,94]</sup> Some specialized collectors will include spinning drums, disks, and mandrels; however, the rotation speed will impact the deposition rate. Therefore, the collector has moved in balanced ways; otherwise, if the collectors move faster than the fibers being deposited, the fiber will starch and break into small pieces and stick to the collector shown in **Figure 1g,h**.<sup>[95]</sup> There are few types of collectors available for the electrospun fibers and structures, including rotating collectors (parallel ring collector, double frame collector, coagulation bath collector), static collectors (parallel electrodes, electrodes array, inline electrode, metal tip electrode, grid, and magnetic field), precision deposited collectors (multiple charged rings based and single charged ring based).<sup>[96,97]</sup>

#### 3.5.1. Electric Current

Electric current is one of the considered factors in the electrospinning technique. The electric current depends on the charge

carrier's movement through the electrospinning distance. Moreover, most charge carriers are obtained by ionizing the air to the sharp needle and the polymer jet solution. The concentration of the charge carriers is noted with the help of the amount of salt present in the polymer solution. The electric current in the jet is also affected by some independent parameters including, solution feed, relative humidity, applied voltage, the conductivity of the solution, needle (hollow) diameter, and few geometrical properties. The current in a jet can be calculated by using the theoretical equation mentioned below

$$I_{\text{total}} \approx EQ^{0.5}K^{0.4} \quad (2)$$

Where,  $I$ —current flow through the jet,  $Q$ —flow rate,  $E$ —field strength, and  $K$  is the solution conductivity. This equation applies to nonaqueous solvents of various polymer solutions. Charles et al., in 1963, reported the invention of electric current and the formation of fibers from the viscous liquid using an air stream-assisted route.<sup>[54]</sup> In 1964, Tylor proposed the impact of the electric current in the shape cone of the solution droplet using the mathematical modeling.<sup>[58]</sup>

### 3.6. Solution Parameters

Solution parameters such as viscosity, conductivity, material selection, surface tension, elasticity, solvent volatility play a significant role in the electrospinning process.

#### 3.6.1. Viscosity

The viscosity of the solution depends on the polymer solution concentration, ambient temperature, molecular weight of the polymer, and impurities in the solution. So, the viscosity can be adjusted by employing the temperature or molecular weight. The relation between molecular weight and viscosity is given by the Mark–Houwink Sakurada equation<sup>[99]</sup>

$$[\eta] = KM^a \quad (3)$$

$M$  is molecular weight,  $\eta$  is viscosity,  $K$  and 'a'  $K$ , and Mark–Houwink parameters or empirically constants parameters. The Mark–Houwink parameter values of  $a$  and  $K$  be contingent on the polymer-solvent. For example, if  $a$  value is 0.5, it indicates theta solvent (where polymer coils act like ideal chains). If  $a$  is 0.8 represents suitable solvents, for flexible polymers stay in the range of 0.5–0.8, and for semiflexible polymers, a value is always greater than 0.8. Furthermore,  $K$  values can be obtained graphically using the line of best fit by measuring the viscosities and molecular weights of series of polymers.<sup>[100]</sup> Fong et al. reported that the reduction of viscosity of a polymer solution makes the formation of beads with longer fiber length along with other parameters such as flow rate also influencing the fiber diameter. Further mentioned that higher polymer concentration creates fewer beads, as shown in Figure 1a–f.<sup>[98]</sup> Lee et al. described that the fiber diameter is related to bead diameter and the distance, thinner the fiber the closure are the beads to each other. This confirms that to obtain consistent fibers, the viscosity of the solution has to be constant.<sup>[101]</sup>

#### 3.6.2. Solution Conductivity

Solution conductivity is significant because increasing the conductivity of the solution surges the stretching of the solution. As a consequence, the solution will carry higher charges. The net charge density is also related to the bead formation and fiber diameter and having a high flow of current favors the bead's thin quality fiber.<sup>[102]</sup> Hence the solution must hold ionic nature to be electric field flow between collector and needle through polymer solution. If the conductivity of the solution is not good enough, then fibers may not form.<sup>[103]</sup> Changing the polymer concentration or solvent concentration by adding the salts can improve the conductivity. Moreover, ion mobility can also affect the conductivity, and this ion conductivity again can be affected by the viscosity of the polymer solution.<sup>[92]</sup> Furthermore, the improvement in solution conductivity also increases the bending instability and increases the jet path, which leads to better quality beads with less thin diameters.<sup>[104]</sup>

#### 3.6.3. Surface Tension

As a stand-alone factor, it is one of the essential factors in the electrospinning route, and if the surface tension is too high, fibers will form and deforms into droplets (instead of in a process known as electro spraying).<sup>[14]</sup> Surface tension, in general, can be overcome by electric fields to produce the polymer solution jets. Fong et al. mentioned that high surface tension would favor the formation of beads, and beads have high surface to volume ratio than a fiber. Hence, with the formation of beads, the surface is left with lower surface energy.<sup>[105]</sup> Jarusuwannapoom et al. reported the different solvents (eighteen) and their role in the electrospun formation, some polymer solutions cannot be electrospun due to their low conductivity high surface tension values. Jarusuwannapoom also described the surface tension of various polymer solvents in tabular form.<sup>[106]</sup>

Moreover, the spinning parameter of the applied voltage, the distance between the tip and collector, and flow rate, surface tension, etc., varies from polymer to polymer. **Table 1** clearly shows the variation of these spinning parameters. The applied voltage varies from 5 to 30 kV based on different applications, mainly 15–20 kV has observed, and the increment in the voltage sometimes creates the bead formation or the reduction in fiber diameter. Similarly, the flow rate is used in the range of 0.005–0.10 mL min<sup>-1</sup>, but 0.3 mL h<sup>-1</sup> is used in many fabrications. Furthermore, the distance between the tip and collector also plays a role in the fiber synthesis, is table the distance varied from 10 to 30 cm, but 15 cm is considered as the optimized when the range increased from 15 to 25 cm to more bead formation observed.<sup>[91,97,107–122]</sup>

#### 3.6.4. Material Choice

Polymers are one of the most critical parameters chosen for the electrospinning technique, and the type of the polymer for the fiber depends upon the specific application. Polyvinylpyrrolidone (PVP), poly(vinyl alcohol) (PVA), polyacrylonitrile (PAN) (Scheme 4), etc., are the most commonly available polymers used

**Table 1.** Electrospinning parameters for the synthesis of various combinations of electrospun nanofibers.

S.No.	Electrospun material	Diameter [nm]	Voltage [kV]	Distance [cm]	Flow rate	Application	Reference
1	PEO/LiClO <sub>4</sub>	—	30	30	—	Humidity sensing	[107]
2	ZnO/PVP	35–150	7	5	0.3 mL h <sup>-1</sup>	Gas sensing	[108]
3	PVA/Au NPs	200	9	17	0.3 mL h <sup>-1</sup>	H <sub>2</sub> O <sub>2</sub> Sensing	[109]
4	PMMA/Ag NPs	318.5 ± 24.9	20	20	1.5 mL h <sup>-1</sup>	SERS application	[110]
5	PVDF/BaTiO <sub>3</sub>	110 ± 40	18	15	0.12 mL h <sup>-1</sup>	Energy harvesting	[111]
6	PVDF/LiCl	—	20	20	0.3 mL h <sup>-1</sup>	Nanogenerator	[112]
7	PVA/PEI/HA	459.7 ± 36.1	18.6	25	0.3 mL h <sup>-1</sup>	Cancer diagnosis	[113]
8	F-PBZ/SiO <sub>2</sub> NP/CA	330	16	15	0.5 mL h <sup>-1</sup>	Oil-polluted water treatment	[114]
9	PVDF	500	25	15	0.5 mL h <sup>-1</sup>	Bone reparation	[115]
10	PVDF/MWCNTs	200 nm–μm	—	—	0.001 mL min <sup>-1</sup>	Wearable sensors	[116]
11	PHBA	270–520	13	12	1 mL h <sup>-1</sup>	Cancer treatment	[117]
12	PVDF/PAPBA	150	25	15	—	Biosensors	[118]
13	H <sub>2</sub> PtCl <sub>6</sub> -HAuCl <sub>4</sub> -PVP	—	20	15	0.3 mL h <sup>-1</sup>	Glucose sensing	[119]
14	CA/Curcumin	104 ± 0.016 nm	20	15	0.3–0.5 mL h <sup>-1</sup>	Lead ion detection	[120]
15	AuNPs@4-MBA	1.99 ± 0.12 μm	12	15	0.5 mL h <sup>-1</sup>	SERS-metal detection	[121]
16	Lignin/PAN	105 nm	24	—	0.3 mL h <sup>-1</sup>	Pb(II),Cu(II) detection	[122]
17	PCL	0.64 Lm–25 nm	15–25	5–10	0.05 and 0.1 mL min <sup>-1</sup>	Synthesis	[91]
18	PS	50–350 nm	10–20	12–35	0.10–0.007 mL min <sup>-1</sup>	Synthesis morphology studies	[97]
19	PEO	10–1000 nm	7–8	15–25	0.0025–0.024 mL min <sup>-1</sup>	Synthesis morphology studies	[97]
20	PC	10–1000 nm	10	35	0.007–0.009 mL min <sup>-1</sup>	Synthesis morphology studies	[97]
21	PMMA	10–1000 nm	10	35	0.007–0.009 mL min <sup>-1</sup>	Synthesis morphology studies	[97]

in tissue engineering, biodegradable scaffolds, and membranes filters, respectively. The molecular weight of the polymer variation makes the property variation of fiber significant. High molecular weight will enhance the solution viscosity.<sup>[106]</sup>

### 3.6.5. Other Parameters

Polymer solutions are prepared from the solvents, so the solvent volatility should be within the desirable range. Even the solution obtained from the solvents with low volatility may result from infused fiber, wet fibers, or even no fibers collection. However, sometimes high solvent volatility provides irregular spinning due to solidification.<sup>[123]</sup> The solvent choice also significantly impacts the fiber production displayed in Figure 1g,h. Different polymer solution has different viscosities which can influence the morphology of the electrospinning fibers.<sup>[79]</sup> The dielectric constant is also one of the parameters that affect the diameter of the fiber and the deposition speed.<sup>[101]</sup>

### 3.7. Environmental Parameters

Other than the solution parameters, temperature and humidity also affect the morphology of the electrospun diameter. Both higher and lower humidity conditions make the fiber diameter larger. The solidification process slows for the aqueous solution for the higher humidity condition, which results in bead defects and thicker fibers. For the lower humidity, faster solvent vaporization increases solidification, leading to increased fiber

diameter.<sup>[124]</sup> The other crucial factor is temperature; the high temperature will make the thinner diameter fibers, temperature rise provides the faster vaporization rate, and the polymer solution's temperature increase and viscosity will be reduced.<sup>[125]</sup>

## 4. Material-Based Electrospinning Nanofibers

### 4.1. Metal-Based Electrospun Nanofibers

In any field of research, nanomaterials play a vital role in the form of many nano-objects, including metals, metal oxides, polymers, metal organic frameworks (MOFs), carbon-based materials, conjugated polymers based on their utilization and their unique properties, such as size, shape, porosity, and surface area. The development of nanomaterial-based electrospun nanofibers has had a high value over the last decade because of the immobilization of these nanomaterials onto nanofibers which opt for new material assets and leads to many applications, including sensors energy electronics.<sup>[126]</sup> As a result, researchers concentrated on the synthesis and development of nanofibers in a well-controlled manner. Indeed, in the 21st century, extensive research and development focused on synthesizing tuneable hybrid nanomaterials, with this approach delivers unique and superior assets rather than using single components of the hybrids. So, this makes it easy to combine the thermally stable, highly conductive inorganic components (metals, metal oxides, glass, carbon, etc.) into flexible and tuneable organic components (biopolymers, copolymers, and polymers).<sup>[127]</sup> The primary strategy for the development of the electrospun nanofibers is to produce the hierarchically ordered self-assembled nanofibers, where



nanofibers are obtained by the direct electrostatic spinning of different polymers solutions with well-dispersed nanomaterials (metal, metal oxide, carbon, ceramics, MOFs, and conjugated polymers for specific application.<sup>[128]</sup>

During the last decade, the synthesis of metal nanostructures, including Ag, Au, Ti, Ni, Co, etc., has been technologically advanced with various sizes and shapes based on their utilization. Moreover, gold and silver nanostructures become a versatile platform for sensing biomedical research, catalysis, and plasmon application. The advanced assets of flexibility and controlled morphology with uniformly distributed electrospun polymer nanofibers have been incorporated with metal nanoparticles.<sup>[129]</sup> Jin et al. reported the PVP/Ag nanoparticles and PVA/PVP/Ag nanoparticles synthesis through the electrospinning method for antimicrobial activity. Primarily the AgNO<sub>3</sub> nanoparticles combine with PVP solution used *N,N*-dimethylformamide (DMF) as the reducing solvent for the Ag<sup>+</sup> ions. Jin used 47% PVP solution with 0.5 wt% of AgNO<sub>3</sub> for 7 days after preparation, and the obtained average diameter of the Ag nanoparticles was 3.4–3.5 nm. However, PVP nanofibers did not accumulate densely, which lead to PVP nanofibers not being strong enough for antimicrobial filters. Hence dissolved Ag contained PVP into PVA solution, PVA is miscible with polyvinylpyrrolidone. So, Ag distributed on PVA nanofibers showed vigorous antimicrobial activity. The average size of the Ag decorated PVA was 6.0 nm.<sup>[130]</sup> Similarly, Yang et al. reported the synthesized Ag NFs contained PAN nanofibers using 0.32 g of AgNO<sub>3</sub> mixed with a 0.5 g PAN solution, and 50 g of DMF was added and stirred for 24 h. The diameter of Ag solution/PAN was 440 nm.

The conductivity of Ag/PAN nanofibers was 10<sup>-7</sup> S cm<sup>-1</sup>.<sup>[131]</sup> Son et al. reported a combination of silver nanoparticles and cellulose acetate (CA) to apply strong antimicrobial activity. 17 kV with 10 cm working distance was opted to synthesize silver nitrate-containing CA electrospun nanofibers. The average diameter of CA/AgNO<sub>3</sub> was in the range of 600–1910 nm concerning various weight ratios. The AgNO<sub>3</sub> in AgNO<sub>3</sub>/CA electrospun is slowly photo reduced into silver nanoparticles. The average diameter of the silver was 3–16 nm, and the cellulose acetate nanofibers showed a better antimicrobial activity.<sup>[132]</sup> Lee et al. described the easy, simple one-step route of synthesizing ultra-fine PAN nanofibers incorporated Ag nanofibers. DMF solvent has been used as a reducing agent for Ag<sup>+</sup> ions reduction. The average diameter of Ag was 5.8 nm, and a voltage of 15 kV was used to produce the PAN/Ag nanoparticles electrospun.<sup>[133]</sup> Kim et al. reported the preparation of 1D arrays of Au nanoparticles and incorporated the poly(ethylene oxide) nanofibers for biosensing, photonics, and electronic applications. 2% of PEO in chloroform and 1% capped Au mixture was stirred 24 h, and 20 kV has been applied to get electrospun of Au NC/PEO. The diameter of the as-obtained nanofibers was in the range of 500–550 nm. This report showed how the simple one-step hybrid electrospinning has excellent potential for various applications, particularly nanoelectronic devices.<sup>[134]</sup> Wei et al. reported the advanced way of producing the conductive nanostructures metallization hybrid nanofibers for the electromagnetic interference shielding effectiveness (EMI SE). The PVA solution with different metals ratios we stirred and 8–12 kV voltage has been maintained. At room temperature, all the prepared solutions were electrospun and sent to the metric collector. The as-obtained different compo-

sition ratio of Cu/Ni annealed at different temperatures, and the metallization electrospun have a diameter in the range of 200–250 nm with the tensile strength of 50 nm.<sup>[135]</sup>

## 4.2. Metal Oxide-Based Electrospun Nanofibers

Nanostructure materials absorbed significant prominence and become promising candidates for many fields due to their unique assets of conductivity, stability, tunable bandgap, catalytic nature, electron transfer kinetics.<sup>[136–138]</sup> However, they have issues of poor selectivity and sometimes low conductivity. Many strategies have been approached to increase selectivity and enhance the device's performance to overcome these issues. Increasing the surface area is one of the superior advantages to obtain better sense catalysis performance electrospun nanofiber, and it is one of the attractive routes for the fabrication of metal oxides-based nanofibers.<sup>[139]</sup> However, direct spinning is impossible with metal oxides, but it is possible at high temperatures to melt. Hence, metal oxides need to bank on the precursor solution. The following steps need to be considered to obtain the metal oxide-based electrospun. a) The compatibility and solubility of metal oxide with the polymer-solvent need to be examined to achieve the required viscosity. b) The electrospinning process of metal oxide nanofibers carried out at room temperature at the precise environment. c) To obtain the crystalline nature of nanofibers, calcination, or sintering method will be approached. The diameter of the as-obtained nanofibers will reduce after the calcination due to the loss of polymer-solvent.<sup>[140]</sup> Hui and his co-workers reported the ultrathin ZnO nanofibers using electrospinning, zinc acetate, and PVA have been used for the electrospinning solution. Electrospinning parameters used were 20 cm distance between the film and the needle tip and a high voltage of 20 kV with a heating rate of 10 °C min<sup>-1</sup> as obtained fine ZnO nanofibers showed a variation in diameter of 300–700 nm for zinc acetate concentration.<sup>[141]</sup> Liang et al. reported the synthesis of In<sub>2</sub>O<sub>3</sub> nanofiber loaded with CuO nanoparticles for H<sub>2</sub>S gas detection. Primarily, the indium oxide precursor was mixed with PVP in the DMF solution. Second, to prepare the CuO-loaded In<sub>2</sub>O<sub>3</sub>, the precursor solution was fixed as In: Cu in the ratio of 5:1. Once the nanofibers were obtained, they were calcinated at 600 °C. As obtained, CuO–In<sub>2</sub>O<sub>3</sub> NFs were used for H<sub>2</sub>S detection. The limit of detection of H<sub>2</sub>S was < 400 ppb at the temperature range of 25–250 °C.<sup>[142]</sup> Namdev More et al. prepared the porous cerium oxide (CO)/PVA electrospun films for the biomedical application of wound healing, platelet ability, and biocompatibility. The PVA and cerium oxide were mixed, and electrospinning parameters were maintained as 20 cm distance between needle and collector and a high voltage of 28.5 kV. The crosslinking of obtained nanofibers was done at 160 °C for 10 min to get heat-treated PVA (HPVA) and PVA. Moreover, the heat-treated HPAV–CO showed high porosity, platelet adhesion, and hemocompatibility. Also, 3 wt% of CO–HPVA showed good biocompatibility through 3-(4, 5-dimethylthiazolyl-2)-2, 5-diphenyltetrazolium bromide (MTT) assay and wound healing.<sup>[143]</sup> Alharbi et al. reported the synthesis of bilayer nanofiber absorbents using PAN/TiO<sub>2</sub>/chitosan and PAN/ZnO/Chitosan nanofibers membranes for the detection of palladium (II) and cadmium (II) ions. The first layer of electrospun nanofibers was prepared as PAN with 2 wt% of

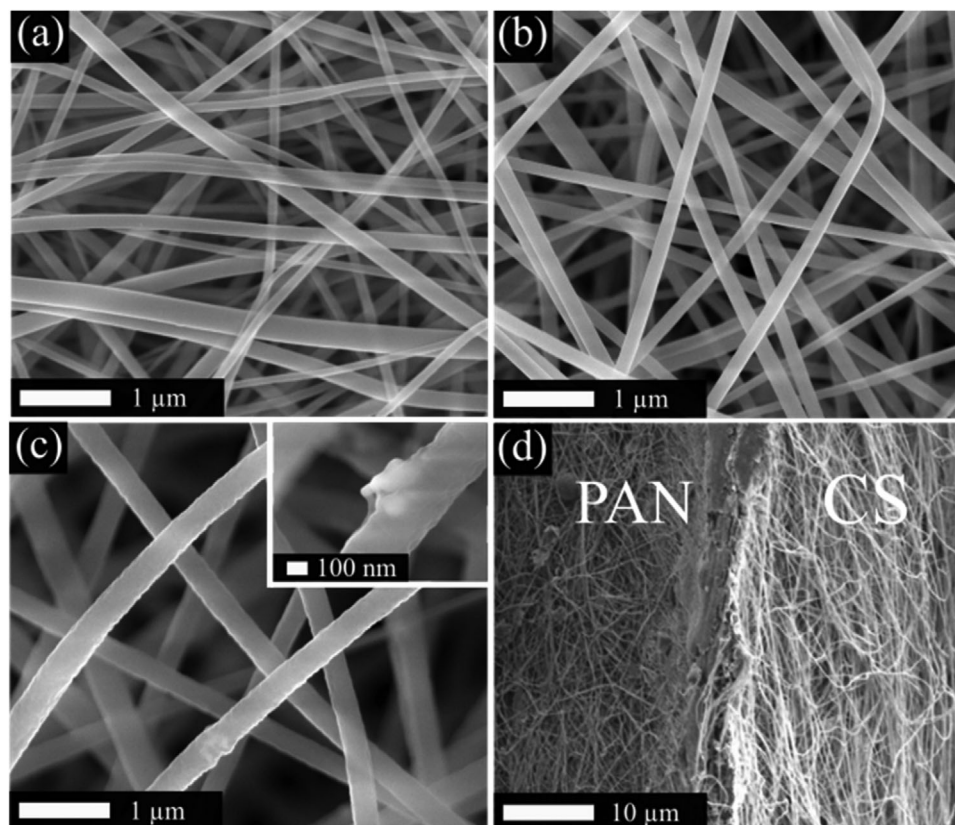


**Figure 2.** SEM images of a) PAN NFs, b) PAN/ZNO-CS NFs, c) PAN/ZnO NFs, d) PAN, and CS bilayer cross section. Reproduced with permission under the CC-BY 4.0 license.<sup>[144]</sup> Copyright 2020, the Authors. Published by MDPI.

ZnO and PAN with 5 wt% of TiO<sub>2</sub> precursors. The other layer was obtained using chitosan and PVA solution (CS/PVA) in **Figure 2a–d** by using a 10 cm distance between needle and collector and a high voltage of 25 kV with a flow of 0.2 mL h<sup>-1</sup>. As prepared, PAN/MO/CS showed an absorption capacity of 102% toward lead (II) and cadmium 405% compared to single layers.<sup>[144]</sup> Tripathy et al. reported synthesizing manganese oxide nanofibers using the manganese precursors with PAN polymer in DMF solution by maintaining a 12 cm distance between needle and collector with a voltage of 1.8 kV cm<sup>-1</sup> as obtained nanofibers were calcinated at 500 °C. The diameter of calcinated Mn<sub>2</sub>O<sub>3</sub> nanofibers was 20–150 nm and used as a working electrode to detect DNA hybridization through the electrochemical route.<sup>[145]</sup>

### 4.3. Carbon-Based Electrospun Nanofibers

The world's first 2D carbon-based lightweight material is referred to as graphene.<sup>[146]</sup> Due to its outstanding properties like high conductivity, high mechanical strength, specific capacitance, hydrophobicity, photocatalytic activity & stability, this is far superior to other materials. Graphene is one thick atom sheet of carbon in a hexagonal structure that looks like a honeycomb lattice. Therefore, graphene has become a promising and potential candidate to act as a nanofiller for the process of electrospinning.

Graphene is a robust nanofiller candidate for the lightweight nanocomposites both for natural polymers and synthetic polymers for electrospinning and has exhibited excellent properties, such as thermal stability, stability, hydrophobicity, conductivity, and mechanical strength.<sup>[147]</sup> Nowadays, considerable advances in the electroconductive graphene-based nanofiller have been made for many applications in science and technology but not limited to energy conversion and storage, biomedical applications, etc.<sup>[148,149]</sup> However, the loading of graphene solution in the electrospinning setup is a very tough task. In general, two methods have been used; one is solution bending/melt mixing or in situ polymerization technique.

Moreover, the second one is the formation of rGO nanofibers in the presence of high temperature or chemical reduction methods.<sup>[150]</sup> Wang et al. reported mixing the Hummers method synthesized graphene oxide with polar polymers, such as PVP and PAN. The PAN solution was added to the oven-dried (1 g) of graphene oxide in the DMF solution and stirred for 8 h to get the homogenous suspension for the spinning process at a voltage of 20 kV. Similarly, PVP with GO was mixed with the help of ethylene glycol as the solvent. Hydrazine hydrate (N<sub>2</sub>H<sub>4</sub>) has been used to reduce the GO–PAN into rGO–PAN and so as rGO–PVP. The conductivity of as-synthesized graphene/PAN, graphene/PVP was measured with the help of TS-8, Probe Tech, and the corresponding values were 7.5 × 10<sup>3</sup> and 2.5 × 10<sup>3</sup> S m<sup>-1</sup>.<sup>[151]</sup> Bera et al. reported the development of nanofibers with

and without graphene composition through the electrospinning technique for the nanogenerator (music and finger tapping) application. PVDF has been used as the polymer, primarily 12 wt% of PVDF in DMF solution was stirred for 30 min to produce  $\beta$ -phase PVDF nanofibers. The following mixture of 0.0025 grams of graphene with PVDF using parameters such as 12 cm distance between syringes to the collector and a voltage of 12 kV was applied with 58% humidity at 30 °C conditions. The field emission scanning electron microscopy (FESEM) showed the diameter difference between PVDF and PVDF/graphene. Finally, obtained PVDF, PVDF/graphene nanofibers were used for the nanogenerator application with the help of silver as electrodes.<sup>[152]</sup> Moyer first chose conductive polyaniline (PANI); however, PANI has limitations of low molecular weight, which can affect the elasticity of spinning and poor stability, and overcome these obstacles, camphor-10-sulfonic acid (HCSA) has been used. The as-obtained solution is doped with PEO polymer. To overcome these limitations, graphene with noncovalent functionalization of PBASE (1-pyrenbutonic acid, succinimidyl ester) via  $\pi$ - $\pi$  stacking, the combinations of PANI (10 mg) & HCSA (13 mg) was dissolved in 14.7 g of chloroform solution and doped with PEO. Finally, the obtained solution is mixed with PBASE. The electrospinning conditions of flow rate 5  $\mu\text{L min}^{-1}$  with 10 kV voltage, a distance of 10 cm between needle tip and collector have been applied for the preparation of PANI/PEO/G-PBASE and PANI/PEO nanofibers. The conductivity of PANI/PEO/G-PBASE was 2.41 times higher than PANI/PEO.<sup>[153]</sup> Enrica et al. reported combining polyactic acid (PLA)-PCL nanofibers in the ratio of 70:30 synthesized through the electrospinning route. Further reported the effect of graphene platelets (GNPs) with different weight ratios of PLA-PCL polymers to produce the PLA-PCL/GNPs nanofibers. The diameter of the PLA-PCL/GNPs nanofibers was in the range of 700–1450 nm. The effect of GNPs on PLA-PCL nanofibers showed an enhancement in the physicochemical properties of electrospun mats.<sup>[154]</sup> Since the last decade, the demand for energy storage and conversion has received more attention, especially in the form of supercapacitors. The specific capacitance mainly depends on the conductivity and high surface area of a material. Hence researchers concentrated on the conductive carbon-based electrospun nanofibers. Thangappan et al. reported the synthesis of graphene oxide by modified hummers method, and  $\text{V}_2\text{O}_5$  was used as a composite material with GO and made  $\text{GO}/\text{V}_2\text{O}_5$  nanofibers through electrospinning method. The diameter of the as-obtained was showed as 90–150 nm and used as electrode material for the supercapacitor application.<sup>[155]</sup>

#### 4.4. 2D Material-Based Electrospinning Nanofibers

Nanostructure materials took the most significant role in many applications. Consequently, material that belongs to a dimensional family similar to graphene structure falls into the analogs of transition metal dichalcogenides (TMDCS), MXenes, and black phosphorus, etc.  $\text{MoS}_2$ -Molybdenum disulfide,  $\text{MoSe}_2$ -Molybdenum diselenide,  $\text{WS}_2$ -Tungsten disulfide,  $\text{WSe}_2$ -Tungsten diselenide, hexagonal Boron Nitrate (hBN) belongs to the TMDCS family.<sup>[156–158]</sup> Moreover, 2D materials can fall into the semiconducting, metallic, semimetallic, and superconducting

materials categories depending on the structural functionalization and chemical compositions.<sup>[159]</sup> 2D materials have the advantage assets of the layer structure, layer tuneable bandgap, mechanical strength, strong quantum Hall Effect high surface to volume ratio.<sup>[160]</sup> Recently MXenes, a 2D transition-metal carbide with outstanding properties of excellent conductivity and high surface area, was developed by Levitt et al. through a simple electrospinning route. For this the group used a simple electrospinning technique to embed the MXenes into carbon nanofibers using PAN polymer in DMF solution. First, MXenes/PAN nanofibers were prepared with different weight ratios and then carbonized to get MXene/carbon nanofibers. The diameter of PAN/MXenes fibers varies from  $179 \pm 33$  to  $958 \pm 190$  nm ranges. After the carbonization, the fiber diameter reduced from  $179 \pm 33$  to  $116 \pm 20$  nm. As obtained, MXenes/carbon electrodes were used for the supercapacitor application with the capacitance value is  $205 \text{ mF cm}^{-2}$  at  $50 \text{ mV s}^{-1}$ .<sup>[161]</sup> Patrik et al. reported synthesizing 2D MXenes/PVA/CNC fiber for enhanced electrical and mechanical properties. Further they utilized PVA polymer solution to prepare the nanofiber with the precursor of MXenes ( $\text{Ti}_3\text{C}_2\text{T}_x$ ). To enhance the mechanical behavior, PVA/MXene nanofiber cellulose nanocrystals (CNC) have been added as shown in **Figure 3**: (I (a–f)). The whole solution was sonicated for 20 min using an ice bath and spinning parameters of 10 cm between screen and needle, and voltage of 17 kV with a flow rate of  $0.3 \text{ mL h}^{-1}$  was applied as obtained nanofibers showed 174–194 nm diameter.<sup>[162]</sup> Jiangtao et al. reported the electrostatic spun  $\text{TiO}_2/\text{WO}_3$  nanofiber decorated  $\text{MoS}_2$  nanosheets for the  $\text{H}_2$  evolution through photocatalytic activity. Precursors of  $\text{TiO}_2/\text{WO}_3$ /PVP/tetrabutyl titanate (TBOT) solution were used to obtain the  $\text{TiO}_2/\text{WO}_3$  nanofibers with a condition of 15 cm distance from the needle tip and the collector with a voltage of 13 kV with a heating rate of  $3 \text{ }^\circ\text{C min}^{-1}$ . As obtained, nanofiber was calcinated at 520 °C for 30 min and found that the diameter of  $\text{TiO}_2/\text{WO}_3$  nanofibers was about 300 nm. Using the hydrothermal technique, the  $\text{TiO}_2/\text{WO}_3$  nanofibers were combined with  $\text{MoS}_2$  to form heterostructure for the enhanced photocatalytic activity for the hydrogen evolution.<sup>[163]</sup> Mei et al. described the fabrication of  $\text{MoS}_2$ /carbon nanofibers to detect Vanillin at a low level of  $0.15 \times 10^{-6} \text{ M}$ . Primarily using auxiliary chemical stripping through the ultrasonication route has been used to obtain the  $\text{MoS}_2$  nanopowder from the bulk. As obtained,  $\text{MoS}_2$  powder was mixed in the combination of PAN and DMF solution with the electrospinning measurements of 15 cm distance between nozzle and tip, with a high voltage of 15 kV. The finally obtained nanofibers were dried at 60 °C and carbonized at 800 °C for 8 h in  $\text{N}_2$ . The obtained 200 nm diameter  $\text{MoS}_2$ -CNF nanofibers showed good selectivity and reproducibility in the linear range of  $0.3\text{--}135 \times 10^{-6} \text{ M}$  toward vanillin sensing.<sup>[164]</sup> Huang et al. reported the synthesis of 2D transition metal carbide MXene composites nanofibers and their utilization in tissue engineering. MXenes were obtained by etching the MAX phase ( $\text{Ti}_3\text{AlC}_2$ ) using LiF and HCl etchants. The obtained MXenes were dispersed into dichloromethane (DCM) and DMF solution and stirred for 2 h using an ice bath; the polymers of Poly(L-lactic acid) (PLLA) and polyhydroxyalkanoates (PHA) were mixed with the above solution to get electrospinning precursor solution. As electrospun, MXenes have functional groups which were beneficial for tissue engineering.<sup>[165]</sup>

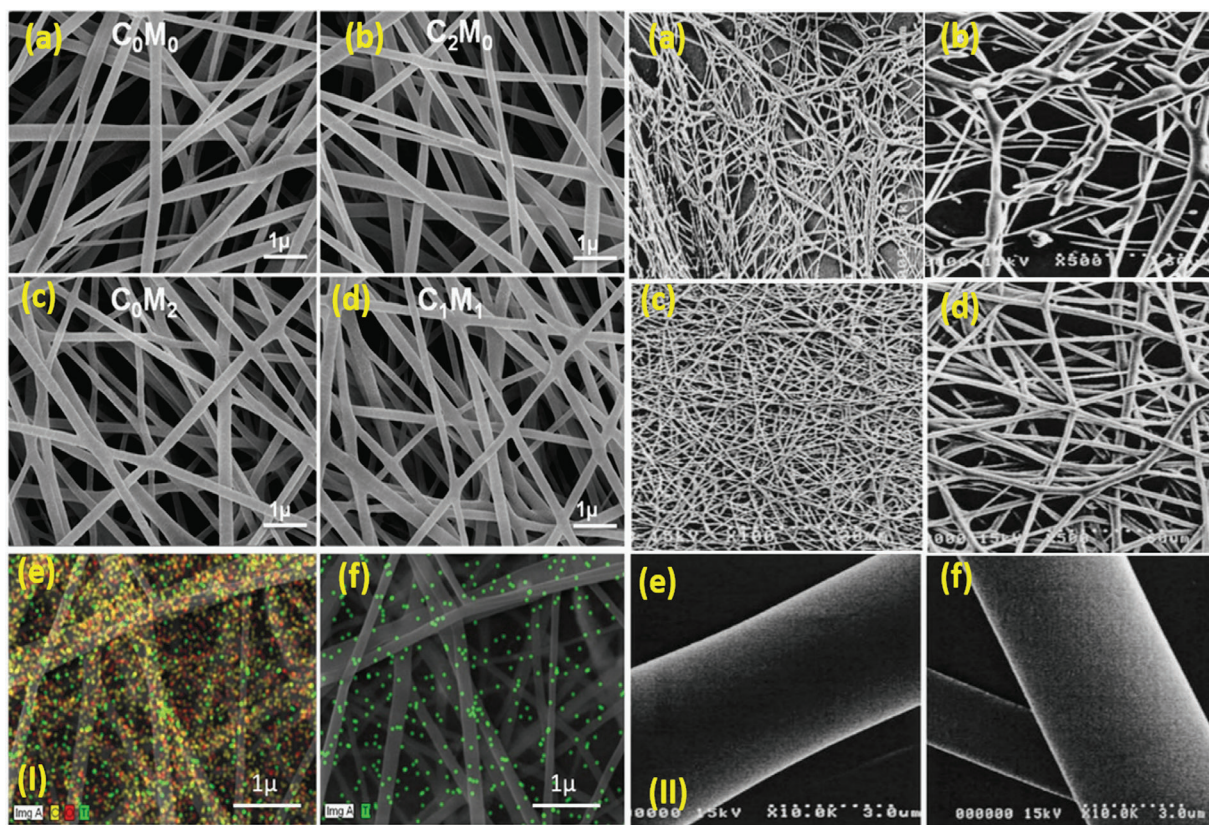


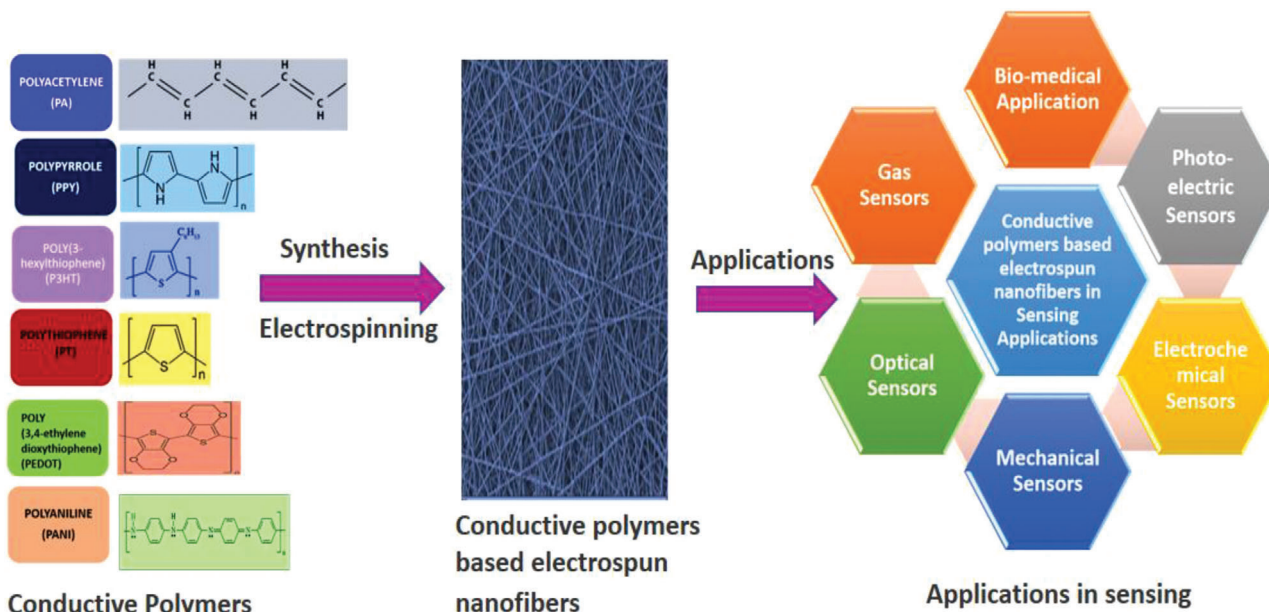
**Figure 3.** (I) a–d) SEM images of PVP with different ratios of  $\text{Ti}_3\text{C}_2\text{T}_x/\text{CNC}$  nanofiber  $\text{CoM}_2$  (CNC wt% 0,  $\text{Ti}_3\text{C}_2\text{T}_x$  wt% 0),  $\text{CoM}_2$  (CNC, wt% 0,  $\text{Ti}_3\text{C}_2\text{T}_x$  wt% 0.014),  $\text{C}_1\text{M}_1$  (CNC, wt% 0.07,  $\text{Ti}_3\text{C}_2\text{T}_x$  wt% 0.07),  $\text{C}_2\text{M}_1$  (CNC, wt% 0.014,  $\text{Ti}_3\text{C}_2\text{T}_x$  wt% 0). e–f) EDS mapping of  $\text{CoM}_2$  O-oxygen, C-yellow, and Ti-green. Reproduced with permission under the CC-BY 4.0 license.<sup>[162]</sup> Copyright 2017, the Authors. Published by PLoS One. (II) SEM images of (PPy nanofibers, a) 0.3 mm b) 60  $\mu\text{m}$  e) 3  $\mu\text{m}$  c) PPy/PVCN nanofibers c) 0.3 mm d) 60  $\mu\text{m}$  f) 3  $\mu\text{m}$ . Reproduced with permission.<sup>[166]</sup> Copyright 2005, Elsevier B.V.

#### 4.5. Conductive Polymer and Biopolymer Based Electrospun Nanofibers

Since the last decade, the emergence of eco-friendly and biofriendly biopolymers research has been accelerated to avoid petroleum-resultant Plastics. Biopolymers are derived from natural plant-based materials, crops, forests, residues, and horticulture.<sup>[167]</sup> Some bio-derived polymers are PLA, polyethylene terephthalate (PET), PE, and polyester, from animal sources-chitosan, from plants-PLA and microorganism-polyhydroxyalkanoates used for tissue engineering applications, drug delivery system, antifungal, antibacterial, and antiviral, wound healing due to their biocompatibility and biodegradability. For unique morphology, 1D electrospun nanofibers through electrospinning have a unique morphology, a high surface area, and good porosity.<sup>[144,165]</sup> Furthermore, the advantage of conductive polymer-based ultrathin electrospun nanofibers provided new opportunities for many applications.<sup>[168]</sup> The conductive polymers-based nanofibers are soft and provide a large surface area, good computability, and tunable electrical properties that can help to enhance sensing properties, including sensitivity, stability, and the limit of detection (LOD), etc.<sup>[169,170]</sup>

Furthermore, the combination of conductive polymers (Scheme 5) with other materials (metals, metals oxides, carbon-

based materials, etc.) form nanocomposite, which provides the new platform for biomedical applications, such as organ implants, tissue engineering, drug delivery system, membranes for water treatment, and even for energy applications.<sup>[171–173]</sup> The conductive polymers include polyacetylene (PA), polypyrrole (PPY), polyaniline (PANI), polythiophene (PT), and its derivatives P3HT-poly(3-hexylthiophene) and PEDOT-poly(3,4-ethylene dioxythiophene). Polymers can be prepared in many methods, and each method has its advantages and disadvantages. Electrospinning is one of the highly versatile and easy one-step techniques to the nanoparticles in the range of nanometer to micrometer range.<sup>[174]</sup> For the conductive polymers, electrospinning has three different routes, direct electrospinning,<sup>[166]</sup> coelectrospinning,<sup>[175]</sup> and electrospun-fiber template method,<sup>[176]</sup> and the synthesis of PPy/PVCN is displayed in Figure 3: II a–f). Qu et al. reported the PAN/PANI nanofibers for the ultrasensitive detection of trimethylamine (TMA). The weight ratio of 1:0.42 PAN and PANI showed high sensitivity with low detection of a limit of 6 ppb toward TMA sensing, the repeatability of PAN/PANI showed an RSD value of 4.7% for the 10 repetitions.<sup>[177]</sup> Nie et al. reported the synthesis of electrospun silica mats with PVA polymer for ammonia gas sensing. PVA with TEOS and Oxalic acid was used to make precursor solution for electrospinning, and then a 10:20 ratio of



**Scheme 5.** Various types of conductive polymers, formation of conductive polymers based electrospun nanofibers, and finally their utilization in sensor application.

PVA solution and silica gel was used to make PVA/silica fibers at a voltage of 20 kV by maintaining a distance of 18 cm between the collector and the needle tip. As obtained, PVA/silica fibers were calcinated at 600–1000 °C to obtain the different ratios of PVA/silica (SNF) mats. These SNFs showed a low detection limit of 400 ppb toward Ammonia at room temperature.<sup>[178]</sup> Bagchi et al. described the Ammonia detection using SnO<sub>2</sub>/PEO with the additive of conductive polymer PPY. The electrospinning deposition was carried out at room temperature with spinning parameters of 8 kV voltage, 0.15 m distance between the tip and collector with a flow rate of 0.01 mL m<sup>-1</sup>, and calcination temperature of 500 °C was used to obtain SnO<sub>2</sub> nanofibers. In the next step, PPY monomers were added to SnO<sub>2</sub> fibers to get Tin oxide/polypyrrole nanofibers. The fibers showed a high sensitivity of 7.45 at a low concentration of Ammonia at 1 ppm.<sup>[179]</sup> Dong et al. reported synthesizing the nonenzymatic glucose sensor based on the conductive polymer/CuCo<sub>2</sub>O<sub>4</sub> carbon nanofiber (CNF). PAN has been used as an electrospinning precursor solution. Poly thiophene-3-boronic acid (PTBA) has been used as a conductive polymer with a CuCo<sub>2</sub>O<sub>4</sub> carbon nanofiber combination. The obtained PTBA/ CuCo<sub>2</sub>O<sub>4</sub>-CNF showed a sensitivity of 708 μA × 10<sup>-3</sup> M<sup>-1</sup>cm<sup>-2</sup> toward enzyme-free glucose detection.<sup>[180]</sup> Part et al. stated a review article about the recent progress of conductive polymers and their utilization in the biomedical field in the form of tissue engineering, drug delivery system, wound healing, etc.<sup>[181]</sup>

#### 4.6. Ceramic-Based Electrospun Nanofibers

Nanostructures Ceramic materials are initiates from upgraded novel assets stand up from the high surface to volume ratio. The particle size at nanolevel deviates from bulk material.<sup>[182,183]</sup> Primarily ceramic nanoparticles are made up of carbides, oxides, carbonates of metal, metalloids, phosphates, such as titanium calci-

nated silicon, etc. They have high favorable properties of chemical inertness, high heat resistance. Especially in the biomedical field, ceramic nanoparticles are considered the drug carriers, proteins, and genes imaging agents.<sup>[184]</sup> Synthesis of ceramics based on the electrospinning route is one of the simple methods to obtain the desired nanosize, better porosity, improved surface properties.<sup>[185,186]</sup> Zhang et al. reported the synthesis of ceramic In<sub>2</sub>O<sub>3</sub> nanofiber using PVP polymer precursor solution, the positive high voltage of 30 kV had been applied with the distance of 15 cm between the collector and tip. The obtained electrospun In<sub>2</sub>O<sub>3</sub> nanofibers showed a diameter of 200–400 nm range.<sup>[187]</sup> Pascariu et al. reported the review article about the ZnO ceramic nanofiber synthesis using different routes and compared those fibers with electrospinning ZnO ceramic nanofibers and their composites with organic materials. They also explained the application of ZnO ceramic nanofibers in sensor application and photocatalysts applications.<sup>[188]</sup>

#### 4.7. Conjugated Polymers-Based Electrospinning Nanofibers

Recently conjugated polymers-based research has witnessed more attraction due to the conductivity, structural, and functional versatility of a lightweight, low-cost processing, solution processibility, and molecular design. Conjugated polymers are polymers that have a conjugated π electron backbone. With the additive of electrospinning, conjugated polymers give extra advantages of high surface volume ratio and high porosity to the conjugated polymers.<sup>[189]</sup> Li et al. reported the synthesis of conjugated polymers nanofibers using the electrospinning of two capillary spinnerets. In this blending Poly[2-methoxy-5-(2-ethylhexyloxy)-1, 4-phenylenevinylene] (MEH-PPV) with another conjugated polymer Polyhexahydrotriazine (PHT), and the diameter of the obtained electrospun fiber was 30–50 nm by maintaining the spinning parameters of 7.5 kV applied voltage, 9 cm distance

between the collector and needle tip with the flow rate of 0.005–0.003 mL h<sup>-1</sup>.<sup>[190]</sup> Long et al. reported the novel synthesis of 2,4-dinitrotoluene (DNT) nanofibers using an electrospinning route with the spinning condition of 25 cm between and tip and the collector, a voltage of 25 kV with the flow rate of 0.12 g mL<sup>-1</sup>. As obtained, nanofibers showed a diameter of 300–400 nm used for the DNT sensing. Moreover, SDS used a porogen to improve the performance of the DNT fluorescent sensor.<sup>[191]</sup> Loganathan et al. reported advantages of conjugated polymers, types of a conjugated polymer, and electrospun conjugated polymers, and their application in the optical sensors (fluorescent and colorimetric sensors).<sup>[192]</sup> The synthesis of materials-based electrospun nanofibers with different parameters is as shown in Table 1.

## 5. Sensor Applications Based on Electrospun Nanofibers

The manipulation of an atomic or molecular level of atoms is called nanotechnology. Nanotechnology has opted significant role in many applications. Mostly nanosensors are one of the most innovative and minuscule devices (sensing measurements are less than 100 nm), which is mainly used in nanoelectronics, molecular engineering, and nanomedicine.<sup>[193,194]</sup> Nanosensors can measure quantitative assets and convert them into human-readable signals, then those signals can be analyzed. Nanosensors are mainly divided into optical sensors, physical sensors, and chemical sensors; all these sensors help the daily life of the human with their ease, comfortability, and cost-effectiveness. Nanosensors play a significant role in biomedical applications.

Moreover, chemical sensors can help detect harmful chemicals like carbon dioxide and lead in agricultural grounds and the environment.<sup>[195]</sup> Nanosensors, with their accuracy and fast measurements, will make the world advance on a technological level. Many sensors are obtained through nanofabrication or nanomanufacturing using materials at the nanoscale level.<sup>[196–198]</sup> Nanomaterials can create novel techniques and devices due to their unique properties and functions. Nanoparticles are synthesized either by a top-down or bottom-up approach to get the desired size for the required application.<sup>[199]</sup> Nanoparticles have enhanced surface area, and electron transfer kinetics make more excellent biological activity, quantum behavior, and analyte reactivity than bulk. Nanomaterials are classified according to their size, shape, and features (color, solubility magnetism, bioavailability, toxicity, strength).<sup>[200]</sup> Nanomaterials are classified as organic and inorganic and even the combinations of metals, oxides of metals, ceramic nanomaterials, polymer, ceramic nanomaterials, and their composites, e.g., polymer matrices reinforced into metal, metal oxides nanoparticles, or carbon nanoparticles. The most important and influential strategy to increase the sensing nature is increasing the specific surface area and enhancing reactivity, electron transfer kinetics, adsorption, etc. In the last decade, electrospinning was one of the most cost-effective and straightforward labs to synthesize nanofibers for the ultrasensing system.<sup>[201,202]</sup> The size and diameter of the nanofibers based on different nanomaterials can be tuneable with the help of spinning parameters such as concentration of precursor solution, high voltage, and distance between the collector and needle tip of equipment. Besides, the versatility process of the chemical combination of electrospun nanofibers provides an exten-

sive range of final assets, including sensitivity, chemical strength, elasticity, porosity, etc.<sup>[203]</sup> All these properties make electrospun nanofibers the potential candidates for many sensing applications.

### 5.1. Electrochemical Sensors

Electrochemistry is one of the most studied multidisciplinary sciences, which has a wide range of applications. Electrochemical studies play a crucial role in sensing, energy field, and water treatment and have both invasive and noninvasive biomedical application fields.<sup>[204,205]</sup> It is an analytical platform of low cost, high sensitivity, and typically fast in nature to detect a very low detection limit of  $\approx \times 10^{-9}$  M /1000 mL<sup>-1</sup>, and they are suitable for miniaturization and come in the category of point of care analysis. The electrochemical analysis is mainly done with the help of cyclic voltammetry (CV). A CV consists of an electrochemical unit cell made of three electrodes, namely counter electrode (usually platinum), reference electrode (Ag/AgCl), and working electrode electrodes can be chosen according to suitable application. Redox property materials are the main concern for electrochemical sensing; generally, GCE (glassy carbon electrode), metal meshes, disposable electrodes, screen printed electrodes, fluorine doped tin oxide (FTO), indium tin oxide (ITO), etc., are working electrodes.<sup>[206–208]</sup> The electrochemical sensing will be coated on the working electrode, making it a modified electrode. There are numerous techniques available in electrochemical analysis based on required application, such as potentiostatic, galvanostatic and conductimetric, chronoamperometry, electrochemical impedance spectroscopy, pulse voltammetry, and linear sweep voltammetry, etc. Electrochemical sensors are mainly enzyme-based and nonenzyme-based sensors.<sup>[209,210]</sup> Nanostructure materials take advantage of ultrahigh sensitivity due to the high surface area to volume ratio, better electron transfer kinetics, and ease of use of the technique. In the road of nanostructure-based electrochemical sensors, simple one-step electrospinning nanofibers showed a better output depending on the diameter of the target nanometer.<sup>[211]</sup> The most commonly used electrospun-based electrochemical sensors help detect glucose **Figure 4a** shows the mechanism of glucose to gluconolactone conversion), H<sub>2</sub>O<sub>2</sub>, urea, ascorbic acid, dopamine, uric acid, neurotransmitters, cancer biomarkers, etc. **Figure 5** represents the electrochemical sensing of ascorbic acid, dopamine and serotonin based on the RuO<sub>2</sub> decorated CeO<sub>2</sub>-Au NFs.

Recently, many flexible and wearable electrochemical sensors based on advanced materials, including metals, metal oxides, 2D materials, and carbon-based materials, occur.<sup>[212]</sup> Gattani et al. reported the current advantages of electrochemical sensors (bio) as a help point of care diagnosis and early detection of metabolic disease detection, such as sweat analysis and hormonal analysis.<sup>[213]</sup> Ke et al. reported the review about electrospinning based electrochemical sensors, which mentioned the detection of H<sub>2</sub>O<sub>2</sub>, glucose with and without enzyme, such as multipurpose sensors based on metal oxides and carbon-based (GO, rGO, CNTs, MWCNTs).<sup>[214]</sup> Guangyue et al. described the synthesis of PVP-based CuO electrospun nanofiber to detect glucose. The modified working electrodes CuO NFs-ITO showed a high sensitivity of 873  $\mu\text{A} \times 10^{-3} \text{ M}^{-1} \text{ cm}^{-2}$  with a low detection limit of 40

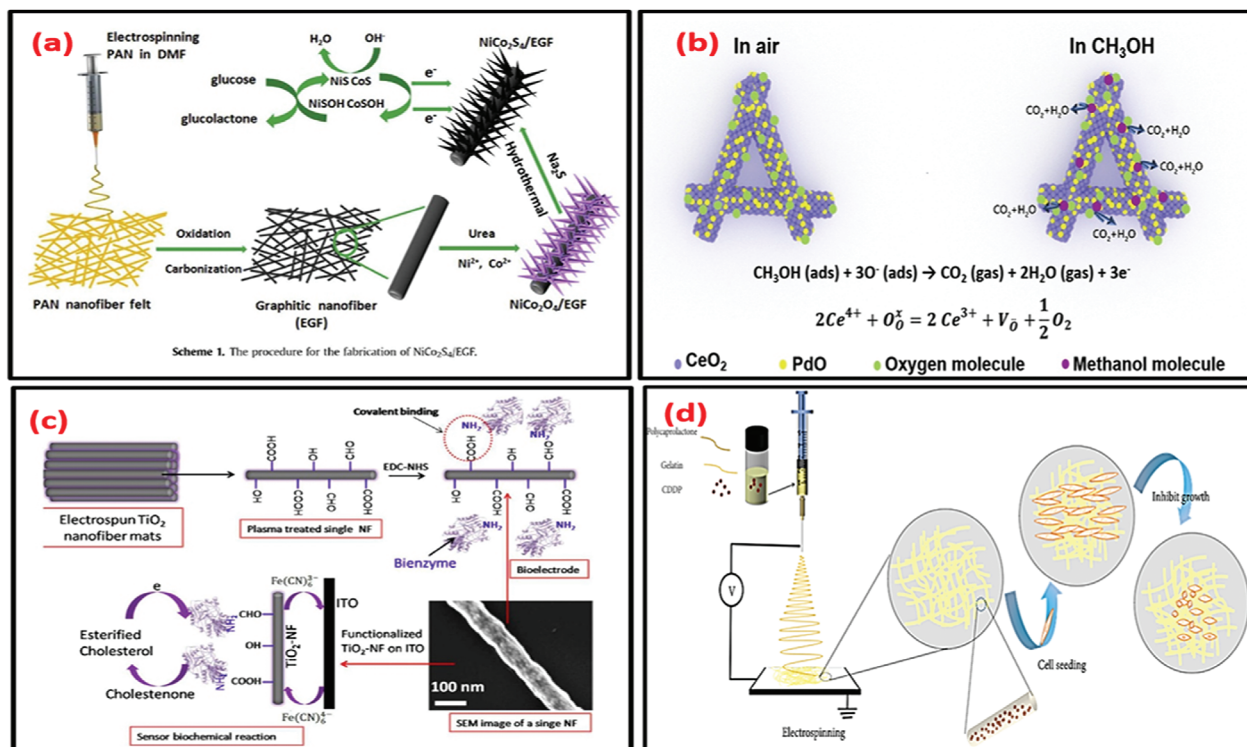


**Figure 4.** a) Mechanism of nonenzymatic glucose sensing of NiCo<sub>2</sub>O<sub>4</sub>/EGF, it showed the oxidation of NiCo<sub>2</sub>O<sub>4</sub> into NiSO<sub>4</sub>, CoSO<sub>4</sub> which helps the conversion of Glucose to Gluconolactone. Reproduced with permission.<sup>[224]</sup> Copyright 2019, Elsevier B.V., b) represents the methanol sensing mechanism of PdO/CeO<sub>2</sub> nanocomposite and it show the reaction of the PdO/CeO<sub>2</sub> in the presence of air and methanol. Reproduced with permission.<sup>[380]</sup> Copyright 2019, Elsevier B.V., c) Biofunctionalized cholesterol mechanism using TiO<sub>2</sub> nanofibers coated ITO. Reproduced with permission.<sup>[482]</sup> Copyright 2014, American Chemical Society, d) Shows the interaction of prostate cancer with the electrospun PCL/Gelatin with loaded CDDP and finally these PG@CDDP for the cancer cell treatment with different periods of time. Reproduced with permission under the terms of the CC-BY license.<sup>[405]</sup> Copyright 2021, the Authors. Published by Hindawi.

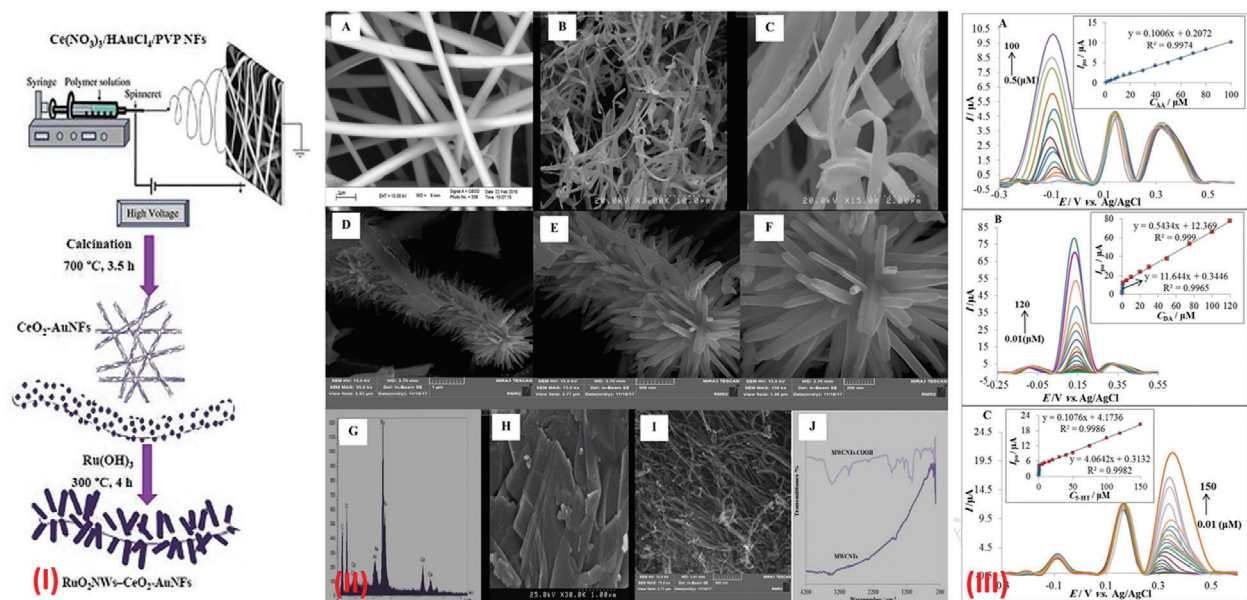


**Figure 5.** (I) schematic of CeO<sub>2</sub>-AuNFs formation and the decoration of RuO<sub>2</sub> decoration of CeO<sub>2</sub>-AuNFs (II) FESEM images of A) electrospun Ce(NO<sub>3</sub>)<sub>3</sub>/HAuCl<sub>4</sub>/PVP nanofibers B,C) CeO<sub>2</sub>-Au NFs D-F) RuO<sub>2</sub> grown on CeO<sub>2</sub>-Au NFs G) EDX of RuO<sub>2</sub>-CeO<sub>2</sub>-Au NFs H) GO I) f-MWCNTs J) FTIR of MWCNTs and f-MWCNTs (III) CV-Differential Pulse Voltammetry (DPV) graphs of A) Ascorbic Acid B) DPV graphs of Dopamine (DA) C) DPV graphs of Serotonin (5-HT) in PBS solution (pH = 7.5). Reproduced with permission.<sup>[234]</sup> Copyright 2018, Elsevier B.V.

$\times 10^{-9}$  M in the linear range of  $0.20 \times 10^{-6}$  M to  $1.3 \times 10^{-3}$  M glucose concentration.<sup>[215]</sup> The below table provides the electrospun nanofibers for the electrochemical detection of various analytes, example of biofunctionalized cholesterol mechanism using  $\text{TiO}_2$  NFs@ ITO shown in Figure 4c. Detection of cancer at the early stages becomes one of the emergent needs of the world. Many technologies have been promoted, showing electrospun nanofiber as the promising platform for sensing related electrochemical biomarkers. Hernández et al. reported the crucial features of the electrospun fiber as high surface area, better porosity, and small size and reported their role in cancer detection and diagnostics. They also mentioned the electrochemical immunosensors, gas sensor fluorescent chemosensor, and gene-sensor.<sup>[216]</sup> The various electrochemical sensors based on electrospun nanofibers are provided in Table 2.

## 5.2. Fluorescent Sensors

Here we explore photonics, an emerging field that has garnered huge attention aimed at developing novel optical nanosensors.<sup>[266]</sup> Optical sensors utilize the principles of scattering, surface plasmon resonance, fluorescence, absorbance chemiluminescence, etc. Moreover, optical sensors are used to detect the fluorescent, colorimetric, and luminescent changes.<sup>[267]</sup> The advanced materials also improve the sensing features of low detection limit, sensitivity, multiplexed detection efficiency, and small size.<sup>[268]</sup> Various nanomaterials metals, oxides of metals, carbon-based materials, advanced materials, etc., have been somewhat explored.<sup>[269,270]</sup> The successful development compared with other nanomaterials electrospun nanofibers can be helpful in the optical sensors with many benefits, such as low cost, easy fabrication, readable and straightforward detections, functionalization, chemical composition, structure, porosity, and high surface to volume ratio. Besides the main advantage of optical sensors after the detection process, the mats/or membranes of an electrospun nanofiber can be taken out because there is no way of contamination.<sup>[271,272]</sup> Fluorescent sensors are the part of the optical sensors that work on absorption by light emission. Sensors based on fluorescence can depend on three types of fluorophores, such as fluorescent labels, enzyme substrates, and fluorescent probes. The fluorescent label is the nanoparticles attached to the receptor directed against a biomarker to a specific analyte.<sup>[273]</sup> Lining et al. reported detecting mercury ion (II) using electrospun nanofibers based fluorescent membrane.

PAN has been used as the polymer solution to get the electrospun nanofibers, DTPTDI (dithioacetal-functionalized perylene diimide) was introduced on the surface of PAN nanofibers surface for the immobilization purpose. Hence the reaction takes between Hg(II) and DTPDI. The selectivity of electrospun nanofibers was analyzed with Fe(III), Fe(II), Hg(II), Na(II), Cu(II) ions. The sensitivity was absorbed in the form of an increase in intensity as Hg concentration increase. The LOD of Hg (II) in water was  $0.00 \text{ mg L}^{-1}$ .<sup>[274]</sup> Afroditi et al. described the synthesis of core-shell nanoparticles decorated cellulose acetate electrospun nanofibers to detect pH and gas sensors through fluorescence. The synthesis of  $\gamma\text{-Fe}_2\text{O}_3/\text{SiO}_2$  core-shell nanoparticles took place and was functionalized with fluorescent molecules

Rhodamine B (RhB) and finally incorporated with cellulose acetate nanofibers. The obtained CA nanofibers showed an average diameter of 770 nm. As obtained, CA decorated  $\gamma\text{-Fe}_2\text{O}_3/\text{SiO}_2$  core-shell NPs were used to detect the Ammonia vapors and pH detection. The nanofibers were immersed in the solution as pH was increased, the fluorescent intensity was decreased, and for ammonia detection, the level was increased up to 12 000 ppm.<sup>[275]</sup>

Furthermore, fluorescent sensors also took much space in the biosensor applications; Jennifer et al. reported the synthesis of PAN and pVDB (poly(4-vinylphenylboronic acid *co*-2-(dimethylamino)ethyl methacrylate-*co*-*n*-butyl methacrylate) blended nanofibers through electrospinning. The obtained PAN@pVDB nanofibers showed a 490–560 nm diameter with a different weight ratio of pVDB. As obtained, PAN@pVDB used the membranes for the fluorescent bacterial (*staphylococcus aureus* or *Escherichia coli*) sensors with distant emission of 530 nm. The PAN@pVDB showed early detection of bacterial settlement.<sup>[276]</sup> The various fluorescent sensors based on electrospun are shown in Table 3.

## 5.3. Colorimetric Sensors

Colorimetric sensors are also part of the optical sensors. Colorimetric sensors have attracted significant attention because of their distinct advantages, including adaptable sensitivity, quick response, simple operation, long linear ranges of the measurable assay.<sup>[306]</sup> Colorimetric sensors are primarily suitable for the clinical point of care diagnosis, gas sensing application, metal ion detection due to the advantages of very low detection limits, simple operation without complicated devices.<sup>[307]</sup> Colorimetric sensors target the color change of a physical parameter, such as thermochromic assemblies. The shift in the color is due to the chemical shift between the molecules by fluorescence enhancement through the turn on or turn off mechanism. Time chemical electrospinning nanofibers transducing optical characteristics becomes a potential candidate for colorimetric sensors, which have been exposed extensively with better sensing properties of selectivity, sensitivity, and limit of detection and response time. The colorimetric sensors are helpful in heavy metal ion detection and medical applications.<sup>[308]</sup> The breath analyzer has become very useful for the early detection of disease and helps in the diagnosis process for cancer treatments. The main thought of this analysis is that volatile organic compounds will increase in cancer patients in the range of ppb levels.<sup>[309]</sup>

Yapor et al. reported the colorimetric sensor for the *Escherichia coli* bacterial activity using electrospun conjugated polymers including polydiacetylene (PDAs), polyurethane (PU), PEO, and their combinations. The color changes occurred at pH 10 but improved from pH 11 to pH 13.<sup>[310]</sup> Zhang et al. described the synthesis of PASP (poly (aspartic acid) electrospun nanofiber for the detection of Cu(II), Fe(III) using the colorimetric sensor. The colorimetric change toward the Cu (II) was white color to a blue color with a low detection limit of  $0.3 \text{ mg L}^{-1}$ , whereas Fe(III) showed LOD of  $0.1 \text{ mg L}^{-1}$  by changing white to yellow color.<sup>[311]</sup> Hyun et al. reported that the colorimetric sensors are the facile and cost-effective sensors for ammonia gas detection using meta-aramid/dye 3 electrospun nanofibers. A fabricated electrospun



**Table 2.** Electrochemical sensors based on electrospun nanofibers.

S.No	Electrospinning material	Sensing material	Diameter [nm]	Application	Limit of detection	References
1	AgNO <sub>3</sub> /Cu(NO <sub>3</sub> ) <sub>2</sub> /PVP	Ag/CuO NFs-ITO	150–200	Glucose	5.17 × 10 <sup>-9</sup> M	[217]
2	Zn(Ac) <sub>2</sub> /Cu(Ac) <sub>2</sub> /	ZnO–CuO HNCs	200	Glucose	0.21 × 10 <sup>-6</sup> M	[218]
3	C <sub>4</sub> H <sub>6</sub> O <sub>4</sub> Ni·4H <sub>2</sub> O /PVP	NA/NiONF/GCE	350	Glucose	0.77 × 10 <sup>-6</sup> M	[219]
4	Polyacrylonitrile/NiAA	NiCFP	200–400	Glucose	1 × 10 <sup>-6</sup> M	[220]
5	Mn(Ac) <sub>2</sub> ·4H <sub>2</sub> O/ Co(Ac) <sub>2</sub> ·4H <sub>2</sub> O/PVP	MCF/GCE	150–250	Glucose	0.01 × 10 <sup>-6</sup> M	[221]
6	WA–ECNF	MnO <sub>2</sub> /Co <sub>3</sub> O <sub>4</sub> @ECNF	—	Glucose	0.3 × 10 <sup>-6</sup> M	[222]
7	PVDF/PEDOT:PSS/THF	ENFM	20–50	Glucose	2.3 × 10 <sup>-6</sup> M	[173]
8	Nickel acetate/Cobalt acetate/PAN/	Ni–CoO/CNF	—	Glucose	0.03 × 10 <sup>-6</sup> M	[223]
9	PAN/ NiCo <sub>2</sub> O <sub>4</sub> /Na <sub>2</sub> S	NiCo <sub>2</sub> S <sub>4</sub> /GCNF	20	Glucose	0.167 × 10 <sup>-6</sup> M	[224]
10	PAN/DMF	CNFs	200	Catechol	0.63 × 10 <sup>-6</sup> M	[225]
11	PAN–CaCO <sub>3</sub> /ptNPs	CNF/PtNP	200–400	H <sub>2</sub> O <sub>2</sub>	1.9 × 10 <sup>-6</sup> M	[226]
12	H <sub>2</sub> PtCl <sub>6</sub> ·6H <sub>2</sub> O/ NiCl <sub>2</sub> ·6H <sub>2</sub> O/ EtOH/PVP	PtNi/NCNFs	200–500	H <sub>2</sub> O <sub>2</sub>	0.037 × 10 <sup>-6</sup> M	[227]
13	PPys/PVP	NCNPFs	140 ± 22	H <sub>2</sub> O <sub>2</sub>	—	[228]
14	Chiston/PVP/MWCNTs	uricase/Chi–CNTsNF/AgNPs/Au	188 ± 15	Uric acid	1 × 10 <sup>-6</sup> M L <sup>-1</sup>	[229]
15	PET/DCM/TFA	AuNP–PET	10	Dopamine	0.5 × 10 <sup>-6</sup> M	[230]
16	PAN/DMF	CNFs/SPE	145 ± 32	Tramadol	0.05–0.016 × 10 <sup>-9</sup> M	[231]
17	Ce(NO <sub>3</sub> ) <sub>3</sub> /HAuCl <sub>4</sub> /PVP	CeO <sub>2</sub> /Au–GCE	100–250	Dopamine	0.056 × 10 <sup>-6</sup> M	[232]
18	DPU/DMF/THF	DATPU/CNTs	726 ± 416	Strain	—	[233]
19	Ce(NO <sub>3</sub> ) <sub>3</sub> /HAuCl <sub>4</sub> /PVP/Ru(OH) <sub>3</sub>	RuO <sub>2</sub> NWs–CeO <sub>2</sub> –AuNFs	<100	Dopamine, Serotonin Ascorbic acid	2.8 × 10 <sup>-9</sup> M 2.4 × 10 <sup>-9</sup> M 160 × 10 <sup>-9</sup> M	[234]
20	PAN/OLC/DMF	OLC–CNFs/GCE	40–200	Dopamine	1.42 × 10 <sup>-6</sup> M	[235]
21	PAN/DMF	WS <sub>2</sub> NSs–CNFs	1000	Dopamine	0.01 × 10 <sup>-6</sup> M	[236]
22	CA/CNs	rGO–Au–SPEs.	—	Glucose	0.1 × 10 <sup>-3</sup> M	[237]
23	PA6/PAH/formic acid	(PA6/ PAH_MWCNTs)	88 ± 24	Dopamine	0.15 × 10 <sup>-6</sup> M L <sup>-1</sup>	[238]
24	PAN/PVP/DMF	Ag–Pt/pCNFs	370	Dopamine	0.11 × 10 <sup>-6</sup> M	[239]
25	DMF/Acetone/PVDF–HFP	rGO/CDs/ GCE	416 ± 10	Dopamine	1.41 × 10 <sup>-6</sup> M	[240]
26	AMH/AgNO <sub>3</sub> /PVA/ethanol	Ag-doped WO <sub>3</sub>	—	SERS	—	[241]
27	PAN/PVP	Ag–Pt/pCNFs/GCE	370	Dopamine	0.11 × 10 <sup>-6</sup> M	[242]
28	PVA/PEI	PVA/PEI/GO <sub>x</sub> /Au NFs	240–360	Glucose	0.9 × 10 <sup>-6</sup> M	[243]
29	Bacteria Cellulose	HRP/Au–BC/GCE	60	H <sub>2</sub> O <sub>2</sub>	1 × 10 <sup>-6</sup> M	[244]
30	PVA	PVA–SbQ/GO <sub>x</sub> /MWCNT	200–600	Glucose	2 × 10 <sup>-6</sup> M	[245]
31	PVA	VA/GO <sub>x</sub> /graphene	—	Glucose	50 × 10 <sup>-6</sup> M	[246]
32	PV6/PAH	PA6/PAH@Au/Tyr/FTO	—	Bisphenol	0.011 × 10 <sup>-6</sup> M	[247]
33	Nylon 6,6	Nylon 6,6/4MWCNT/PBIBA	—	Glucose	9 × 10 <sup>-6</sup> M	[248]
34	PVP	CuO–NiO/GCE	200–300	Glucose	0.08 × 10 <sup>-6</sup> M	[249]
35	PVA	Magnetic nanofibers (MNFs)	70–120	Morphine	1.9 × 10 <sup>-9</sup> M	[250]
36	PAN	NiCo <sub>2</sub> O <sub>4</sub> /CNF	320–400	glucose	1.5 × 10 <sup>-6</sup> M	[251]
37	PAN–Oxime	Ag NPs–PAN–Oxime NFs	400	CA 125 ovarian cancer	0.0042 U mL <sup>-1</sup>	[252]
38	AgNO <sub>3</sub> /Co(Ac) <sub>2</sub> /PVP	Au–Ag/Co <sub>3</sub> O <sub>4</sub> NFs	150–200	H <sub>2</sub> O <sub>2</sub> –breast cancer cells	—	[253]
39	PCL	CuO/PCL@PPy/ITO	150–200	Gucose-saliva	0.8 × 10 <sup>-6</sup> M	[254]
40	PAN	Fe <sub>3</sub> O <sub>4</sub> PANNFs/ITO	—	Vitamin D3	0.12 ng mL <sup>-1</sup>	[255]
41	PAN	Au decorated ECNFs	—	Breast Cancer	0.45 ng mL <sup>-1</sup>	[256]
42	PAN	PAN/PPy NFs	160	A549 –Lung cancer	1.2 × 10 <sup>3</sup> cells mL <sup>-1</sup>	[257]
43	PAN	PtNPs/PAN	—	H <sub>2</sub> O <sub>2</sub>	—	[258]
44	PAN	ZrO <sub>2</sub> @GNF	0.8–1.0 μm	Osteopontin determination	4.76 fg mL <sup>-1</sup>	[259]
45	PAN	MWCNT/ZnO	—	Atrazine	—	[260]
46	PANI/PDMS	PANI NFs	256	COX–2enzyme	0.01 pg mL <sup>-1</sup>	[261]

(Continued)

**Table 2.** (Continued).

S.No	Electrospinning material	Sensing material	Diameter [nm]	Application	Limit of detection	References
47	PA6/PAH	PA6/PAH/MWCNTs	—	CA19-9	1.84 U mL <sup>-1</sup>	[262]
	PA6/PAH	PA6/PAH/AuNPs	—	CA19-9	1.57 U mL <sup>-1</sup>	
48	PAN	MWCNT-ZnO	300–400	Anti-CA125	0.00113 U mL <sup>-1</sup>	[263]
49	PAN	Ni-CNF	85.3	Glucose	0.57 × 10 <sup>-6</sup> M	[264]
50	PVDF/PEDOT: PSS	Au/PVDF/PEDOT:PSS/GOx	100 ± 50	Glucose	1.84 U mL <sup>-1</sup> 1.57 U mL <sup>-1</sup>	[265]

**Table 3.** Fluorescent sensors based on the electrospun nanofibers.

S.No	Electrospinning material	Sensing material	Diameter [nm]	Application	Limit of detection	References
1	TMOPP/PS/DMF	TMOPP-PS	300–400	Nitroaromatic explosive detection	—	[277]
2	Polystyrene	CB-PS/G-NH <sub>2</sub>	—	Picric acid detection	228 ppb	[278]
3	Polyurethane	Polyurethane/HTTP glass chip	300–400	Nitroaromatics and TNT	—	[279]
4	Poly(NIPAAm-co-NMA-co-RHPMA/ (PNNR1- PNNR3) /methanol	PNNR	298 ± 70	Cu <sup>2+</sup> detection	—	[280]
			268 ± 23			
5	PSMA	PSMA/TPE	—	<i>E.Coli</i> bacteria detection	—	[281]
6	PEI/PVA	QDs/PEI/PVA	—	Biomarker	—	[282]
7	PAN	Polycrystalline/BYF-EY/PAN/	—	Temperature sensor	—	[283]
8	PVP	PVP_Eu <sup>3+</sup> NFs	179 ± 52	Ammonia detection	—	[284]
9	PAN	CDs/mesoSiO <sub>2</sub> /PAN	380–550	Fe(III) detection,	3.95 × 10 <sup>-6</sup> M	[285]
10	PAN	PAN/Ag/SiO <sub>2</sub>	—	Pb <sup>2+</sup> , Mn <sup>2+</sup> , Cd <sup>2+</sup> , Fe <sup>3+</sup> , Ni <sup>2+</sup> and Hg <sup>2+</sup> ions detection	—	[195]
11	PCL	AuNC*PCL-NF	280 ± 40	Hg <sup>2+</sup> detection	50 PPT	[286]
12	PMMA/MEH-PPV	PMMA/MEH-PPV	169 nm	Optical devices, chemical sensor	—	[287]
13	Ethyl cellulose (EC)	EMIMBF <sub>4</sub>	400–685	Hg (II) detection	0.07 × 10 <sup>-9</sup> M	[288]
14	PHBMA/THF	3,4-dihydroxy-4 -aminostilbene (DHAS)	—	Organophosphorus nerve agents detection	—	[289]
15	Polystyrene	Polymer P	400–500	Nitroaromatic, explosive sensor	—	[290]
16	P-PS	P-PS NFs	400–500	Heme protein analysis	1.2 × 10 <sup>-8</sup> M	[291]
17	Polystyrene (PS)	CPBQDs/PS FM	800	Ultrasensitive fluorescent sensor	0.01 ppm	[292]
18	PVP/PCL	PVP/PCL/Ag/RCSPs	923 ± 288	Wound healing	—	[293]
19	Polyethylene oxide PEO	PEO/MePyCz	0.8–1.6 μm	Portable explosive detector	—	[294]
20	Cellulose acetate (CA)	DNA-AuNP-CANF	150–250	Nucleic acids Sensing	0.08 × 10 <sup>-9</sup> M	[295]
21	(Poly(NIPAAm-co-NMA)	(Poly(NIPAAm-co-NMA)/F-Phen	300–570	Cu <sup>2+</sup> detection	1 × 10 <sup>-5</sup> –1 × 10 <sup>-4</sup> M	[296]
22	PCL	Ag@SiO <sub>2</sub> -PCL	—	Ag	1.5 ng mL <sup>-1</sup>	[297]
23	PVA	CDs/AuNCs-PVA@CA NFM	260	Cyanide detection	0.15 × 10 <sup>-6</sup> M	[298]
24	poly(HEMA-co-NMA)	Poly(HEMA-co-NMA-co-RhBN2AM)	200–350	Hg (II) sensing	10 <sup>-7</sup> M	[299]
25	EVOH	EVOH-PABA-Py	1–13 μm	Cu <sup>2+</sup> detection	—	[300]
26	PVP	YTO: Ho <sup>3+</sup> /Yb <sup>3+</sup>	300–400	Temperature Sensor	—	[301]
27	CA	CA/Fe/QDs	30–90	Mercury (II) and	—	[302]
		CA/Fe/QDs		Lead (II) ions detection		
28	PMMA/ethyl cellulose	PMMA/EC/DPAINH	300–550	Cu <sup>2+</sup> detection	3.8 × 10 <sup>-14</sup> M 1.4 × 10 <sup>-13</sup> M	[303]
29	Poly(HEMA-co-NMA-co-NBD)	Poly(HEMA-co-NMA-co-NBD)/ SRhBOH	300–550	Naked eye sensors	10 <sup>-4</sup> M	[304]
30	Polystyrene/ polyethylene oxide/carbazole	PEO/PyCz	0.8–1.2 μm	Nitro explosives and	—	[305]
		PS/PyCz		Watery interferents		

**Table 4.** Colorimetric sensors based on electrospun nanofibers.

S.No.	Electrospinning material	Sensing material	Diameter [nm]	Application [cell type/drug]	LOD	References
1	Nylon 6 NFN	Nylon 6 NFN sensor	150–250	Formaldehyde detection	50 ppb	[313]
2	NFM	PA66/CoCl <sub>2</sub> ·6H <sub>2</sub> O	100	Humidity sensor	—	[314]
3	Cellulose acetate (CA)	Br–PADAP/CA	147	Uranyl sensor	50 ppb	[315]
4	Diacetylene(DA)/PEO	PCDA–AN 2	1 μm	Organic solvent	—	[316]
5	CA	RBD/CA	750 ± 270	Cu <sup>2+</sup>	018 ppm	[317]
6	TCF–H	PAA–TCF–H	200–450	Ammonia Gas	—	[318]
7	PVA	AuNC*–NFM	180 ± 40	Hg <sup>2+</sup> detection	1 ppb	[319]
8	Polysulfone	AuNC/FNFM	520–650	H <sub>2</sub> O <sub>2</sub> detection	500 × 10 <sup>–9</sup> M	[320]
9	NFN	PANI/PA-6 NFN	435 and 650	Cu <sup>2+</sup> detection	1 ppb	[321]
10	PAN	N-CDs	200	Cu <sup>2+</sup> detection	5 × 10 <sup>–9</sup> M	[322]

colorimetric sensor detected the ammonia gas in the range of 1–10 ppm with 10 s response time at room temperature.<sup>[312]</sup> The various combinations of electrospun fibers and their colorimetric applications are shown in **Table 4**.

#### 5.4. Gas Sensors

Noninvasive health monitoring, disease detection, and environmental protection have become the most demanded concern in the continuous research in nanoscience and technology due to industrialization and the rapidly growing population, which causes extreme air pollution.<sup>[323,324]</sup> So, there is an urge to protect the environment and ecosystem. Hence real-time monitoring sensors are highly essential for protection. The various types of gases detection methane (from mining), hydrocarbons (oil refineries), NO<sub>2</sub> (vehicle exhaust), Ammonia (fertilizers), and VOCs (human breath) need to be detected. Hence, low-cost, rapid, highly sensitive, and reliable small-size sensors have emerged, which are more preferable.<sup>[325,326]</sup> Moreover, nanomaterial-based human breath analyzers have become promising candidates for many disease detections rather than traditional blood tests and computed tomography (CT) routes. Breath biomarkers mainly depend on volatile organic compound, **Figure 6** shows the acetone (VOC) sensing based on the Rh doped SnO<sub>2</sub> nanofibers, which is the cost-effective and noninvasive way of detecting disease. The essential sensing parameters of sensitivity, stability, response time, recovery time, low detection limit, selectivity, repeatability, everything depends on adsorption and desorption. The most important properties are high porosity, better surface area, and mechanical strength of the nanostructure's material.<sup>[327]</sup> Many methods were opted out of them; electrospinning nanofibers have fulfilled all the required gas sensing parameters. Furthermore, even though electrospun semiconducting materials are the most promising candidates, they still have limited stability, toxicity, and high temperature to avoid these issues, semiconductive materials are combined with composites, including metals, metal oxides, polymer, and carbon-based materials.<sup>[328,329]</sup> **Figure 4b** shows the methanol sensing mechanism based on electrospun PdO/CeO<sub>2</sub>. Singh et al. reported the review articles about ZnO nanostructures for the gas sensing applications due to their outstanding properties, such as

semiconducting nature, low cost, high sensing responsiveness. Various techniques have prepared ZnO, including nanofibers through electrospinning route with a combination of metals (Ag, Pt, Au, Ni, Co, Cr, Tb, La, In, etc.), polymers (P3HT, PEIE, PANI, etc.), and carbon-based materials (CNFs, CNTs, rGO, GO) for detecting H<sub>2</sub>, NO<sub>2</sub>, ethanol, ethane, acetone, CO, VOCs, etc., at different temperatures.<sup>[330]</sup> Mercante et al. reported the hybrid ceramic electrospun nanofibers for the gas sensing application as a mini-review. The overview for the preparation of ceramic nanofibers (CNF) has been explained. Moreover, the importance of gas sensing and use of the CNF for sensing application using different gases and VOC at different combinations of meta doped CNF, hybrid CNFs, and carbon-based CNFs have been displayed for the sensing parameters of sensitivity, detection limit, selectivity, response, and recovery time as a table.<sup>[331]</sup> Joshua et al. described the synthesis of PS(polystyrene) and PHB (polyhydroxybutyrate),-tetraphenylporphyrin (H2TPP), and graphitized carbon with CTAB nanofiber with the spinning parameters of 6 kV DC voltage by maintaining 8 cm distance from the collector and needle tip with a flow rate of 700 μL h<sup>–1</sup> as-fabricated PS/PHB/H2TPP/MGC was coated on the interdigitated electrode to detect the toluene and acetic acid at a temperature of 60–70 °C. The limit of detection of ascorbic acid was 1 ppm, and toluene was 3 ppm.<sup>[332]</sup> Different type of gas sensing application based on the electrospun nanofiber has been shown in **Table 5**.

#### 5.5. Biomedical Applications

In recent years the attraction toward health care has advanced, and science and technology are trending to self-access or self-monitoring of specific individuals. Consequently, health care focuses more on the biomedical application for the well-being of patients (individuals).<sup>[384,385]</sup> Hence, monitoring health care has been seen as a point of care devices implants of the body parts, early disease detection in invasive or noninvasive ways, cancer biomarkers, wound dressing, wound healing, and tissue engineering.<sup>[386,387]</sup> In the biomedical field, many kinds of biosensors have been used for different biomedical applications to detect the information of clinical chemistry. Tissue engineering is reflected as regenerative medicine. It is a multidisciplinary

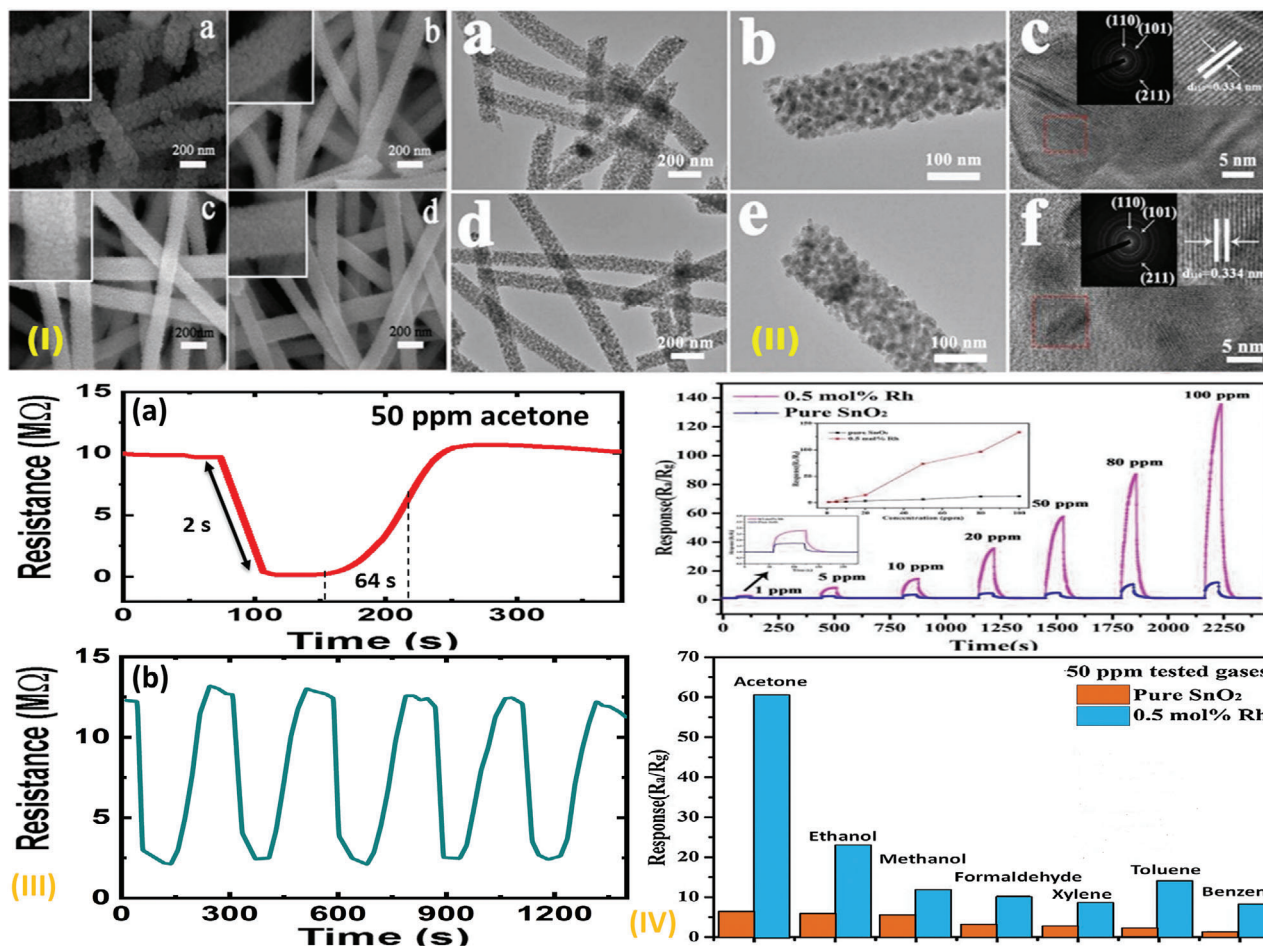


**Figure 6.** (I) FESEM images of Rh doped SnO<sub>2</sub> nanofibers of a) pure. b) 0.2 mol%. c) 0.5 mol%. d) 1 mol%. (II) TEM images of a,b) pure SnO<sub>2</sub> nanofibers. d,e) The 0.5 mol% Rh doped SnO<sub>2</sub> nanofibers c,f) SEAD pattern of pure SnO<sub>2</sub> and 0.5 mol% Rh doped SnO<sub>2</sub> nanofibers. (III) Acetone sensing a) response and recovery time of 0.5 mol% Rh doped SnO<sub>2</sub> nanofibers. b) Repeatability (five cycles) of 0.5 mol% Rh doped SnO<sub>2</sub> nanofibers at 50 ppm with 200 °C (IV) Interfering gas response of 0.5 mol% Rh doped SnO<sub>2</sub> at 50 ppm with 200 °C. Adapted with permission.<sup>[340]</sup> Copyright 2017, Elsevier.

field that includes biology, medicine, material science, and engineering. Tissue engineering uses scaffolds to regenerate a new extracellular matrix developed by disease or injury.<sup>[388]</sup> The three critical parameters required for tissue engineering are seeding and attachment of cells, scaffold fabrications, and incorporation of cell signaling factors. Out of three, scaffold fabrication is one of the most challenging tasks. However, it is the primary and vital procedure by multiple techniques, such as freeze-drying, electrospun-based self-assembly, 3D printing, even successful tissue engineering mainly depends on the behavior and morphology of scaffolds. For example **Figure 7(I)** represents tissue engineering application using PCL/CP electrospun fibers and gentamicin-loaded collagen/PCL nanofibers (GCP). Because of the outstanding properties of high surface area, tunable porosity, mechanical strength, and high surface-to-volume ratio of versatile electrospinning nanofibers or mats, it is an excellent candidate for tissue engineering (Biomedical application).<sup>[389–393]</sup> Wound dressings were first obtained from the animal's fats and plant fiber to cover wounds. As the technology improved, artificial materials came into the matter and were prepared us-

ing advanced methods. The main two requirements for wound dressing and healing are dressing should have hemostasis properties and antibacterial features to prevent the infection surrounded by the bacteria. Researchers reported that electrospinning mats really have enough space to improve the wound and promote wound healing, and they are also used for rapid hemostasis because of the large surface area.<sup>[394–396]</sup> Electrospinning nanofibers are called the carriers for the drug loading or drug delivery system because of the control of the released drug at the desired quantity **Figure 7(I)** displays the cumulative drug release activity of CAM-loaded PCL nanofibers. The drug loading of the electrospinning techniques can be done by co-electrospinning multiset, side by side, surface immobilization, and emulsion spinning. Moreover, electrospinning provides an opportunity to encapsulate drugs or biomolecules into nanofibers. Wang and his team reported that the bioactive drugs were loaded into the bilayer membrane and that they can release nanofibrous scaffolds separately without loss of functionality and structural integrity.<sup>[397,398]</sup> Rahmati et al. reported the tissue engineering application based on the electrospun nanofibers

**Table 5.** Gas sensors based on electrospun nanofibers.

S.No	Electrospinning material	Sensing material	Diameter [nm]	Application	Limit of detection	References
1	PVA/Glycerol	WO <sub>3</sub> /PVA	130 ± 20	H <sub>2</sub> S sensing	100 ppb	[333]
2	PVP/DMF	Bimetallic Mo-W oxide	—	Acetone sensing	0.019 ppm	[334]
3	PVP	Bi-doped SnO <sub>2</sub>	30–40	NO detection	50 ppb	[335]
4	PVA	Cu-doped ZnO	100	H <sub>2</sub> S sensing	—	[336]
5	PVP/In(NO <sub>3</sub> ) <sub>3</sub> ·5H <sub>2</sub> O	In <sub>2</sub> O <sub>3</sub>	60	Ethanol sensing	—	[337]
6	PVP	Cr <sub>2</sub> O <sub>3</sub> -ZnO	80–130	Ethanol sensing	1 ppm	[338]
7	PVP/DMF	ZnO	95	Acetone sensing	—	[339]
8	PVP/DMF	NiO-WO <sub>3</sub>	—	Acetone sensing	—	[340]
9	PVP/DMF	GO-WO <sub>3</sub>	100–150	Acetone sensing	—	[341]
10	PVP/DMF	WO <sub>3</sub> NFs	200	NH <sub>3</sub> sensing	—	[342]
11	PVA	CuO-ZnO	80–100	H <sub>2</sub> S sensing	—	[343]
12	PVP	CuO/SnO <sub>2</sub>	—	H <sub>2</sub> S sensing	< 10 ppb	[344]
13	PVP/DMF	La <sub>2</sub> O <sub>3</sub> -WO <sub>3</sub>	200 nm	Acetone sensing	0.8 ppm	[345]
14	PVA	Mesoporous In <sub>2</sub> O <sub>3</sub> NFs	150–200	CO sensing	—	[346]
15	PVP, PAN	α-Fe <sub>2</sub> O <sub>3</sub> /SnO <sub>2</sub>	160	Acetone sensing	—	[347]
16	PVA	PVA/CdO	125–425	Formaldehyde sensing	5 ppm	[348]
17	PVP	InYbO	75 ± 5	Ethanol sensing	1 ppm	[349]
18	PVP	TiO <sub>2</sub>	60	Ethanol sensing	0.7 ppm	[350]
19	PVP	Ca-In <sub>2</sub> O <sub>3</sub> NTs	80	Ethanol sensing	—	[351]
20	PVP	IO-Au-0.42 NFs	120	Ethanol sensing	1 ppm	[352]
21	PVP	CaO-SnO <sub>2</sub>	300	NO <sub>x</sub> Sensing	—	[353]
22	PVP/DMF	Ni-doped In <sub>2</sub> O <sub>3</sub>	75	Ethanol sensing	—	[354]
23	PVP/DMF	In <sub>2</sub> O <sub>3</sub> -ZnO	60–80	Ethanol sensing	—	[355]
24	PVP	InYbO	75	VOC-DMF	5 ppb	[356]
25	PEO	SnO <sub>2</sub>	—	VOC- tetrahydrocannabinol	0.0008 V ppm <sup>-1</sup>	[357]
26	PMMA	PANI/PMMA	—	Ammonia sensing	10 ppm	[358]
27	t-Boc/PANI	t-Boc/PAN	1.6 ± 0.6 μm	NH <sub>3</sub> sensing	10 ppm	[359]
28	PVA	PVA/ TiO <sub>2</sub>	310 ± 30	LPG sensing	—	[360]
29	PVA	Sn/NiO	—	Triethylamine	—	[361]
30	PPy	PPy/SRGO	—	NH <sub>3</sub> sensing	—	[362]
31	PVP	TiO <sub>2</sub> /PVP	41–281	H <sub>2</sub> Sensing	—	[363]
32	PVP/ EtOH	Co <sub>3</sub> O <sub>4</sub> /PVP NFs	200–400	CO sensing	—	[364]
33	PVA	PVA/Cr(OH) <sub>3</sub>	150–200	Ethanol sensing	—	[365]
34	PVP/DMF	PA6/TiO <sub>2</sub> /PANI	100–300	Ammonia sensing	—	[366]
35	PVP/DMF	SmFeO <sub>3</sub> NFs	70–120	Ethylene glycol	—	[367]
36	PVA	rGO/ZnO	150	NO <sub>2</sub> sensing	—	[368]
37	PVA	rGO/ZnO NFs	190	H <sub>2</sub> sensing	0.1 ppm	[369]
38	PVA	rGO-loaded ZnFe <sub>2</sub> O <sub>4</sub> NFs	50–100	H <sub>2</sub> S sensing	1 ppm	[370]
39	PVA	ZnFe <sub>2</sub> O <sub>4</sub> NFs	30–100	H <sub>2</sub> S Sensing	1 ppm	[371]
40	PVP	PdO <sub>x</sub> @SnO <sub>x</sub>	—	NO <sub>2</sub> sensing	10 ppb	[372]
41	PVP	TiO <sub>2</sub> /SnO <sub>2</sub>	341 ± 29, 206 ± 17	Ethanol sensing	5 ppm	[373]
42	PVP	Pt/ SnO <sub>2</sub> , Au/ SnO <sub>2</sub>	250–350	H <sub>2</sub> S, acetone sensing	0.6, 1.2 ppm	[374]
43	PAN	NiO doped SnO <sub>2</sub>	150–250	H <sub>2</sub> S sensing	—	[375]
44	PVA	CuZnFe <sub>2</sub> O <sub>4</sub>	18 ± 9	H <sub>2</sub> sensing	—	[376]
45	PVA	V <sub>2</sub> O <sub>5</sub> nanowires	80–146	Acetone sensing	—	[377]
46	PVA/PVP	α-Fe <sub>2</sub> O <sub>3</sub> @NiO CSNF	90–180	HCHO sensing	1 ppm	[378]
47	PVP/DMF	Pr-BiFeO <sub>3</sub>	146.7	Formaldehyde sensing	—	[379]
48	PVP/DMF	PdO/CeO <sub>2</sub> NFs	75–85	Methanol sensing	402 ppb	[380]
49	P3HB	SnO <sub>2</sub> /PANI/P3HB	—	Ethanol sensing	50 ppm	[381]
50	PAN	PAN/PANI	—	Trimethylamine sensing	6 ppb	[382]
51	PVA	PVA/WO <sub>3</sub>	—	Acetaldehyde sensing	50 ppb	[383]

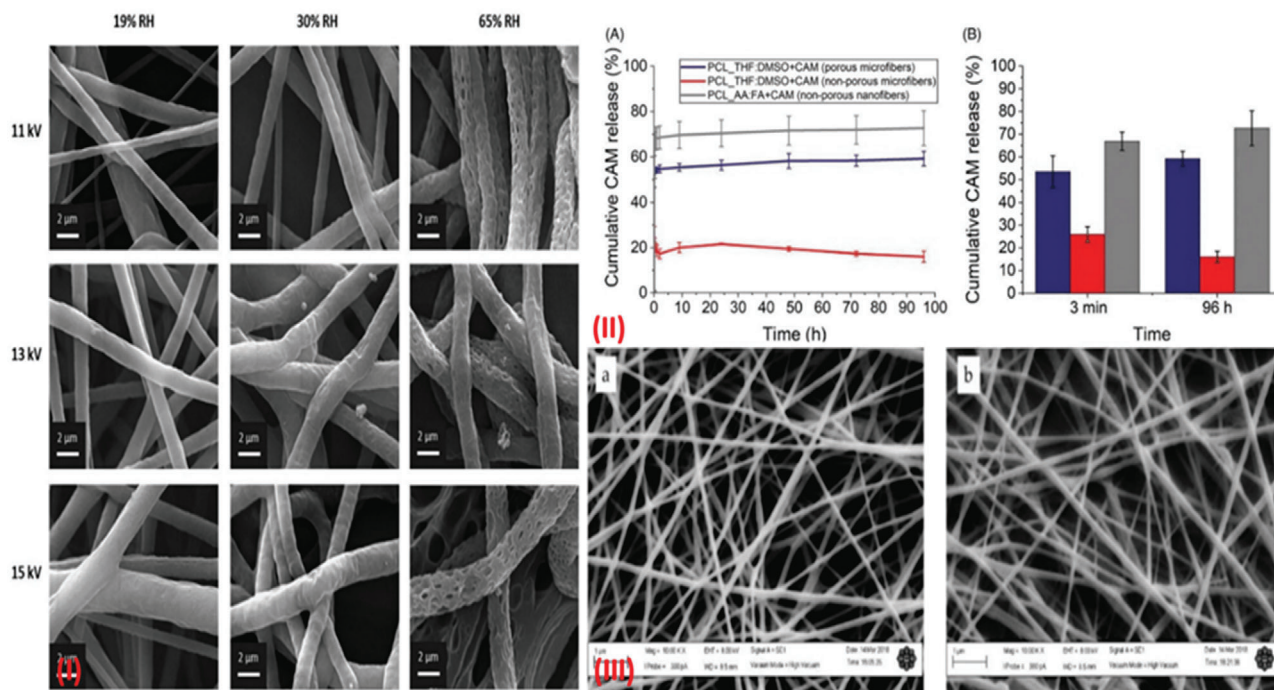


**Figure 7.** (I) SEM images of PCL nanofibers (used THF: DMSO solution) and chloramphenicol (CAM)-loaded PCL nanofibers with different humidity and applied conditions. (II) A) Cumulative drug release activity of CAM-loaded PCL (THF: DMSO) nanofibers in PBS at 37 °C. B) Drug release percentage after releasing the drug in 3 min and 96 h at 37 °C. Reproduced with permission.<sup>[397]</sup> Copyright 2020, Taylor & Francis Group, LLC., (III) a) PCL/ CP electrospun fibers b) gentamicin-loaded collagen/PCL nanofibers (GCP) for the tissue engineering application. Reproduced with permission under the CC-BY 4.0 license.<sup>[433]</sup> Copyright 2018, the Authors. Published by MDPI.

and the importance of the scaffold nanofibers and their crucial role in skin, bone, and nerve tissue engineering with different polymer electrospun nanofiber gives different combinations as per desired application.<sup>[399]</sup> Jian et al. explained that the preparation poly(lactic-co-glycolic acid) (PLGA) as main polymers was added with different weight ration combinations of the drug. Finally, they obtained the nanofibers through spinning by applying a high voltage of 22 kV.<sup>[400]</sup> Moreover, Figure 4d reveals the treatment of prostate cancer with help of PCL/Gelatin with NFs loaded CDDP, and the electrospun nanofiber-based for various biomedical applications are shown in **Table 6**.

## 5.6. Mechanical Sensors

The main object of the nanosensors is to measure the physical, mechanical, and chemical changes associated with markers of interest.<sup>[438]</sup> The sensors (electrical, chemical, optical, physical, and mechanical, etc.) is an exciting and dynamic field of research study at the early stages and make a comprehensive multidisciplinary list of applications in many fields including, environmental, sensors, biomedical, energy (self-powered bio-fuels), particularly disease diagnosis, etc.<sup>[439]</sup> Out of many synthesis methods, electrospinning nanofibers provide a platform to impart more attractive sensing properties, such as improved electrical conductivity, biocompatibility, optical effects, quantum confinement effect, the enhanced surface to volume ratio, high porosity. Nanofibers posed an advanced asset in detecting the high concentration of targets present in the low-density sam-

ples due to their high surface area. Mechanical sensors are the detection system that allows ultrasensitive detection and measures the modifications in the mechanical force at the molecular level.<sup>[440]</sup> They are mainly involved in detecting forces, displacement modification, and mass variations. The added advantage of mechanical sensors is sensitivity to masses. Mechanical sensors can detect the mechanical forces caused by pressure, force, torque, strain, where bending remains a challenge.<sup>[441]</sup> The primary motivation for mechanical sensors are flexible, artificial, self-powered, wearable, electronic, disease detection and diagnosis, and monitoring.<sup>[442]</sup> **Figure 8** indicates the rGO/TPU based strain sensor fabrication and utilization as a human motions detector with different conditions. Jalalian et al. reported the (Na, K)NbO<sub>3</sub> (NKN) based electrospun nanofibers for the polarizable and flexible scaffolds for tissue engineering application based on piezoelectricity. To prepare electrospinning solution, PVP/NKN has been used with the spinning condition of 1.8 kV cm<sup>-1</sup> voltage, flow rate 0.5 mL h<sup>-1</sup>, and 8 cm distance between the collector and the needle tip. After the formation of the fibers, they are annealed at the temperature of 800 °C for 1 h, and the diameter also varied as 350 and 200 nm before and after the calcination at 800 °C as obtained PVP/NKN nanofibers were tested using (PFM) piezoresponse force microscopy technique at low signals. The PVP/NKN showed a polarization of  $P_{max}$  as 21.2  $\mu\text{C cm}^{-2}$  which led to a potential candidate for the polarisable scaffolds for the bioengineering application.<sup>[443]</sup> Singh et al. reported the electrospun PVDF nanofibers with spinning conditions of 15 cm distance between collector and needle tip, a voltage 5 kV, and a flow rate of 2 mL h<sup>-1</sup>. The PVDF showed a diameter of  $184 \pm$

**Table 6.** Electrospun-based biomedical applications.

S.No	Electrospinning material	Sensing material	Diameter [nm]	Application	Property	References
1	PVP	TiO <sub>2</sub> NFs decorated Ti	32–44	Osteosarcoma (MG63) evolution	—	[401]
2	PEG–PLLA	BCNU-loaded PEG–PLLA	690–1350	D.D.S (BCNU)	—	[402]
3	Collagen, Gelatin	PlnDI and heparin-BSA/ Collagen/Gelatin	3–6 μm	T.E ((human osteosarcoma cells)	—	[403]
4	PCL	PGC-C18	2–6 μm 6800–8400	Colorectal cancer (HT-29)	90 days	[404]
5	PHBV, PHBV/CP	PHBV/CP	270–520	Gastric cancer (MKN28)	80% 72 h	
6	PCL	Curcumin/PCL, PCL/aloe, neem/PCL	222–518	Breast cancer (MCF7)	42% 24	[406]
7	PCL	NaGdF <sub>4</sub> :Yb/Er@NaGdF <sub>4</sub> : Yb@mSiO <sub>2</sub> -PEG /DOX	400–600	Lung cancer (A459) Orthotropic cancer	96%	[407]
8	PCL	QCh/-co-PLA/DOX	310–830	Hela cell	100% 48 h	[408]
9	PEO/PLGA	PLGA/PEO	5 ± 1 μm	Tissue engineering (nHDF)	7 days	[409]
10	PLLA	PLLA/Co-I	319 ± 123	Bone T.E. (MG63)	22 days INC	[410]
11	Fibrinogen	Fibrinogen NFs	0.32 6 0.11 mm	T.E. (Cardiac fibroblasts)	2–7 days	[411]
12	PEO/Chiston	PS/HA	300	Prostate cancer (DU145)	24 h	[412]
13	PLLA	PLLA/titanocene dichloride	870–4270	Lung cancer (SPCA-1)	68.2%	[413]
14	PVP/TBT	PVP/TBT/Ti NFs	100–300	Colorectal cancer (HCT116) Gastric cancer (BGC823)	—	[414]
15	PCL	PCL/MgO, PCL–K/MgO	0.2–2.2 μm	Tissue engineering (Keratin)	7 days	[415]
16	PCL/collagen	PCL/collagen NFs	290–340	Tissue engineering (skeletal muscle)	7 days	[416]
17	PVP	GF–nTiO <sub>2</sub>	72	Breast cancer (EGFR2 or ErbB2)	—	[417]
18	PEO	PEO/Keratin	0.90 ± 0.22 μm	Tissue engineering (Keratin)	7 days	[418]
19	Chiston/PCL	TNZ–PCHNF	143.55 ± 8.5	Periodontitis treatment	21 days	[419]
20	PAA/PVA	PAA/PVA/Au NPs	315 ± 90	SERS-4-aminothiophenol	LOD- 10–8 M	[420]
21	PCL/TCN	FTCN: BCD	200–500	Periodontitis treatment	14 days	[421]
22	PLLA	PLLA/DMOG	—	Diabetic wound, chronic wound	97%-15 days NO	[422]
23	Polyurethane	4 (G4) poly- (amidoamine), dendrimers	393	Wound healing	Release-9 h	[423]
24	EVOH	EVOH/graphene	500	Intelligent food packaging	—	[424]
25	PVA/Plur/PEI	PVA–Plur–PEI/TiO <sub>2</sub>	255	Wound dressing	—	[425]
26	PCL	PCL/(cilostazol) CIL NFs	0.77–2.97 μm	Vascular implants	—	[426]
27	PCL	Span 60; PCL; SLS	—	Infection treatment	—	[427]
28	PCL	PCL/GelMA-CEX	280–330	Wound dressing	—	[428]
29	PVA/HA	PVA/HA/CNC NFs	122–222	Wound healing	24 and 48 h	[429]
30	Cs/PVA/nHA	Cs/PVA/nHA/Cu/Ag NFs	500	Wound dressing	24 h	[430]
31	PLA	PLA/PLLA NFs	300	Tissue engineering	—	[431]
32	PLGA/PEO	PLGA/PEO NFs	280 PLGA 760 PEO	Skin tissue engineering	—	[432]
33	Collegen/PCL	Collegen/PCL/ gentamicin	130	Skin tissue engineering	72 h	[433]
34	PLLA/PANi	PLLA/PANI	195 ± 30	Nerve tissue engineering	—	[434]
35	HA/PLGA	HA/PLGA/NFs	266.6 ± 7.3	Bone tissue engineering	7 days	[435]
36	CA/PVP	CA/PVP/MLT	1.7 μm	D.D.S-Melatonin	—	[436]
37	Thiram/HPβCD	Thiram/HPβCD-IC-NF	—	D.D.S-pesticides	—	[437]

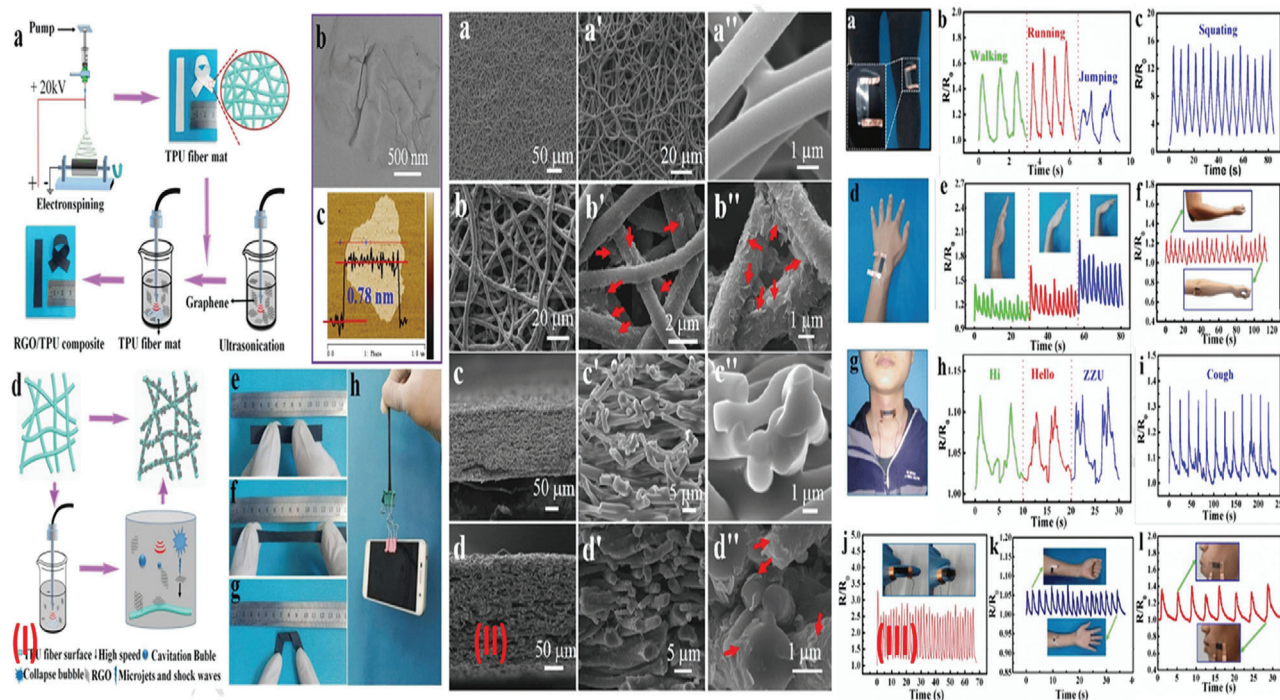


**Figure 8.** (I) a) Schematics of formation of PU/rGO strain sensor b,c) TEM and AFM morphology. d) schematic formation rGO anchored TPU. (e, f, g) rGO/TPU sensor stretching, bending, and twisting conditions. h) images of rGO/TPU stain sensor on the phone. (II) SEM images (a-a'') pure TPU nanofiber mats. (b-b'') images rGO/TPU strain sensor. (c-c'') cross-section of TPU mats. (d-d'') cross-section of rGO/TPU stain sensor. The arrows (red) show the rGO absorbed TPU (III) rGO/TPU based strain sensor to detect human motions. a) Assembly of rGO/TPU sensor on stocking b,c) strain sensor rGO/TPU walking, running, jumping, and squatting responsive. d) Image of rGO/TPU strain sensor attached to the wrist. e) Wrist attached rGO/TPU sensor response. f) rGO/TPU strain sensor cycling bending (under elbow) response. g) Image of strain sensor on the throat. h,i) rGO/TPU strain sensor concerning coughs and speaks Hi, Hello, and ZZU. j-l) Finger, arm, and cheek response of the rGO/TPU strain sensor. Reproduced with permission.<sup>[446]</sup> Copyright 2017, Elsevier Ltd.

96 nm, and strain value was measured, and the tolerance of  $\pm 0.2$  cm is found for the string deflection. The sensitivity of the strain sensor was  $150 \text{ mV } \epsilon^{-1}$  (%), which proves this type of sensor can be used in sports rockets.<sup>[444]</sup> Yuchao et al. described the preparation of polyimide (PI) electrospun nanofibers for the flexible capacitive pressure sensor with a spinning condition of 11 kV high voltage with  $0.45 \text{ mL h}^{-1}$  flow rate. The obtained PI nanofibers showed a high sensitivity of  $2.204 \text{ kPa } 1$  at  $3.5\text{--}4.1 \text{ Pa}$  in the linear range of  $0\text{--}1.388 \text{ MPa}$  with a detection limit of  $3.5 \text{ Pa}$  at a deficient level. These sensing features prove the PI nanofibers can be candidates for health monitoring and robotics (intelligence).<sup>[445]</sup> The electrospun nanofiber based several mechanical sensors are displayed in Table 7.

### 5.7. Resistive Sensors

The change or shift in the electrical resistance when the sensor surface is exposed to the target is referred to as resistive sensors. The electrospun-based nanofibers or nanofibrous membranes have been given more attention due to their features of fast response and recovery time, sensitivity, and stability. Moreover, nanofibrous membranes are formed either by organic, inorganic, or hybrid fibers.<sup>[483]</sup> Modafeeri et al. reported the synthesis of electrospun  $\text{V}_2\text{O}_5$  nanofibers to detect Ammonia using the

resistive sensor. Polyvinyl acetate (PVAC) has been used to synthesize  $\text{PVAC}/\text{V}_2\text{O}_5$  nanofibers with 17 kV applied voltage with collector and needle distance of 14 cm and a flow rate of  $5 \text{ mL h}^{-1}$  conditions obtained, nanofiber was calcinated at  $300\text{--}500 \text{ }^\circ\text{C}$ . The Ammonia molecule reacted with the oxygen molecule on the surface, causing electric resistance and enhancing the sensitivity toward the target gas.  $\text{V}_2\text{O}_5/\text{PVAC}$  used operating voltage between  $200$  and  $250 \text{ }^\circ\text{C}$ , the response and recovery times were  $50$  and  $350 \text{ s}$ , respectively, and the LOD was  $100 \text{ ppb}$ .<sup>[484]</sup> Wang et al. reported the thermoplastic polyurethane (TPU)/rGO electrospun fibrous mats for the flexible electric resistive strain sensor. The TPU/rGO fibers are obtained at a high voltage of  $20 \text{ kV}$ . As obtained, rGO/TPU was tested with the help of two probes and four probe instruments, and mechanical properties were tested with ultrasonication technique, the high specific elongation ( $670 \pm 20$ ) of rGO/TPU was higher itself. The mechanical properties play a role in strain sensors. rGO/TPU showed a reversible strain regime.<sup>[446]</sup> Lee et al. reported the electrospun PEBA (polyether block amide) and coated with PEDOT:PSS and used top and bottom electrodes for the pressure sensor. Primarily PEBA nanofibers were synthesized. PEBA is not conductive, and to make it conductive, PEDOT:PSS was drop cast on the outside electrospun film with time  $10\text{--}100 \text{ min}$ . ITO-PET was used as the counter electrode, and the pressure sensors were fabricated by sandwiching the as obtain thin films between two electrodes.



**Table 7.** Electrospun-based mechanical sensors.

S.No.	Electrospinning material	Sensing material	Diameter [nm]	Application	Property	References
1.	PVDF	PVDF nanofiber	20–800	Piezoelectric force sensor	42 mV N <sup>-1</sup> (S)	[447]
2	PVDF–TrFE	PVDF–TrFE	1.45 ± 0.18 μm	Pressure sensor	—	[448]
3	PVDF–TrFE	PVDF–TrFE/PDMS	520 ± 15	Flexible and stretchable piezoelectric sensor	120 mV μm <sup>-1</sup> (S)	[449]
4	PVDF/BaTiO <sub>3</sub>	PVDF/BaTiO <sub>3</sub>	1–1.2 μm	Piezoelectric pressure tactile sensor	18.0 V N <sup>-1</sup> w(S)	[450]
5	PVDF–TrFE	PVDF–TrFE/PDMS	250 ± 30	Acoustic based biomedical sensors.	11 V Pa <sup>-1</sup>	[451]
6	PVA	PEDOT:PSS–PVA	250	Ultrahigh-strain sensors	—	[452]
7	PVDF–TrFE	P(VDF–TrFE)/ PDMS/MWCNT	200 ± 20	TENG Nanogenerators for wearable's	1.98 mW cm <sup>-3</sup> (PD)	[453]
	PVDF–TrFE	P(VDF–TrFE)/ PDMS/MWCNT	200 ± 20	PENG Nanogenerators for wearable's	0.689 mW cm <sup>-3</sup> (PD)	[453]
8	PVDF–HFP	PVDF–HFP/ PEDOT NFs	480 ± 34	Pressure sensor	13.5 kPa <sup>-1</sup> (S)	[454]
9	PVDF	CNF/PEI aerogel/PVDF NFs	15–110	TENG-self-powered sensor	13.3 W m <sup>-2</sup> (PD)	[455]
10	PVDF	PVDF/Nylon	550–790	TENG–Self powdered UV detectors	26.6 W m <sup>-2</sup> (PD)	[456]
11	PU/PANi	PANi/PU mats	100–200	Strain sensors-in wearable's and robotics	0.75, curvature = 0.4 cm <sup>-1</sup>	[457]
12	PVDF/MWCNTs	PVDF/MWCNTs/OMMT	200–300	PENG Nanogenerators	10.9 mV N <sup>-1</sup> (S)	[458]
					—	
13	PVDF/CNT	PVDF/CNT	130–160	Piezoelectric sound absorber	—	[459]
14	PVDF/PPY	PVDF/PPY mats	450–860	Pressure sensor	—	[460]
15	(P(VDF–TrFE)	BaTiO <sub>3</sub> /P(VDF–TrFE)	525 ± 126	Energy harvesting for self-monitoring	—	[461]
16	PAN/PI	PAN/PI/CNFs	400 nm	Tactile pressure sensor	—	[462]
17	CA	CA/rGO	—	Strain sensors	—	[463]
18	TPU	TPU/Ti <sub>3</sub> C <sub>2</sub> Tx	—	Strain sensors	70%	[464]
19	TPU	TPUEM/CNTs/AgNPs	1.67 μm	Human motion detection-strain sensor	7066	[465]
20	PANI/PVDF	PANI/PVDF NFs	—	Detect the pressure and finger	22%	[466]
21	PVDF–TrFE	P(VDF–TrFE) (shell)-PVP/PEDOT: PSS (core) nanofibers	1 μm	Energy harvesting for self-monitoring	4000 μV mmH <sup>-1</sup>	[467]
22	PVDF	PVDF/AuNPs	324 ± 18	Piezoelectric scaffold for nerve tissue engineering	—	[468]
23	PVDF	PVDF/(POSS–EGCG)	936 ± 223 to 1094 ± 394	Piezoelectric scaffold for nerve tissue engineering	—	[469]
24	P(VDF–TrFE)	P(VDF–TrFE)	575 ± 139	Piezoelectric cardiovascular tissues using stem cells	Tensile strength: 21.42 MPa	[470]
25	P(VDF–TrFE)	P(VDF–TrFE)	—	Flexible nanogenerators and nanopressure sensors	—	[471]
26	PVDF	PVDF	332	Piezoelectric Vibration sensor	—	[472]
27	PDA/TPU	PDA/RGO/TPU	—	Human Motion sensor	—	[473]
28	P(VDF–TrFE)	P(VDF–TrFE)	360	Biosensor	Sensitivity 50 V N <sup>-1</sup>	[474]
29	PU/PVDF	PU/PVDF	1.41 ± 0.32 μm	Piezoelectric-wound healing	d33 = 11.24 ± 1.2 pC N <sup>-1</sup>	[475]
30	P(VDF–TrFE)	P(VDF–TrFE)/ZnO	1035–1227	Scaffolds tissue engineering	—	[476]
31	P(VDF–TrFE)	P(VDF–TrFE)/ 0.78Bi <sub>0.5</sub> Na <sub>0.5</sub> TiO <sub>3</sub> –0.22SrTiO <sub>3</sub>	100–300	Frequency sensor applications	—	[477]
32	P(VDF–TrFE)	P(VDF–TrFE)/rGO	—	Piezoresistive pressure sensors	15.6 kPa <sup>-1</sup> (S)	[478]
33	PVDF	PVDF/Ag Nanowires	100–300	Force sensors	—	[479]
34	PVDF	PVDF/BaTiO <sub>3</sub> NPs	200	Wearable smart textiles and implantable biosensors	—	[480]
35	PVDF	PVDF	200 ± 96	Skeletal muscle tissue engineering (muscle regeneration)	—	[481]

When the pressure is applied, there is the shift between the electrospun mat and electrodes that produce the sensitive current and can be observed with the broadband of pressure and tunable sensitivity.<sup>[485]</sup>

### 5.8. Photoelectric Sensors

Photoelectric sensors are a device used as the light transmitter (infrared) to determine an object's absence, presence, and distance. In general, photoelectric sensors contain both optics along electronics. Lue et al. reported the synthesis and characterization of TiO<sub>2</sub>/PPy (using PVP) coaxial nanocable using electrospinning route with parameters of 10 kV applied voltage, 15 cm distance between tip and collector with a flow rate of 0.1 mL h<sup>-1</sup>. As prepared PPy/TiO<sub>2</sub>, the conductive property of PPy and photoelectric property of TiO<sub>2</sub> make a better combination and can be applied in photoelectric transformation.<sup>[486]</sup> Shi and co-workers reported the synthesis of PVP, TEOS, and SiO<sub>2</sub> electrospun nanofibers and embedded them with Au NPs through the electrospinning method. As prepared, SiO<sub>2</sub>/Au NPs showed surface plasmon response at 550 nm, which is the absorption band of the gold nanoparticles, whereas pure silicon showed no electric response. However, the combination of SiO<sub>2</sub>/Au NPs can make the potential applications in optoelectronics as optical switches.<sup>[487]</sup> Hee et al. reported the versatile photoelectric material ZnO and PVDF-TrEF electrospun nanofibers film for the effective photodetector application.<sup>[488]</sup> Reddy et al. Reported the electrospun synthesis of NiO/Si self-powered photoelectric sensor for the photodetection application. P-NiO nanowires were directly deposited on the n-Si through the electrospinning technique. The diameter of NiO/Si nanowires was around 60–75 nm, as showed by FESEM. As obtained, P-NiO/n-Si showed a photoelectric responsibility of 9.1 mA W<sup>-1</sup>.<sup>[489]</sup> Pan and co-workers reported the synthesis of GaN electrospun nanofibers. Pan also compared the photoconductance of GaN nanowires and electrospun GaN nanofibers; GaN nanofiber showed 830 times higher photoconductance than GaN nanowire in the presence of UV light. This is due to the high surface-to-volume ratio of nanofibers.<sup>[490]</sup>

### 5.9. Mass Sensitive Sensor

Mass sensitive sensors work on the principle of a slight change in the mass that creates or forms a readable electric signal. The resultant mass change can be measured as a frequency shift. Mass sensitive change sensor also referred to as QCM (quartz crystal microbalance). Sauerbrey first demonstrated mass change sensitive sensors in 1959, and they described the relation between frequencies to change in mass of quartz. He also mentioned that the change in the mass on the quartz surface is directly proportional to oscillating crystal frequency change.<sup>[491]</sup> Ding et al. reported PAA/PVA nanofiber synthesis through electrospinning and QCM techniques to detect ammonia gas. As synthesized PAA/PVA nanofiber showed a diameter of 100–400 nm. To increase the resistance of PAA/PVA, compound crosslinking treatment has been approached. The concentration of the ammonia tank will affect the detection sensitivity of QCM.<sup>[492]</sup>

Aditya et al. reported the PAN polymer-based QCM for the detection of saffrole. Saffrole is the primary drug produced from the ATS (amphetamine-type stimulant), AMDA (N-methyl-3,4-methylenedioxyamphetamine), also called ecstasy. As obtained, 240 ± 10 nm PAN electrospun nanofibers showed good sensitivity of 4.6 Hz L mg<sup>-1</sup> toward the detection of saffrole. Mohammad et al. described the detection of ethanol sensing using PVP nanofibers through QCM detection. 12% of PVP concentration showed good permeability.<sup>[493]</sup> Wang et al. reported the synthesis of PEI/PVA membranes through electrospinning coated on QCM to detect formaldehyde. The fibers coated QCM was exposed to 10–255 ppm of formaldehyde.<sup>[494]</sup>

### 5.10. Other Sensors

Ultrasensitive sensors based on the electrospun nanofibers are gaining massive demand as sensors in many applications, including medical diagnostics, environmental applications, and many more fields due to extremely long, small-diameter nanofibers and their enlarged surface to volume ratio, high porosity, and easy process of synthesis.<sup>[495]</sup> Surface acoustic wave devices, here the electro spray or electrospinning has been using. Xiuli et al. reported the synthesis of SAW sensor using PVP/LiTaO<sub>3</sub> through electrospinning route to detect H<sub>2</sub> gas, the 58% concentrated PVP solution produced smooth and uniform nanofibers and showed better performance toward H<sub>2</sub> gas.<sup>[496]</sup> Augustine et al. reported the SAW sensor based on the P(VDF-TrFE)/ZnO nanocomposite using electrospinning for the biosensor application of cell proliferation and detect the quality of the cell in the cell culture.<sup>[497]</sup> Besides, chemical sensors also play a key role in environmental protection by detecting harmful gases (hazardous gases, volatile organic compounds (VOCs), hydrocarbons) using nanostructures (nanofibers) through the electrospinning method, and the electrospun nanofibers have been mentioned in Table 5. Another one of the essential fields is food technology, such as the food packing process, enzyme immobilization, where nanofibers can work as nanofood carriers.<sup>[498]</sup> Arkoun et al. reported the synthesis of PEO/chitosan electrospun nanofiber to apply the antibacterial activity of pathogenic (*Staphylococcus aureus*, *Esherichia coli*, and *Listeria innocua*, etc.) linked to food contamination.<sup>[499]</sup> Ghorani et al. reported a review about the synthesis of electrospun nanofibers and their use as nanocarriers and encapsulation for the food sector.<sup>[500]</sup>

## 6. Electrospinning Importance in Sensing Applications

The electrospinning technique is a versatile way for obtaining distinct nanofibers. Since the invention of nanotechnology, nanomaterials with different morphology plays a significant role in the research community with many applications, including material science, biomedical, energy, sensing, and environmental applications.<sup>[501,502]</sup> Many methods have been used to synthesize nanostructures, including sol-gel, hydrothermal, coprecipitation, self-assembly, template synthesis, and electrospinning. Many routes have been utilized to obtain the desired structure, in which electrospinning is the facile route to obtain the

nanofibers and nanofibrous mats.<sup>[503]</sup> Furthermore, the electrospinning method has the unique assets of high surface volume ratio, better porosity, tunable conductivity, and flexibility.

Additionally, it is a simple and economical lab setup procedure.<sup>[86]</sup> The morphology of the electrospun nanofibers can be controlled using the spinning parameters of the applied voltage, the distance between the needle tip and collector, flow rate, collector's morphology, solvent choice, conductivity, viscosity, molecular weight, temperature, and humidity.<sup>[92]</sup> Moreover, fabricated electrospun nanofibers with different material interfaces, including metals, oxides of metals, carbon-based materials, advanced materials, polymers, and biodegradable biopolymers, can avoid agglomeration enhances the electron-transport and electron transfer kinetics, enhancing their performance in sensing and biosensing. Electrospinning is one of the most emergent routes to synthesis electrospun nanofibers in the field of scaffolds of nerve, skin, and bone tissue engineering, antibacterial wound dressing, and healing, drug delivery systems,<sup>[425–437]</sup> and biosensing of glucose, dopamine, ascorbic acid, H<sub>2</sub>O<sub>2</sub>, etc.

## 7. Conclusions, Challenges, and Future Trends

Over the past two decades, the versatile electrospinning technique for the synthesis and development of nanofibers, nanofibrous mats, scaffolds are one of the simple, cost-effective, unique, and eco-friendly methods and widely used in various applications including sensing(bio), biomedical, optical, chemical, ultrasensitive sensors, made with a better understanding of the electrospinning principle and better control of the nanofiber material. A wide variety of polymer, copolymers, synthetic polymers, and composites (metals, metal oxides, 2D materials, and carbon-based materials) have been blended into the electrospinning method to get the nanofibers with optimal conditions. The factors that affect the morphology of the nanofibers are solution parameters (concentration of the solution, viscosity, solvent volatility, molecular weight, etc.), electrospinning parameters (applied voltage, distance between the collector and needle tip, flow rate of solution, and morphology of collectors) temperature and humidity effects. Notable examples of biosensing (glucose, dopamine, H<sub>2</sub>O<sub>2</sub>, ascorbic acid, etc.), water treatment, biomedical applications including, drug delivery system, tissue engineering (bone, skin, and nerve), mechanical applications of energy harvesters in the form of biofuel cells or self-powered wearable sensors, color-changing the property of colorimetric sensors, photoresistive sensors, and quartz crystal microbalance-based sensors owing to unique properties of high surface volume ratio, better porosity, mechanical properties, stacking of functional groups, alignment, biocompatibility, and biodegradability. Therefore, based on the properties mentioned above electrospinning technique plays a vital role in many applications especially sensing and biomedical tissue engineering applications. However, despite having excellent properties, slight instability in the poor infiltration of cells into electrospun scaffolds and the low yield of the product are significant drawbacks of the electrospinning route.

On the other hand, the leading electrospinning parameter of high voltage can cause dangers to human resources and is not suitable for biomolecules. However, progress has been made to overcome the challenges of large-scale or large volume production, functionality and diversity enhancement of the electrospun

nanofibers, environmental concern, and enhancement in cell infiltration ability make them 3D scaffolds. Future trends to obtain the nanofibers electrospinning set can be needleless or multineedle hold great production challenge, solving the environmental issues and safety matters in solvent evaporation during the spinning process: solvent recovery systems or green chemistry techniques for melt electrospinning.

## Acknowledgements

This publication was supported by Qatar University Internal Grant No. IRCC-2020-013, respectively. The findings achieved herein are solely the responsibility of the authors. This work also collaborated with DST-SERB (file no. EEQ/2020/000158), CNST, IST, JNTU Hyderabad. Open Access funding was provided by the Qatar National Library.

## Conflict of Interest

The authors declare no conflict of interest.

## Keywords

electrospun nanofibers, polymers, sensors, synthetic polymers

Received: June 7, 2021

Revised: August 6, 2021

Published online: September 16, 2021

- [1] C. Yonzon, D. A. Stuart, X. Zhang, A. D. McFarland, C. L. Haynes, R. P. Van Duyne, *Talanta* **2005**, 67, 438.
- [2] Y. Cui, *Science* **2001**, 293, 1289.
- [3] E. Bakker, M. Telting-Diaz, *Anal. Chem.* **2002**, 74, 2781.
- [4] J. Janata, A. Bezegh, *Anal. Chem.* **1988**, 60, 62.
- [5] K. Vijay Vardan, C. Lin Feng, *Nanomedicine: Design and Applications of Magnetic Nanomaterials, Nanosensors and Nanosystems*, John Wiley & Sons, Chichester, UK **2008**, p. 175.
- [6] J. Riu, A. Maroto, F. Rius, *Talanta* **2006**, 69, 288.
- [7] P. J. Vikesland, *Nat. Nanotechnol.* **2018**, 13, 651.
- [8] R. Sha, T. K. Bhattacharyya, *Electrochim. Acta* **2020**, 349, 136370.
- [9] B. Din, X. Wang, J. Yu, *Electrospinning: Nanofabrication and Applications*, Elsevier, New York **2019**, p. 832.
- [10] B. Kannan, H. Cha, I. C. Hosie, *Nano-Size Polymers*, Springer, Cham **2016**, p. 309.
- [11] H. S. Salehuddin, E. N. Mohamad, W. N. L. Mahadi, A. Muhammad Afifi, *Mater. Manuf. Processes* **2018**, 33, 479.
- [12] H. M. Ibrahim, A. Klingner, *Polym. Test.* **2020**, 90, 106647.
- [13] *Regenerated Cellulose Fibres* (Ed: C. Woodings), Woodhead Publishing, Cambridge, **2004**.
- [14] M. Andersson, Q. Jia, A. Abella, X.-Y. Lee, M. Landreh, P. Purhonen, H. Hebert, M. Tenje, C. V. Robinson, Q. Meng, G. R. Plaza, J. Johansson, A. Rising, *Nat. Chem. Biol.* **2017**, 13, 262.
- [15] F. Vollrath, D. P. Knight, *Nature* **2001**, 410, 541.
- [16] S. Kumar, V. B. Gupta, *Manufactured Fibre Technology*, Springer, Dordrecht **1997**.
- [17] A. Valizadeh, S. Mussa Farkhani, *IET Nanobiotechnol.* **2014**, 8, 83.
- [18] W. Gilbert, *On the Magnet*, Chiswick Press, London **1600**.
- [19] R. Hooke, *1665 Micrographia*, Royal Society, London **2003**.
- [20] W. Gilbert, P. F. Mottelay, *De Magnete*, Dover Publications, New York **1991**.

- [21] G. Stephen, *Philos. Trans. R. Soc. London* **1731**, 37, 227.
- [22] G. M. Bose, *Die Electricität nach ihrer Entdeckung und Fortgang mit poetischer Feder entworfen*, Joh. Joacjim Ahlfelden, Wittenberg **1744**.
- [23] J. A. Nollet, *Philos. Trans. R. Soc. London* **1748**, 45, 187.
- [24] L. Rayleigh, *London, Edinburgh Dublin Philos. Mag. J. Sci.* **1882**, 14, 184.
- [25] JAF Plateau, *Statique Expérimentale et Théorique des Liquides Soumis aux Seules Forces Moléculaires*, Gautheir-Villars, Paris **1873**, p. 485.
- [26] R. Lord, *Proc. London Math. Soc.* **1878**, 10, 4
- [27] J. W. Strutt, *Proc. R. Soc. Lond.* **1879**, 29, 71.
- [28] J. W. Strutt, *Proc. R. Soc. London* **1879**, 28, 405.
- [29] R. R. Mather, *Manufactured Fibre Technology*, Chapman and Hall, New York **1997**.
- [30] C. J. Luo, S. D. Stoyanov, E. Stride, E. Pelan, M. Edirisinghe, *Chem. Soc. Rev.* **2012**, 41, 4708.
- [31] C. V. Boys, *Proc. Phys. Soc. London* **1887**, 9, 8.
- [32] Anon, The X-ray medicine, The New York Times, **1896**.
- [33] Anon, The historical company, **1897**.
- [34] J. F. Cooley, United Kingdom Patent, **1900**, 6385, 19.
- [35] J. F. Cooley, Apparatus for Electrically Dispersing Fluids, *US Patent 692631A*, **1902**
- [36] W. J. Morton, Method of Dispersing Fluid, *US Patent. 705691*, **1902**
- [37] Anon, Calandar of the Imperial University of Kyoto, **1905**.
- [38] E. F. Burton, W. B. Wiegand, *London, Edinburgh Dublin Philos. Mag. J. Sci.* **1912**, 23, 148.
- [39] J. Zeleny, *Phys. Rev.* **1907**, 25, 305.
- [40] J. Zeleny, *Phys. Rev.* **1908**, 26, 448.
- [41] J. Zeleny, *Phys. Rev.* **1908**, 26, 129.
- [42] J. Zeleny, *Phys. Rev.* **1914**, 3, 69.
- [43] J. Zeleny, **1915**, 18, 71.
- [44] J. Zeleny, *Phys. Rev.* **1917**, 10, 1.
- [45] J. Zeleny, *Phys. Rev.* **1920**, 16, 102.
- [46] K. Hagiwara, *J. Jpn. Soc. Mech. Eng.* **1924**, 22, 27.
- [47] K. Hagiwara, *Canada Patent 271440*, **1927**.
- [48] K. Hagiwara, *Canada Patent 293884*, **1927**.
- [49] H. Kiyohiko, *US Patent 1699615*, **1929**.
- [50] W. Macky, *N. Z. J. Sci. Technol.* **1930**, 19, 193.
- [51] W. Macky, *Proc. R. Soc. London, Ser. A* **1931**, 133, 565.
- [52] A. Formhals, US Patent 1,975,504, **1934**.
- [53] A. Formhals, US Patent and Trademark Office **1944**.
- [54] B. Vonnegut, R. L. Neubauer, *J. Colloid Sci.* **1952**, 7, 616.
- [55] V. G. Drozin, *J. Colloid Sci.* **1955**, 10, 158.
- [56] G. I. Taylor, *Proc. R. Soc. London, Ser. A* **1964**, 280, 383.
- [57] G. I. Taylor, *Proc. R. Soc. London, Ser. A* **1966**, 291, 145.
- [58] G. I. Taylor, *Proc. R. Soc. London, Ser. A* **1969**, 313, 453.
- [59] J. R. Melcher, E. P. Warren, *J. Fluid Mech.* **1971**, 47, 127.
- [60] E. T. Layton, *Technology and Culture*, Johns Hopkins University Press, Baltimore, MD **1974**, p. 31.
- [61] G. E. Martin, I. D. Cockshott, F. J. T. Fildes, US Patent 4044404, **1977**.
- [62] D. H. Reneker, A. L. Yarin, H. Fong, S. Koombhongse, *J. Appl. Phys.* **2000**, 87, 4531.
- [63] Y. M. Shin, M. M. Hohman, M. P. Brenner, G. C. Rutledge, *Polymer* **2001**, 42, 09955.
- [64] A. L. Yarin, S. Koombhongse, D. H. Reneker, *J. Appl. Phys.* **2001**, 89, 3018.
- [65] M. M. Hohman, M. Shin, G. Rutledge, M. P. Brenner, *Phys. Fluids* **2001**, 13, 2201.
- [66] M. M. Hohman, M. Shin, G. Rutledge, M. P. Brenner, *Phys. Fluids* **2001**, 13, 2221.
- [67] Y. M. Shin, M. M. Hohman, M. P. Brenner, G. C. Rutledge, *Appl. Phys. Lett.* **2001**, 78, 1149.
- [68] H. Dai, J. Gong, H. Kim, D. Lee, *Nanotechnology* **2002**, 13, 674.
- [69] G. Larsen, R. Velarde-Ortiz, K. Minchow, A. Barrero, I. G. Loscertales, *J. Am. Chem. Soc.* **2003**, 125, 1154.
- [70] J.-S. Park, *Adv. Nat. Sci. Nanosci. Nanotechnol.* **2011**, 1, 043002.
- [71] M. Mirjalili, S. Zohoori, *J. Nanostruct. Chem.* **2016**, 6, 207.
- [72] Md. M Hasan, A. K. M. M. Alam, K. Abu Nayem, *ESJ* **2014**, 10, 265.
- [73] P. K. Panda, *Trans. Indian Ceram. Soc.* **2007**, 66, 65.
- [74] S. T. Aruna, L. S. Balaji, S. S. Kumar, B. S. Prakash, *Renewable Sustainable Energy Rev.* **2017**, 67, 673.
- [75] I. S. Chronakis, *J. Mater. Process. Technol.* **2005**, 167, 283.
- [76] J. Xue, J. Xie, W. Liu, Y. Xia, *Acc. Chem. Res.* **2017**, 50, 1976.
- [77] S. Park, K. Park, H. Yoon, J. Son, T. Min, G. Kim, *Polym. Int.* **2007**, 56, 1361.
- [78] Y.-Z. Long, X. Yan, X.-X. Wang, J. Zhang, M. Yu, *Electrospinning: Nanofabrication and Applications*, Elsevier, New York **2019**, p. 21.
- [79] S. De Vrieze, T. Van Camp, A. Nelvig, B. Hagström, P. Westbroek, K. De Clerck, *J. Mater. Sci.* **2009**, 44, 1357.
- [80] V. Beachley, X. Wen, *Mater. Sci. Eng. C* **2009**, 29, 663.
- [81] D. H. Reneker, A. L. Yarin, *Polymer* **2008**, 49, 2387.
- [82] Y. Peng, Y. Dong, H. Fan, P. Chen, Z. Li, Q. Jiang, *Desalination* **2013**, 316, 53.
- [83] E. Kijeńska, M. P. Prabhakaran, W. Swieszkowski, K. J. Kurzydowski, S. Ramakrishna, *J. Biomed. Mater. Res.* **2012**, 100B, 1093.
- [84] C. Feng, K. C. Khulbe, T. Matsuura, S. Tabe, A. F. Ismail, *Sep. Purif. Technol.* **2013**, 102, 118.
- [85] B. Ostrowska, J. Jaroszewicz, E. Zaczynska, W. Tomaszewski, W. Swieszkowski, K. J. Kurzydowski, *Bull. Polish Acad. Sci. Tech. Sci.* **2014**, 62, 551.
- [86] A. Haider, S. Haider, I.-K. Kang, *Arabian J. Chem.* **2018**, 11, 1165.
- [87] M. J. Laudenslager, W. M. Sigmund, *Encyclopedia of Nanotechnology*, Springer, New York **2012**, p. 769.
- [88] J. M. Deitzel, J. Kleinmeyer, D. Harris, N. C. Beck Tan, *Polymer* **2001**, 42, 261.
- [89] T. Mazoochi, M. Hamadani, M. Ahmadi, V. Jabbari, *Int. J. Ind. Chem.* **2012**, 3, 2.
- [90] K. P. Matabola, R. M. Moutloali, *J. Mater. Sci.* **2013**, 48, 5475.
- [91] L. A. Bosworth, S. Downes, *J. Polym. Environ.* **2012**, 20, 879.
- [92] E. Adomaviciute, S. Stanys, *Fibres Text. East. Eur.* **2011**, 19, 34.
- [93] S. Megelski, J. S. Stephens, D. B. Chase, J. F. Rabolt, *Macromolecules* **2002**, 35, 8456.
- [94] C. Gao, L. Zhang, J. Wang, M. Jin, Q. Tang, Z. Chen, Y. Cheng, R. Yang, G. Zhao, *J. Mater. Chem. B* **2021**, 9, 3106.
- [95] A. Baji, Y.-W. Mai, S.-C. Wong, M. Abtahi, P. Chen, *Compos. Sci. Technol.* **2010**, 70, 703.
- [96] C. J. Angammana, S. H. Jayaram, *Part. Sci. Technol.* **2016**, 34, 72.
- [97] L. Buttafoco, N. G. Kolkman, P. Engbers-Buijtenhuijs, A. A. Poot, P. J. Dijkstra, I. Vermes, J. Feijen, *Biomaterials* **2006**, 27, 724.
- [98] H. Fong, I. Chun, D. H. Reneker, *Polymer* **1999**, 40, 4585.
- [99] L. H. Sperling, *Introduction to Physical Polymer Science*, Wiley, Hoboken, NJ **2005**.
- [100] S. Zhao, X. Wu, L. Wang, Y. Huang, *J. Appl. Polym. Sci.* **2004**, 91, 242.
- [101] K. H. Lee, H. Y. Kim, H. J. Bang, Y. H. Jung, S. G. Lee, *Polymer* **2003**, 44, 4029.
- [102] X. Zong, K. Kim, D. Fang, S. Ran, B. S. Hsiao, B. Chu, *Polymer* **2002**, 43, 4403.
- [103] J. Du, X. Zhang, *J. Appl. Polym. Sci.* **2008**, 109, 2935.
- [104] J. S. Choi, S. W. Lee, L. Jeong, S.-H. Bae, B. C. Min, J. H. Youk, W. H. Park, *Int. J. Biol. Macromol.* **2004**, 34, 249.
- [105] A. Jaworek, A. Krupa, M. Lackowski, A. T. Sobczyk, T. Czech, S. Ramakrishna, S. Sundarajan, D. Pliszka, *Fibres Text. East. Eur.* **2009**, 17, 77.
- [106] T. Jarusuwanapoom, W. Hongrojjanawiwat, S. Jitjaicham, L. Wannatong, M. Nithitanakul, C. Pattamaprom, P. Koombhongse, R. Rangkupan, P. Supaphol, *Eur. Polym. J.* **2005**, 1, 409.
- [107] D. Aussawasathien, J.-H. Dong, L. Dai, *Synth. Met.* **2005**, 154, 37.
- [108] J.-A. Park, J. Moon, S.-J. Lee, S.-C. Lim, T. Zyung, *Curr. Appl. Phys.* **2009**, 9, S210.

- [109] J. Wang, H.-B. Yao, D. He, C.-L. Zhang, S.-H. Yu, *ACS Appl. Mater. Interfaces* **2012**, *4*, 1963.
- [110] Y. Bao, C. Lai, Z. Zhu, H. Fong, C. Jiang, *RSC Adv.* **2013**, *3*, 8998.
- [111] A. Baji, Y.-W. Mai, Q. Li, Y. Liu, *Compos. Sci. Technol.* **2011**, *71*, 1435.
- [112] F. Mokhtari, M. Latifi, M. Shamsirsaz, M. Khelghatdoost, S. Rahmani, *J. Text. Inst.* **2017**, *108*, 1917.
- [113] Y. Zhao, Z. Fan, M. Shen, X. Shi, *Adv. Mater. Interfaces* **2015**, *2*, 1500256.
- [114] Y. Shang, Y. Si, A. Raza, L. Yang, X. Mao, B. Ding, J. Yu, *Nanoscale* **2012**, *4*, 7847.
- [115] C. Ribeiro, D. M. Correia, I. Rodrigues, L. Guardão, S. Guimarães, R. Soares, S. Lanceros-Méndez, *Mater. Lett.* **2017**, *209*, 118.
- [116] Z. H. Liu, C. T. Pan, C. K. Yen, L. W. Lin, J. C. Huang, C. A. Ke, *Appl. Surf. Sci.* **2015**, *346*, 291.
- [117] Y.-J. Kim, H.-I. Bae, O. K. Kwon, M.-S. Choi, *Int. J. Biol. Macromol.* **2009**, *45*, 65.
- [118] A. I. Gopalan, K.-P. Lee, K. M. Manesh, P. Santhosh, J. H. Kim, J. S. Kang, *Talanta* **2007**, *71*, 1774.
- [119] Y. Liu, Y. Ding, Y. Zhang, Y. Lei, *Sens. Actuators, B* **2012**, *171–172*, 954.
- [120] S. Raj, D. R. Shankaran, *Sens. Actuators, B* **2016**, *226*, 318.
- [121] H. Zhang, M. Cao, W. Wu, H. Xu, S. Cheng, L.-J. Fan, *Nanoscale* **2015**, *7*, 1374.
- [122] S. Demiroğlu Mustafov, A. K. Mohanty, M. Misra, M. Ö. Seydibeyoğlu, *Carbon* **2019**, *147*, 262.
- [123] C. Mit-Uppatham, M. Nithitanakul, P. Supaphol, *Macromol. Symp.* **2004**, *216*, 293.
- [124] N. A. Yuya, W. Kai, B. S. Kim, I. S. Kim, *J. Mater. Sci. Eng. Adv. Technol.* **2010**, *2*, 97.
- [125] H. Icoğlu, R. Oğulata, *EKSTIL VE KONFEKSIYON* **2013**, *23*, 313.
- [126] W. Peng, D. Tang, *Front. Bioeng. Biotechnol.* **2016**, *10*, 9.
- [127] J. Yoon, H.-S. Yang, B.-S. Lee, W.-R. Yu, *Adv. Mater.* **2018**, *30*, 1704765.
- [128] D. He, B. Hu, Q.-F. Yao, K. Wang, S.-H. Yu, *ACS Nano* **2009**, *3*, 3993.
- [129] H. Wu, R. Zhang, X. Liu, D. Lin, W. Pan, *Chem. Mater.* **2007**, *19*, 3506.
- [130] W.-J. Jin, H. K. Lee, E. H. Jeong, W. H. Park, J. H. Youk, *Macromol. Rapid Commun.* **2005**, *26*, 1903.
- [131] Q. B. Yang, D. M. Li, Y. L. Hong, Z. Y. Li, C. Wang, S. L. Qiu, Y. Wei, *Synth. Met.* **2003**, *137*, 973.
- [132] W. K. Son, J. H. Youk, T. S. Lee, W. H. Park, *Macromol. Rapid Commun.* **2004**, *25*, 1632.
- [133] H. K. Lee, E. H. Jeong, C. K. Baek, J. H. Youk, *Mater. Lett.* **2005**, *59*, 2977.
- [134] G.-M. Kim, A. Wutzler, H.-J. Radosch, G. H. Michler, P. Simon, R. A. Sperling, W. J. Parak, *Chem. Mater.* **2005**, *17*, 4949.
- [135] K. Wei, H.-R. Kim, B.-S. Kim, I.-S. Kim, *Nanofibers – Production, Properties and Functional Applications*, IntechOpen, London **2011**.
- [136] K. Mondal, A. Sharma, *RSC Adv.* **2016**, *6*, 94595.
- [137] A. Mirzaei, S. G. Leonardi, G. Neri, *Ceram. Int.* **2016**, *42*, 15119.
- [138] J.-Y. Chen, C.-C. Kuo, C.-S. Lai, W.-C. Chen, H.-L. Chen, *Macromolecules* **2011**, *44*, 2883.
- [139] Q. Hu, Z. Wang, X. Huang, Y. Qin, H. Yang, X. Ren, Q. Zhang, J. Liu, C. He, *Energy Environ. Sci.* **2020**, *13*, 5097.
- [140] H. Wu, W. Pan, *J. Am. Ceram. Soc.* **2006**, *89*, 699.
- [141] Z. U. Abideen, J.-H. Kim, J.-H. Lee, J.-Y. Kim, A. Mirzaei, H. W. Kim, S. S. Kim, *J. Korean Ceram. Soc.* **2017**, *54*, 366.
- [142] X. Liang, T.-H. Kim, J.-W. Yoon, C.-H. Kwak, J.-H. Lee, *Sens. Actuators, B* **2015**, *209*, 934.
- [143] N. More, D. Ranglani, S. Khariche, G. Kapusetti, *J. Appl. Polym. Sci.* **2020**, *137*, 49426.
- [144] H. F. Alharbi, M. Y. Haddad, M. O. Aijaz, A. K. Assaifan, M. R. Karim, *Coatings* **2020**, *10*, 285.
- [145] S. Tripathy, S. R. Krishna Vanjari, V. Singh, S. Swaminathan, S. G. Singh, *Biosens. Bioelectron.* **2017**, *90*, 378.
- [146] K. S. Novoselov, V. I. Fal'Ko, L. Colombo, P. R. Gellert, M. G. Schwab, K. Kim, *Nature* **2012**, *490*, 192.
- [147] F. Meng, W. Lu, Q. Li, J.-H. Byun, Y. Oh, T.-W. Chou, *Adv. Mater.* **2015**, *27*, 5113.
- [148] G. Sun, L. Sun, H. Xie, J. Liu, *Nanomaterials* **2016**, *6*, 129.
- [149] J. J. Grant, S. C. Pillai, S. Hehir, M. McAfee, A. Breen, *ACS Biomater. Sci. Eng.* **2021**, *7*, 1278.
- [150] M. H. Chakrabarti, C. T. J. Low, N. P. Brandon, V. Yufit, M. A. Hashim, M. F. Irfan, J. Akhtar, E. Ruiz-Trejo, M. A. Hussain, *Electrochim. Acta* **2013**, *107*, 425.
- [151] Y. Wang, J. Tang, S. Xie, J. Liu, Z. Xin, X. Liu, L. A. Belfiore, *RSC Adv.* **2015**, *5*, 42174.
- [152] B. Bera, D. Mandal, M. D. Sarkar, *Imp. J. Interdiscip. Res.* **2016**, *2*, 1411.
- [153] A. Moayeri, A. Aji, *Synth. Met.* **2015**, *200*, 7.
- [154] E. Chiesa, R. Dorati, S. Pisani, G. Bruni, L. G. Rizzi, B. Conti, T. Modena, I. Genta, *Polymers* **2020**, *12*, 1390.
- [155] R. Thangappan, S. Kalaiselvam, A. Elayaperumal, R. Jayavel, *Solid State Ionics* **2014**, *268*, 321.
- [156] D. J. Late, A. Bhat, C. S. Rout, *Fundamentals and Sensing Applications of 2D Materials*, Elsevier, New York **2019**, p. 5.
- [157] P. Miró, M. Audiffred, T. Heine, *Chem. Soc. Rev.* **2014**, *43*, 6537.
- [158] Y. Chen, C. Tan, H. Zhang, L. Wang, *Chem. Soc. Rev.* **2015**, *44*, 2681.
- [159] G. Fiori, F. Bonaccorso, G. Iannaccone, T. Palacios, D. Neumaier, A. Seabaugh, S. K. Banerjee, L. Colombo, *Nat. Nanotechnol.* **2014**, *9*, 768.
- [160] P. V. Shinde, M. K. Singh, *Fundamentals and Sensing Applications of 2D Materials*, Elsevier, New York **2019**, p. 91.
- [161] A. S. Levitt, M. Alhabeb, C. B. Hatter, A. Sarycheva, G. Dion, Y. Gogotsi, *J. Mater. Chem. A* **2019**, *7*, 269.
- [162] P. Sobolčiak, A. Ali, M. K. Hassan, M. I. Helal, A. Tanvir, A. Popelka, M. A. Al-Maadeed, I. Krupa, K. A. Mahmoud, *PLoS One* **2017**, *12*, e0183705.
- [163] J. Zhao, P. Zhang, J. Fan, J. Hu, G. Shao, *Appl. Surf. Sci.* **2018**, *430*, 466.
- [164] M. Qianwen, D. Yaping, L. Li, W. Anqing, D. Dingding, Z. Yijun, *J. Electroanal. Chem.* **2019**, *833*, 297.
- [165] R. Huang, X. Chen, Y. Dong, X. Zhang, Y. Wei, Z. Yang, W. Li, Y. Guo, J. Liu, Z. Yang, H. Wang, L. Jin, *ACS Appl. Bio. Mater.* **2020**, *3*, 2125.
- [166] T. S. Kang, S. W. Lee, J. Joo, J. Y. Lee, *Synth. Met.* **2005**, *153*, 61.
- [167] A. Kakoria, S. Sinha-Ray, *Fibers* **2018**, *6*, 45.
- [168] B. Sun, Y.-Z. Long, S.-L. Liu, Y.-Y. Huang, J. Ma, H.-D. Zhang, G. Shen, S. Xu, *Nanoscale* **2013**, *5*, 7041.
- [169] K. Puttananjegowda, A. Takshi, S. Thomas, *IEEE Sens. Lett.* **2020**, *4*, 4500204.
- [170] P. Zhan, W. Zhai, N. Wang, X. Wei, G. Zheng, K. Dai, C. Liu, C. Shen, *Mater. Lett.* **2019**, *236*, 60.
- [171] F. Zha, W. Chen, Lu Hao, C. Wu, M. Lu, L. Zhang, D. Yu, *Soft Matter* **2020**, *16*, 6591.
- [172] K. Ramanathan, M. A. Bangar, M. Yun, W. Chen, N. V. Myung, A. Mulchandani, *J. Am. Chem. Soc.* **2005**, *127*, 496.
- [173] L. Xia, Z. Wei, M. Wan, *J. Colloid Interface Sci.* **2010**, <https://doi.org/10.1016/j.jcis.2009.09.029>.
- [174] D. H. Reneker, I. Chun, *Nanotechnology* **1996**, *7*, 216.
- [175] M. Mahdavi, N. Mahmoudi, F. Rezaie Anaran, A. Simchi, *Marine Drugs* **2016**, *14*, 128.
- [176] S. Aznar-Cervantes, M. I. Roca, J. G. Martinez, L. Meseguer-Olmo, J. L. Cenis, J. M. Moraleda, T. F. Otero, *Bioelectrochemistry* **2012**, *85*, 36.
- [177] C. Qu, P. Zhao, C. Wu, Y. Zhuang, J. Liu, W. Li, Z. Liu, J. Liu, *Sens. Actuators, B* **2021**, *338*, 129822.
- [178] Q. Nie, Z. Pang, D. Li, H. Zhou, F. Huang, Y. Cai, Q. Wei, *Colloids Surf. A* **2018**, *537*, 532.

- [179] S. Bagchi, C. Ghanshyam, *J. Phys. D: Appl. Phys.* **2017**, *50*, 105302.
- [180] Y. Ding, H. Sun, C. Ren, M. Zhang, K. Sun, *Materials* **2020**, *13*, 2874.
- [181] Y. Park, J. Jung, M. Chang, *Appl. Sci.* **2019**, *9*, 1070.
- [182] R. Ramaseshan, S. Sundarrajan, R. Jose, S. Ramakrishna, *J. Appl. Phys.* **2007**, *102*, 111101.
- [183] H. Wu, W. Pan, D. Lin, H. Li, *J. Adv. Ceram.* **2012**, *1*, 2.
- [184] S. Thomas, B. S. P. Harshita, P. Mishra, S. Talegaonkar, *Curr. Pharm. Des.* **2015**, *21*, 6165.
- [185] D. Li, J. T. Mccann, Y. Xia, M. Marquez, *J. Am. Ceram. Soc.* **2006**, *89*, 1861.
- [186] Y. Dai, W. Liu, E. Formo, Y. Sun, Y. Xia, *Polym. Adv. Technol.* **2011**, *22*, 326.
- [187] Y. Zhang, J. Li, Q. Li, L. Zhu, X. Liu, X. Zhong, J. Meng, X. Cao, *Scr. Mater.* **2007**, *56*, 409.
- [188] P. Pascariu, M. Homocianu, *Ceram. Int.* **2019**, *45*, 11158.
- [189] P. Baek, L. Voorhaar, D. Barker, J. Travas-Sejdic, *Acc. Chem. Res.* **2018**, *51*, 1581.
- [190] D. Li, A. Babel, S. A. Jenekhe, Y. Xia, *Adv. Mater.* **2004**, *16*, 2062.
- [191] Y. Long, H. Chen, Y. Yang, H. Wang, Y. Yang, N. Li, K. Li, J. Pei, F. Liu, *Macromolecules* **2009**, *42*, 6501.
- [192] L. Veeramuthu, M. Venkatesan, F.-C. Liang, J.-S. Benas, C.-J. Cho, C.-W. Chen, Y. Zhou, R.-H. Lee, C.-C. Kuo, *Polymers* **2020**, *12*, 587.
- [193] J. T. Devreese, *MRS Bull.* **2007**, *32*, 718.
- [194] R. Bogue, *Sens. Rev.* **2009**, *29*, 310.
- [195] S. M. Mousavi, S. A. Hashemi, M. Zarei, A. M. Amani, A. Babapoor, *Med. Chem.* **2018**, *08*, 2161.
- [196] N. Chauhan, S. Soni, P. Agrawal, Y. P. S. Balhara, U. Jain, *Process Biochem.* **2020**, *91*, 241.
- [197] S. H. Nile, V. Baskar, D. Selvaraj, A. Nile, J. Xiao, G. Kai, *Nano-Micro Lett.* **2020**, *12*, 45.
- [198] M. Ramezani, S. M. Taghdisi, R. Yazdian-Robati, F. Oroojalian, K. Abnous, M. Alibolandi, *Nanosensors for Smart Cities*, Elsevier, New York **2020**, p. 285.
- [199] W. K. Choi, T. H. Liew, H. G. Chew, F. Zheng, C. V. Thompson, Y. Wang, M. H. Hong, X. D. Wang, L. Li, J. Yun, *Small* **2008**, *4*, 330.
- [200] B. Farhang, *Global Issues in Food Science and Technology*, Elsevier, New York **2009**, p. 401.
- [201] S. Zhang, Z. Jia, T. Liu, G. Wei, Z. Su, *Sensors* **2019**, *19*, 3977.
- [202] A. Macagnano, E. Zampetti, E. Kny, *Electrospinning for High Performance Sensors*, Springer, Cham, Switzerland **2015**, pp. 1–329.
- [203] B. Robb, B. Lennox, *Electrospinning for Tissue Regeneration*, Elsevier, New York **2011**, p. 51.
- [204] B. J. Privett, J. H. Shin, M. H. Schoenfish, *Anal. Chem.* **2008**, *80*, 4499.
- [205] J. R. Stetter, W. R. Penrose, S. Yao, *J. Electrochem. Soc.* **2003**, *150*, S11.
- [206] N. R. Stradiotto, H. Yamanaka, M. V. B. Zannoni, *J. Braz. Chem. Soc.* **2003**, *14*, 159.
- [207] X. Zhang, J. Huangxian, W. Joseph, *Electrochemical Sensors, Biosensors and Their Biomedical Application*, Academic Press, San Diego, CA **2011**.
- [208] Y. Shao, J. Wang, H. Wu, J. Liu, I. A. Aksay, Y. Lin, *Electroanalysis* **2010**, *22*, 1027.
- [209] G. Wang, X. He, L. Wang, A. Gu, Y. Huang, B. Fang, B. Geng, X. Zhang, *Microchim. Acta* **2013**, *180*, 161.
- [210] H. Lee, Y. J. Hong, S. Baik, T. Hyeon, D. H. Kim, *Adv. Healthcare Mater.* **2018**, *7*, 1701150.
- [211] A. Senthamizhan, B. Balusamy, T. Uyar, *Anal. Bioanal. Chem.* **2016**, *408*, 1285.
- [212] K. Dhara, D. R. Mahapatra, *Microchim. Acta* **2018**, *185*, 49.
- [213] A. Gattani, S. V. Singh, A. Agrawal, M. H. Khan, P. Singh, *Anal. Biochem.* **2019**, *579*, 25.
- [214] K. Chen, W. Chou, L. Liu, Y. Cui, P. Xue, M. Jia, *Sensors* **2019**, *19*, 3676.
- [215] G. Liu, B. Zheng, Y. Jiang, Y. Cai, J. Du, H. Yuan, D. Xiao, *Talanta* **2012**, *101*, 24.
- [216] S. N. H. Hernández, G. Chauhan, *Mater. Today: Proc.* **2020**, S2214785320377452.
- [217] B. Zheng, G. Liu, A. Yao, Y. Xiao, J. Du, Y. Guo, D. Xiao, Q. Hu, M. M. F. Choi, *Sens. Actuators, B* **2014**, *195*, 431.
- [218] C. Zhou, L. Xu, J. Song, R. Xing, S. Xu, D. Liu, H. Song, *Sci. Rep.* **2015**, *4*, 7382.
- [219] Y. Zhang, Y. Wang, J. Jia, J. Wang, *Sens. Actuators, B* **2012**, *171–172*, 580.
- [220] Y. Liu, H. Teng, H. Hou, T. You, *Biosens. Bioelectron.* **2009**, *24*, 3329.
- [221] Y. Zhang, L. Luo, Z. Zhang, Y. Ding, S. Liu, D. Deng, H. Zhao, Y. Chen, *J. Mater. Chem. B* **2014**, *2*, 529.
- [222] Z. Yin, K. Allado, A. T. Sheardy, Z. Ji, D. Arvapalli, M. Liu, P. He, X. Zeng, J. Wei, *Cryst. Growth Des.* **2021**, *21*, 1527.
- [223] Q. Mei, R. Fu, Y. Ding, L. Li, A. Wang, D. Duan, D. Ye, *J. Electroanal. Chem.* **2019**, *847*, 113075.
- [224] Q. Guo, T. Wu, L. Liu, Y. He, D. Liu, T. You, *J. Alloys Compd.* **2020**, *819*, 153376.
- [225] D. Li, Z. Pang, X. Chen, L. Luo, Y. Cai, Q. Wei, *Beilstein J. Nanotechnol.* **2014**, *5*, 346.
- [226] Y. Li, M. Zhang, X. Zhang, G. Xie, Z. Su, G. Wei, *Nanomaterials* **2015**, *5*, 1891.
- [227] H. Guan, Y. Zhao, J. Zhang, Y. Liu, S. Yuan, B. Zhang, *Sens. Actuators, B* **2018**, *261*, 354.
- [228] X. Zhang, D. Liu, B. Yu, T. You, *Sens. Actuators, B* **2016**, *224*, 103.
- [229] A. Numnuam, P. Thavarungkul, P. Kanatharana, *Anal. Bioanal. Chem.* **2014**, *406*, 3763.
- [230] A. Rostami, A. Hadjizadeh, S. Mahshid, *J. Mater. Sci.* **2020**, *55*, 7969.
- [231] Z. Jahromi, E. Mirzaei, A. Savardashtaki, M. Afzali, Z. Afzali, *Microwchem. J.* **2020**, *157*, 104942.
- [232] Y. Tong, Z. Li, X. Lu, L. Yang, W. Sun, G. Nie, Z. Wang, Ce Wang, *Electrochim. Acta* **2013**, *95*, 12.
- [233] Y. Wang, W. Li, Y. Zhou, L. Jiang, J. Ma, S. Chen, S. Jerrams, F. Zhou, *J. Mater. Sci.* **2020**, *55*, 12592.
- [234] H. Asadi Samie, M. Arvand, *J. Alloys Compd.* **2019**, *782*, 824.
- [235] O. C. Ozoemena, L. J. Shai, T. Maphumulo, K. I. Ozoemena, *Electrocatalysis* **2019**, *10*, 381.
- [236] H. Y. Yue, P. F. Wu, S. Huang, X. Gao, S. S. Song, W. Q. Wang, H. J. Zhang, X. R. Guo, *J. Electroanal. Chem.* **2019**, *833*, 427.
- [237] A. Ahmadi, S. M. Khoshfetrat, S. Kabiri, L. Fotouhi, P. S. Dorraji, K. Omidfar, *IEEE Sensors J.* **2021**, *21*, 9210.
- [238] L. A. Mercante, A. Pavinatto, L. E. O. Iwaki, V. P. Scagion, V. Zucolotto, O. N. Oliveira, L. H. C. Mattoso, D. S. Correa, *ACS Appl. Mater. Interfaces* **2015**, *7*, 4784.
- [239] Z. X. Deng, J. W. Tao, W. Zhang, H. J. Mu, H. J. Wu, Y. B. Wang, X. X. Xu, W. Zheng, *Mater. Chem. Phys.* **2021**, *257*, 123827.
- [240] V. Sharma, G. Anit Kaur, N. Gupta, M. Shandilya, *FlatChem* **2020**, *24*, 100195.
- [241] K. Juntaracena, T. Yuangkaew, M. Horpratum, N. Triroj, P. Jaroenapibal, *IOP Conf. Ser.: Mater. Sci. Eng.* **2021**, *1070*, 012004.
- [242] Y. Huang, Y.-E. Miao, S. Ji, W. W. Tjiu, T. Liu, *ACS Appl. Mater. Interfaces* **2014**, *6*, 12449.
- [243] E. Sapountzi, M. Braiek, F. Vocanson, J.-F. Chateaux, N. Jaffrezic-Renault, F. Lagarde, *Sens. Actuators, B* **2017**, *238*, 392.
- [244] T. Zhang, W. Wang, D. Zhang, X. Zhang, Y. Ma, Y. Zhou, L. Qi, *Adv. Funct. Mater.* **2010**, *20*, 1152.
- [245] E. Sapountzi, M. Braiek, C. Farre, M. Arab, J.-F. Chateaux, N. Jaffrezic-Renault, F. Lagarde, *J. Electrochem. Soc.* **2015**, *162*, B275.
- [246] C. M. Wu, S. A. Yu, S. L. Lin, *eXPRESS Polym. Lett.* **2014**, *8*, 565.
- [247] L. A. Mercante, L. E. O. Iwaki, V. P. Scagion, O. N. Oliveira, L. H. C. Mattoso, D. S. Correa, *Electrochem* **2021**, *2*, 41.
- [248] S. Demirci Uzun, F. Kayaci, T. Uyar, S. Timur, L. Toppare, *ACS Appl. Mater. Interfaces* **2014**, *6*, 5235.

- [249] Y. Xu, Y. Ding, L. Zhang, X. Zhang, *Compos. Commun.* **2021**, *25*, 100687.
- [250] G. Bahrami, H. Ehzari, S. Mirzabeigy, B. Mohammadi, E. Arkan, *Mater. Sci. Eng. C* **2020**, *106*, 110183.
- [251] L. Liu, Z. Wang, J. Yang, G. Liu, J. Li, L. Guo, S. Chen, Q. Guo, *Sens. Actuators, B* **2018**, *258*, 920.
- [252] L. Farzin, S. Sadjadi, M. Shamsipur, S. Sheibani, M. H. Mousazadeh, *Mater. Sci. Eng. C* **2019**, *97*, 679.
- [253] Y. Zhang, D. Deng, X. Zhu, S. Liu, Y. Zhu, L. Han, L. Luo, *Anal. Chim. Acta* **2018**, *1042*, 20.
- [254] T. Xu, W. Jin, Z. Wang, H. Cheng, X. Huang, X. Guo, Y. Ying, Y. Wu, F. Wang, Y. Wen, H. Yang, *Nanomaterials* **2018**, *8*, 133.
- [255] D. Chauhan, P. K. Gupta, P. R. Solanki, *Mater. Sci. Eng. C* **2018**, *93*, 145.
- [256] M. Adabi, S. S. Esnaashari, M. Adabi, *J. Porous Mater.* **2021**, *28*, 415.
- [257] E. Kivrak, A. Ince-Yardimci, R. Ilhan, P. B. Kirmizibayrak, S. Yilmaz, P. Kara, *Anal. Bioanal. Chem.* **2020**, *412*, 7851.
- [258] P. Li, M. Zhang, X. Liu, Z. Su, G. Wei, *Nanomaterials* **2017**, *7*, 236.
- [259] S. Zhou, M. Hu, X. Huang, N. Zhou, Z. Zhang, M. Wang, Y. Liu, L. He, *Microchim. Acta* **2020**, *187*, 219.
- [260] P. Supraja, V. Singh, S. R. K. Vanjari, S. Govind Singh, *Microsyst. Nanoeng.* **2020**, *6*, 3.
- [261] R. Asmatulu, Z. Veisi, M. N. Uddin, A. Mahapatro, *Fibers Polym.* **2019**, *20*, 966.
- [262] J. C. Soares, L. E. O. Iwaki, A. C. Soares, V. C. Rodrigues, M. E. Melendez, J. H. T. G. Fregnani, R. M. Reis, A. L. Carvalho, D. S. Corrêa, O. N. Oliveira, *ACS Omega* **2017**, *2*, 6975.
- [263] K. B. Paul, V. Singh, S. R. K. Vanjari, S. G. Singh, *Biosens. Bioelectron.* **2017**, *88*, 144.
- [264] M. Adabi, M. Adabi, *J. Dispersion Sci. Technol.* **2021**, *42*, 262.
- [265] K. Puttananjogowda, A. Taksi, S. Thomas, *J. Electrochem. Soc.* **2020**, *167*, 037553.
- [266] C. McDonagh, C. S. Burke, B. D. Maccraith, *Chem. Rev.* **2008**, *108*, 400.
- [267] A. D. Tjandra, J. Y. H. Chang, S. Ladame, R. Chandrawati, *Bioengineering Innovative Solutions for Cancer*, Elsevier, New York **2020**, p. 23.
- [268] J. Shi, Y. Zhu, X. Zhang, W. R. G. Baeyens, A. M. García-Campaña, *TrAC Trends Anal. Chem.* **2004**, *23*, 351.
- [269] X. Wang, C. Drew, S.-H. Lee, K. J. Senecal, J. Kumar, L. A. Samuelson, *Nanoletters* **2002**, *2*, 1273.
- [270] J. Soleymani, M. Hasanzadeh, M. H. Somi, A. Jouyban, *TrAC Trends Anal. Chem.* **2018**, *107*, 169.
- [271] S.-J. Choi, L. Persano, A. Camposeo, J.-S. Jang, W.-T. Koo, S.-J. Kim, H.-J. Cho, I.-D. Kim, D. Pisignano, *Macromol. Mater. Eng.* **2017**, *302*, 1600569.
- [272] S. Ponce-Alcántara, D. Martín-Sánchez, A. Pérez-Márquez, J. Maudes, N. Murillo, J. García-Rupérez, *Opt. Mater. Express* **2018**, *8*, 3163.
- [273] L. Rey-Barroso, S. Peña-Gutiérrez, C. Yáñez, F. J. Burgos-Fernández, M. Vilaseca, S. Royo, *Opt. Sens.* **2021**, *21*, 252.
- [274] L. Ma, K. Liu, M. Yin, J. Chang, Y. Geng, K. Pan, *Sens. Actuators, B* **2017**, *238*, 120.
- [275] A. Petropoulou, S. Kralj, X. Karagiorgis, I. Savva, E. Loizides, M. Panagi, T. Krasia-Christoforou, C. Riziotis, *Sci. Rep.* **2020**, *10*, 367.
- [276] J. Quirós, A. J. R. Amaral, G. Pasparakis, G. R. Williams, R. Rosal, *React. Funct. Polym.* **2017**, *121*, 23.
- [277] Y. Yang, H. Wang, K. Su, Y. Long, Z. Peng, N. Li, F. Liu, *J. Mater. Chem.* **2011**, *21*, 11895.
- [278] K. Li, R.-H. Yu, C.-M. Shi, F.-R. Tao, T.-D. Li, Y.-Z. Cui, *Sens. Actuators, B* **2018**, *262*, 637.
- [279] P. Anzenbacher, L. Mosca, M. A. Palacios, G. V. Zyryanov, P. Koutnik, *Chem. – Eur. J.* **2012**, *18*, 12712.
- [280] W.-C. Wu, H.-J. Lai, *J. Polym. Res.* **2016**, *23*, 223.
- [281] L. Zhao, Y. Chen, J. Yuan, M. Chen, H. Zhang, X. Li, *ACS Appl. Mater. Interfaces* **2015**, *7*, 5177.
- [282] T. Yang, P. Hou, L. L. Zheng, L. Zhan, P. F. Gao, Y. F. Li, C. Z. Huang, *Nanoscale* **2017**, *9*, 17020.
- [283] L. Ma, K. Liu, M. Yin, J. Chang, Y. Geng, K. Pan, *Sens. Actuators B: Chem.* **2017**, *238*, 120.
- [284] I. A. A. Terra, R. C. Sanfelice, V. P. Scagion, N. B. Tomazio, C. R. Mendonça, L. A. O. Nunes, D. S. Correa, *J. Appl. Polym. Sci.* **2019**, *136*, 47775.
- [285] S. Li, S. Zhou, H. Xu, L. Xiao, Yi Wang, H. Shen, H. Wang, Q. Yuan, *J. Mater. Sci.* **2016**, *51*, 6801.
- [286] A. Senthamizhan, A. Celebioglu, T. Uyar, *Sci. Rep.* **2015**, *5*, 10403.
- [287] A. P. Roque, L. A. Mercante, V. P. Scagion, J. E. Oliveira, L. H. C. Mattoso, L. De Boni, C. R. Mendonca, D. S. Correa, *J. Polym. Sci. Part B: Polym. Phys.* **2014**, *52*, 1388.
- [288] S. Kacmaz, K. Ertekin, A. Suslu, Y. Ergun, E. Celik, U. Cocen, *Mater. Chem. Phys.* **2012**, *133*, 547.
- [289] R. Anandakathir, U. Ojha, E. T. Ada, R. Faust, J. Kumar, *J. Macromol. Sci., Part A: Pure Appl. Chem.* **2009**, *46*, 1217.
- [290] Y. Long, H. Chen, H. Wang, Z. Peng, Y. Yang, G. Zhang, N. Li, F. Liu, J. Pei, *Anal. Chim. Acta* **2012**, *744*, 82.
- [291] H. Wang, Z. Peng, Y. Long, H. Chen, Y. Yang, N. Li, F. Liu, *Talanta* **2012**, *94*, 216.
- [292] Y. Wang, Y. Zhu, J. Huang, J. Cai, J. Zhu, X. Yang, J. Shen, H. Jiang, C. Li, *J. Phys. Chem. Lett.* **2016**, *7*, 4253.
- [293] X. Ji, R. Li, G. Liu, W. Jia, M. Sun, Y. Liu, Y. Luo, Z. Cheng, *Mater. Des.* **2021**, *207*, 109864.
- [294] W. Xue, Y. Zhang, J. Duan, D. Liu, Y. Ma, N. Shi, S. Chen, L. Xie, Y. Qian, W. Huang, *J. Mater. Chem. C* **2015**, *3*, 8193.
- [295] H. Wang, D. Wang, Z. Peng, W. Tang, N. Li, F. Liu, *Chem. Commun.* **2013**, *49*, 5568.
- [296] H.-J. Lin, C.-Y. Chen, *J. Mater. Sci.* **2016**, *51*, 1620.
- [297] B. J. Yun, J. E. Kwon, K. Lee, W.-G. Koh, *Sens. Actuators, B* **2019**, *284*, 140.
- [298] Y. Hu, X. Lu, X. Jiang, P. Wu, *J. Hazard. Mater.* **2020**, *384*, 121368.
- [299] B.-Y. Chen, C.-C. Kuo, C.-J. Cho, F.-C. Liang, R.-J. Jeng, *Dyes Pigm.* **2017**, *143*, 129.
- [300] X. Cui, T. Li, J. Li, Y. An, L. An, X. Zhang, Z. Zhang, *Spectrochim. Acta, Part A* **2019**, *207*, 173.
- [301] E. Hu, P. Lin, E. Y.-B. Pun, J. Yuan, H. Lin, X. Zhao, *J. Electrochem. Soc.* **2020**, *167*, 027510.
- [302] S. Ahmadian-Fard-Fini, D. Ghanbari, O. Amiri, M. Salavati-Niasari, *Carbohydr. Polym.* **2020**, *229*, 115428.
- [303] M. Z. Ongun, K. Ertekin, M. Gocmenturk, Y. Ergun, A. Suslu, *Spectrochim. Acta, Part A* **2012**, *90*, 177.
- [304] B.-Y. Chen, C.-C. Kuo, Y.-S. Huang, S.-T. Lu, F.-C. Liang, D.-H. Jiang, *ACS Appl. Mater. Interfaces* **2015**, *7*, 2797.
- [305] W. Wu, N. Shi, J. Zhang, X. Wu, T. Wang, L. Yang, R. Yang, C. Ou, W. Xue, X. Feng, L. Xie, W. Huang, *J. Mater. Chem. A* **2018**, *6*, 18543.
- [306] E. Schoolaert, R. Hoogenboom, K. De Clerck, *Adv. Funct. Mater.* **2017**, *27*, 1702646.
- [307] H. Aldewachi, T. Chalati, M. N. Woodrooffe, N. Bricklebank, B. Sharrock, P. Gardiner, *Nanoscale* **2018**, *10*, 18.
- [308] A. Senthamizhan, B. Balusamy, T. Uyar, *Curr. Opin. Biomed. Eng.* **2020**, <https://doi.org/10.1016/j.cobme.2019.08.002>.
- [309] G. Peng, U. Tisch, O. Adams, M. Hakim, N. Shehada, Y. Y. Broza, S. Billan, R. Abdah-Bortnyak, A. Kuten, H. Haick, *Nat. Nanotechnol.* **2009**, *4*, 669.
- [310] J. P. Yapor, A. Alharby, C. Gentry-Weeks, M. M. Reynolds, A. K. M. M. Alam, Y. V. Li, *ACS Omega* **2017**, *2*, 7334.
- [311] C. Zhang, H. Li, Q. Yu, L. Jia, L. Y. Wan, *ACS Omega* **2019**, *4*, 14633.
- [312] H. J. Oh, B. J. Yeang, Y. K. Park, H. J. Choi, J. H. Kim, Y. S. Kang, Y. Bae, J. Y. Kim, S. J. Lim, W. Lee, W.-G. Hahm, *Polymers* **2020**, *12*, 1585.

- [313] X. Wang, Y. Si, J. Wang, B. Ding, J. Yu, S. S. Al-Deyab, *Sens. Actuators, B* **2012**, *163*, 186.
- [314] M.-H. You, X. Yan, J. Zhang, X.-X. Wang, X.-X. He, M. Yu, X. Ning, Y.-Z. Long, *Nanoscale Res. Lett.* **2017**, *12*, 360.
- [315] L. Hu, X.-W. Yan, Q. Li, X.-J. Zhang, D. Shan, *J. Hazard. Mater.* **2017**, *329*, 205.
- [316] J. Yoon, Y.-S. Jung, J.-M. Kim, *Adv. Funct. Mater.* **2009**, *19*, 209.
- [317] N. Tungsombatvisit, T. Inprasit, D. Rohmawati, P. Pisitsak, *Fibers Polym.* **2019**, *20*, 481.
- [318] T. A. Khattab, S. Abdelmoez, T. M. Klapötke, *Chem. – Eur. J.* **2016**, *22*, 4157.
- [319] A. Senthamizhan, A. Celebioglu, T. Uyar, *J. Mater. Chem. A* **2014**, *2*, 12717.
- [320] A. Senthamizhan, B. Balusamy, Z. Aytac, T. Uyar, *Anal. Bioanal. Chem.* **2016**, *408*, 1347.
- [321] B. Ding, Y. Si, X. Wang, J. Yu, L. Feng, G. Sun, *J. Mater. Chem.* **2011**, *21*, 13345.
- [322] Y. Li, Z. Liu, L. Bai, Y. Liu, *New J. Chem.* **2019**, *43*, 1812.
- [323] X. Zhou, Z. Xue, X. Chen, C. Huang, W. Bai, Z. Lu, T. Wang, *J. Mater. Chem. B* **2020**, *8*, 3231.
- [324] M. Imran, N. Motta, M. Shafiei, *Beilstein J. Nanotechnol.* **2018**, *9*, 2128.
- [325] B. De Lacy Costello, A. Amann, H. Al-Kateb, C. Flynn, W. Filipiak, T. Khalid, D. Osborne, N. M. Ratcliffe, *J. Breath Res.* **2014**, *8*, 014001.
- [326] B. Ding, M. Wang, J. Yu, G. Sun, *Sensors* **2009**, *9*, 1609.
- [327] P. Shankar, J. Bosco Balaguru Rayappan, *Sci. Lett. J.* **2015**, *4*.
- [328] I.-D. Kim, A. Rothschild, *Polym. Adv. Technol.* **2011**, *22*, 318.
- [329] B. Ding, M. Yamazaki, S. Shiratori, *Sens. Actuators, B* **2005**, *106*, 477.
- [330] V. S. Bhati, M. Hojamberdiev, M. Kumar, *Energy Rep.* **2020**, *6*, 46.
- [331] L. A. Mercante, R. S. Andre, L. H. C. Mattoso, D. S. Correa, *ACS Appl. Nano Mater.* **2019**, *2*, 4026.
- [332] J. Avossa, R. Paolesse, C. Di Natale, E. Zampetti, G. Bertoni, F. De Cesare, G. Scarascia-Mugnozza, A. Macagnano, *Nanomaterials* **2019**, *9*, 280.
- [333] W. Hittini, Y. E. Greish, N. N. Qamhie, M. A. Alnaqbi, D. Zeze, S. T. Mahmoud, *Org. Electron.* **2020**, *81*, 105659.
- [334] J. Zhang, H. Lu, H. Lu, G. Li, J. Gao, Z. Yang, Y. Tian, M. Zhang, C. Wang, Z. He, *J. Alloys Compd.* **2019**, *779*, 531.
- [335] Z. Ma, K. Yang, C. Xiao, L. Jia, *J. Hazard. Mater.* **2021**, *416*, 126118.
- [336] M. Zhao, X. Wang, L. Ning, J. Jia, X. Li, L. Cao, *Sens. Actuators, B* **2011**, *156*, 588.
- [337] W. Zheng, X. Lu, W. Wang, Z. Li, H. Zhang, Y. Wang, Z. Wang, C. Wang, *Sens. Actuators, B* **2009**, *142*, 61.
- [338] W. Wang, Z. Li, W. Zheng, H. Huang, C. Wang, J. Sun, *Sens. Actuators, B* **2010**, *143*, 754.
- [339] X. Yu, F. Song, B. Zhai, C. Zheng, Y. Wang, *Phys. E* **2013**, *52*, 92.
- [340] X. Kou, N. Xie, F. Chen, T. Wang, L. Guo, C. Wang, Q. Wang, J. Ma, Y. Sun, H. Zhang, G. Lu, *Sens. Actuators, B* **2018**, *256*, 861.
- [341] J. Zhang, H. Lu, C. Yan, Z. Yang, G. Zhu, J. Gao, F. Yin, C. Wang, *Sens. Actuators, B* **2018**, *264*, 128.
- [342] J.-Y. Leng, X.-J. Xu, N. Lv, H.-T. Fan, T. Zhang, *J. Colloid Interface Sci.* **2011**, *356*, 54.
- [343] A. Katoch, S.-W. Choi, J.-H. Kim, J. H. Lee, J.-S. Lee, S. S. Kim, *Sens. Actuators, B* **2015**, *214*, 111.
- [344] Y. Zhao, X. He, J. Li, X. Gao, J. Jia, *Sens. Actuators, B* **2012**, *165*, 82.
- [345] C. Feng, C. Wang, P. Cheng, X. Li, B. Wang, Y. Guan, J. Ma, H. Zhang, Y. Sun, P. Sun, J. Zheng, G. Lu, *Sens. Actuators, B* **2015**, *221*, 434.
- [346] S. K. Lim, S.-H. Hwang, D. Chang, S. Kim, *Sens. Actuators, B* **2010**, *149*, 28.
- [347] X. Li, H. Zhang, C. Feng, Y. Sun, J. Ma, C. Wang, G. Lu, *RSC Adv.* **2014**, *4*, 27552.
- [348] K. R. Kishore, D. Balamurugan, B. G. Jeyaprakash, *Mater. Sci. Semi-cond. Process.* **2021**, *121*, 105296.
- [349] L. Jun, Q. Chen, W. Fu, Y. Yang, W. Zhu, J. Zhang, *ACS Appl. Mater. Interfaces* **2020**, *12*, 38425.
- [350] C. De Pascali, M. A. Signore, A. Taurino, L. Francioso, A. Macagnano, J. Avossa, P. Siciliano, S. Capone, *IEEE Sensors J.* **2018**, *18*, 7365.
- [351] C. Zhao, H. Gong, G. Niu, F. Wang, *Sens. Actuators, B* **2019**, *299*, 126946.
- [352] B. Huang, Y. Wang, Q. Hu, X. Mu, Y. Zhang, J. Bai, Q. Wang, Y. Sheng, Z. Zhang, E. Xie, *J. Mater. Chem. C* **2018**, *6*, 10935.
- [353] C. Jiang, S. Xu, G. Zhang, L. Li, Y. Yang, K. Shi, *CrystEngComm* **2013**, *15*, 2482.
- [354] J. Bai, Q. Wang, Y. Wang, X. Cheng, Z. Yang, X. Gu, B. Huang, G. Sun, Z. Zhang, X. Pan, J. Y. Zhou, E. Xie, *J. Colloid Interface Sci.* **2020**, *560*, 447.
- [355] B. Huang, C. Zhao, M. Zhang, Z. Zhang, E. Xie, J. Zhou, W. Han, *Appl. Surf. Sci.* **2015**, *349*, 615.
- [356] Q. Chen, J. Li, W. Fu, Y. Yang, W. Zhu, J. Zhang, *Sens. Actuators, B* **2020**, *323*, 128676.
- [357] P. Mehrabi, J. Hui, S. Janfaza, A. O'brien, N. Tasnim, H. Najjaran, M. Hoorfar, *Micromachines* **2020**, *11*, 190.
- [358] V. Kumar, A. Mirzaei, M. Bonyani, K.-H. Kim, H. W. Kim, S. S. Kim, *TrAC Trends Anal. Chem.* **2020**, *129*, 115938.
- [359] K. Uh, T. Kim, C. W. Lee, J.-M. Kim, *Macromol. Mater. Eng.* **2016**, *301*, 1320.
- [360] G. F. El Fawal, H. S. Hassan, M. R. El-Aassar, M. F. Elkady, *Arab. J. Sci. Eng.* **2019**, *44*, 251.
- [361] J. Yang, W. Han, J. Ma, C. Wang, K. Shimano, S. Zhang, Y. Sun, P. Cheng, Y. Wang, H. Zhang, G. Lu, *Sens. Actuators, B* **2021**, *320*, 129971.
- [362] A. Shahmoradi, A. Hosseini, A. Akbarinejad, N. Alizadeh, *Anal. Chem.* **2021**, *93*, 6706.
- [363] N. Z. Al-Hazeem, N. M. Ahmed, M. Z. Matjafri, M. Bououdina, *Microsyst. Technol.* **2021**, *27*, 293.
- [364] C. Busacca, A. Donato, M. Lo Faro, A. Malara, G. Neri, S. Trocino, *Sens. Actuators, B* **2020**, *303*, 127193.
- [365] R. Hao, J. Yuan, Q. Peng, *Chem. Lett.* **2006**, *35*, 1248.
- [366] Z. Pang, J. Fu, L. Luo, F. Huang, Q. Wei, *Colloids Surf. A* **2014**, *461*, 113.
- [367] T. Han, S. Y. Ma, X. L. Xu, X. H. Xu, S. T. Pei, Y. Tie, P. F. Cao, W. W. Liu, B. J. Wang, R. Zhang, J. L. Zhang, *Mater. Lett.* **2020**, *268*, 127575.
- [368] Z. U. Abideen, A. Katoch, J.-H. Kim, Y. J. Kwon, H. W. Kim, S. S. Kim, *Sens. Actuators, B* **2015**, *221*, 1499.
- [369] Z. U. Abideen, H. W. Kim, S. S. Kim, *Chem. Commun.* **2015**, *51*, 15418.
- [370] N. Van Hoang, C. M. Hung, N. D. Hoa, N. Van Duy, I. Park, N. Van Hieu, *Sens. Actuators, B* **2019**, *282*, 876.
- [371] N. Van Hoang, C. M. Hung, N. D. Hoa, N. Van Duy, N. Van Hieu, *J. Hazard. Mater.* **2018**, *360*, 6.
- [372] H. Lahlou, S. Claramunt, O. Monereo, D. Prades, J. M. Fernandez-Sanjuá, N. Bonet, F. M. Ramos, A. Cirera, *Mater. Today: Proc.* **2021**, <https://doi.org/10.1016/j.matpr.2020.04.674>.
- [373] F. Li, H. Song, W. Yu, Q. Ma, X. Dong, J. Wang, G. Liu, *Mater. Lett.* **2020**, *262*, 127070.
- [374] J.-S. Jang, S.-J. Kim, S.-J. Choi, N.-H. Kim, M. Hakim, A. Rothschild, I.-D. Kim, *Nanoscale* **2015**, *7*, 16417.
- [375] P. Jiang, D. Tang, C. Chen, X. Chen, M. Zhang, *Nanotechnology* **2020**, *31*, 145503.
- [376] O. Erdem Yilmaz, R. Erdem, *Int. J. Hydrogen Energy* **2020**, *45*, 26402.
- [377] M. Ezhilan, A. J. Jbb, J. B. Balaguru Rayappan, *Mater. Res. Bull.* **2021**, *139*, 111276.
- [378] J. Cao, Z. Wang, R. Wang, S. Liu, T. Fei, L. Wang, T. Zhang, *J. Mater. Chem. A* **2015**, *3*, 5635.
- [379] Y. Tie, S. Y. Ma, S. T. Pei, Q. X. Zhang, K. M. Zhu, R. Zhang, X. H. Xu, T. Han, W. W. Liu, *Sens. Actuators, B* **2020**, *308*, 127689.

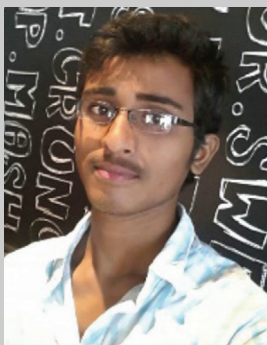


- [380] Q. Hu, B. Huang, Y. Li, S. Zhang, Y. Zhang, X. Hua, G. Liu, B. Li, J. Zhou, E. Xie, Z. Zhang, *Sens. Actuators, B* **2020**, *307*, 127638.
- [381] V. Inderan, M. M. Arafat, A. S. M. A. Haseeb, K. Sudesh, H. L. Lee, *Nanotechnology* **2020**, *31*, 425503.
- [382] F. Temel, I. Ozyaytekin, *Sens. Actuators, A* **2021**, *326*, 112688.
- [383] M. Ezhilan, A. J. Jbb, K. J. Babu, J. B. B. Rayappan, *J. Alloys Compd.* **2021**, *863*, 158407.
- [384] V. S. Saji, H. C. Choe, K. W. K. Yeung, *Int. J. Nano Biomater.* **2010**, *3*, 119.
- [385] A. P. Ramos, M. A. E. Cruz, C. B. Tovani, P. Ciancaglini, *Biophys. Rev.* **2017**, *9*, 79.
- [386] S. Emilian Leucuta, *Curr. Clin. Pharmacol.* **2010**, *5*, 257.
- [387] R. H. Kraus, B. Wright, *Biomedical Applications of Nanotechnology*, Wiley, New York, **2007**, p. 65, Ch. 3.
- [388] R. Ravichandran, S. Sundarrajan, J. R. Venugopal, S. Mukherjee, S. Ramakrishna, *Macromol. Biosci.* **2012**, *12*, 286.
- [389] M. Fathi-Achachelouei, H. Knopf-Marques, C. E. Ribeiro Da Silva, J. Barthès, E. Bat, A. Tezcaner, N. E. Vrana, *Front. Bioeng. Biotechnol.* **2019**, *7*, 113.
- [390] S. Datta, G. Menon, *Biotechnological Applications of Polyhydroxyalkanoates*, Springer, Berlin **2019**, p. 409.
- [391] T. Lu, Y. Li, T. Chen, *Int. J. Nanomed.* **2013**, *8*, 337.
- [392] W. Lin, M. Chen, T. Qu, J. Li, Yi Man, *J. Biomed. Mater. Res.* **2020**, *108*, 1311.
- [393] M. Rahmati Nejad, M. Yousefzadeh, A. Solouk, *Mater. Sci. Eng. C* **2020**, *110*, 110692.
- [394] M. Liu, X.-P. Duan, Y.-M. Li, D.-P. Yang, Y.-Z. Long, *Mater. Sci. Eng. C* **2017**, *76*, 1413.
- [395] J. A. Gerstenhaber, R. Brodsky, R. B. Huneke, P. I. Lelkes, *Wound Med.* **2014**, *5*, 9.
- [396] F. Aavani, S. Khorshidi, A. Karkhaneh, *J. Med. Eng. Technol.* **2019**, *43*, 38.
- [397] C. Ramos, G.-M. Lanno, I. Laidmäe, A. Meos, R. Härmas, K. Kogermann, *Int. J. Polym. Mater. Polym. Biomater.* **2020**, *1*, 880.
- [398] B. Balusamy, A. Celebioglu, A. Senthamizhan, T. Uyar, *J. Controlled Release* **2020**, *326*, 482.
- [399] M. Rahmati, D. K. Mills, A. M. Urbanska, M. R. Saeb, J. R. Venugopal, S. Ramakrishna, M. Mozafari, *Prog. Mater. Sci.* **2021**, *117*, 100721.
- [400] J. Wu, Z. Zhang, J.-G. Gu, W. Zhou, X. Liang, G. Zhou, C. C. Han, S. Xu, Y. Liu, *J. Controlled Release* **2020**, *320*, 337.
- [401] C. Dumitriu, A. B. Stoian, I. Titorencu, V. Pruna, V. V. Jinga, R.-M. Latonen, J. Bobacka, I. Demetrescu, *Mater. Sci. Eng. C* **2014**, *45*, 56.
- [402] X. Xu, X. Chen, X. Xu, T. Lu, X. Wang, L. Yang, X. Jing, *J. Controlled Release* **2006**, *114*, 307.
- [403] C. L. Casper, W. Yang, M. C. Farach-Carson, J. F. Rabolt, *Biomacromolecules* **2007**, *8*, 1116.
- [404] S. T. Yohe, V. L. M. Herrera, Y. L. Colson, M. W. Grinstaff, *J. Controlled Release* **2012**, *162*, 92.
- [405] Y. Jin, P. Sun, T. Wu, J. Wang, X. Huang, S. Zuo, Z. Cui, J. Chen, L. Li, N. Suo, X. Jin, D. Zhang, *J. Nanomater.* **2021**, <https://doi.org/10.1155/2021/9956466>.
- [406] R. Sridhar, S. Ramanan, J. R. Venugopal, S. Sundarrajan, D. Pliszka, S. Sivasubramanian, P. Gunasekaran, M. Prabhakaran, K. Madhaiyan, A. Sahayaraj, K. H. C. Lim, S. Ramakrishna, *J. Biomater. Sci., Polym. Ed.* **2014**, *25*, 985.
- [407] Y. Chen, S. Liu, Z. Hou, P. Ma, D. Yang, C. Li, J. Lin, *Nano Res.* **2015**, *8*, 1917.
- [408] M. G. Ignatova, N. E. Manolova, R. A. Toshkova, I. B. Rashkov, E. G. Gardeva, L. S. Yossifova, M. T. Alexandrov, *Biomacromolecules* **2010**, *11*, 1633.
- [409] E. H. Gang, C. S. Ki, J. W. Kim, J. Lee, B. G. Cha, K. H. Lee, Y. H. Park, *Fibers Polym.* **2012**, *13*, 685.
- [410] J. F. Paletta, F. Mack, H. Schenderlein, C. Theisen, J. Schmitt, Jh. Wendorff, S. Agarwal, S. Fuchs-Winkelmann, M. Schofer, *eCells Mater.* **2011**, *21*, 384.
- [411] M. C. Mcmanus, E. D. Boland, D. G. Simpson, C. P. Barnes, G. L. Bowlin, *J. Biomed. Mater. Res.* **2007**, *81A*, 299.
- [412] G. Ma, Y. Liu, C. Peng, D. Fang, B. He, J. Nie, *Carbohydr. Polym.* **2011**, *86*, 505.
- [413] P. Chen, Q.-S. Wu, Y.-P. Ding, M. Chu, Z.-M. Huang, W. Hu, *Eur. J. Pharm. Biopharm.* **2010**, *76*, 413.
- [414] N. Zhang, Y. Deng, Q. Tai, B. Cheng, L. Zhao, Q. Shen, R. He, L. Hong, W. Liu, S. Guo, K. Liu, H.-R. Tseng, B. Xiong, X.-Z. Zhao, *Adv. Mater.* **2012**, *24*, 2756.
- [415] M. Boakye, N. Rijal, U. Adhikari, N. Bhattarai, *Materials* **2015**, *8*, 4080.
- [416] J. S. Choi, S. J. Lee, G. J. Christ, A. Atala, J. J. Yoo, *Biomaterials* **2008**, *29*, 2899.
- [417] Md. A. Ali, K. Mondal, Y. Jiao, S. Oren, Z. Xu, A. Sharma, L. Dong, *ACS Appl. Mater. Interfaces* **2016**, *8*, 20570.
- [418] W. T. Sow, Y. S. Lui, K. W. Ng, *Nanomedicine* **2013**, *8*, 531.
- [419] G. Khan, S. K. Yadav, R. R. Patel, N. Kumar, M. Bansal, B. Mishra, *Int. J. Biol. Macromol.* **2017**, *103*, 1311.
- [420] Z. Liu, Z. Yan, L. Jia, P. Song, L. Mei, L. Bai, Y. Liu, *Appl. Surf. Sci.* **2017**, *403*, 29.
- [421] A. P. F. Monteiro, C. M. S. L. Rocha, M. F. Oliveira, S. M. L. Gontijo, R. R. Agudelo, R. D. Sinisterra, M. E. Cortés, *Carbohydr. Polym.* **2017**, *156*, 417.
- [422] X. Ren, Y. Han, J. Wang, Y. Jiang, Z. Yi, H. Xu, Q. Ke, *Acta Biomater.* **2018**, *70*, 140.
- [423] B. V. Worley, R. J. Soto, P. C. Kinsley, M. H. Schoenfish, *ACS Biomater. Sci. Eng.* **2016**, *2*, 426.
- [424] S. Torres-Giner, Y. Echegoyen, R. Teruel-Juanes, J. Badia, A. Ribes-Greus, J. Lagaron, *Nanomaterials* **2018**, *8*, 745.
- [425] M. R. El-Aassar, G. F. El Fawal, N. M. El-Deeb, H. S. Hassan, X. Mo, *Appl. Biochem. Biotechnol.* **2016**, *178*, 1488.
- [426] M. Rychter, A. Baranowska-Korczyk, B. Milanowski, M. Jarek, B. M. Maciejewska, E. L. Coy, J. Lulek, *Pharm. Res.* **2018**, *35*, 32.
- [427] M. A. Badawi, L. K. El-Khordagui, *Eur. J. Pharm. Sci.* **2014**, *58*, 44.
- [428] H. R. Bakhsheshi-Rad, A. F. Ismail, M. Aziz, M. Akbari, Z. Hadisi, M. Daroonparvar, X. B. Chen, *Mater. Lett.* **2019**, *256*, 126618.
- [429] Y. Hussein, E. M. El-Fakharany, E. A. Kamoun, S. A. Loutfy, R. Amin, T. H. Taha, S. A. Salim, M. Amer, *Int. J. Biol. Macromol.* **2020**, *164*, 667.
- [430] D. Kharaghani, M. Q. Khan, Y. Tamada, H. Ogasawara, Y. Inoue, Y. Saito, M. Hashmi, I. S. Kim, *Polym. Test.* **2018**, *72*, 315.
- [431] A. C. Areias, C. Ribeiro, V. Sencadas, N. Garcia-Giralt, A. Diez-Perez, J. L. Gómez Ribelles, S. Lanceros-Méndez, *Soft Matter* **2012**, *8*, 5818.
- [432] O. Mirdailami, M. Soleimani, R. Dinarvand, M. R. Khoshayand, M. Norouzi, A. Hajarizadeh, M. Dodel, F. Atyabi, *J. Biomed. Mater. Res.* **2015**, *103*, 3374.
- [433] W. Abdul Khodir, A. Abdul Razak, M. Ng, V. Guarino, D. Susanti, *J. Funct. Biomater.* **2018**, *9*, 36.
- [434] M. P. Prabhakaran, L. Ghasemi-Mobarakeh, G. Jin, S. Ramakrishna, *J. Biosci. Bioeng.* **2011**, *112*, 501.
- [435] L. Lao, Y. Wang, Y. Zhu, Y. Zhang, C. Gao, *J. Mater. Sci.: Mater. Med.* **2011**, *22*, 1873.
- [436] M. Vlachou, S. Kikionis, A. Siamidi, K. Tragou, E. Ioannou, V. Rousis, A. Tsoinis, *J. Pharm. Sci.* **2019**, *108*, 970.
- [437] S. Gao, Y. Liu, J. Jiang, X. Li, F. Ye, Y. Fu, L. Zhao, *Colloids Surf., B* **2021**, *201*, 111625.
- [438] A. Jouyban, E. Rahimpour, *Talanta* **2020**, *2020*, 121383.
- [439] A. Munawar, Y. Ong, R. Schirhagl, M. A. Tahir, W. S. Khan, S. Z. Bajwa, *RSC Adv.* **2019**, *9*, 6793.
- [440] J. Huang, M. Zhao, Y. Hao, D. Li, J. Feng, F. Huang, Q. Wei, *Adv. Electron. Mater.* **2021**, *7*, 2000840.

- [441] M. J. Yee, N. M. Mubarak, E. C. Abdullah, M. Khalid, R. Walvekar, R. R. Karri, S. Nizamuddin, A. Numan, *Nano-Struct. Nano-Objects* **2019**, *18*, 100312.
- [442] M. Pasquale, *Sens. Actuators, A* **2003**, *106*, 142.
- [443] A. Jalalian, A. M. Grishin, *Appl. Phys. Lett.* **2014**, *104*, 243701.
- [444] R. K. Singh, S. W. Lye, J. Miao, *Sens. Actuators, A* **2020**, *303*, 111841.
- [445] Y. Zhu, Y. Wu, G. Wang, Z. Wang, Q. Tan, L. Zhao, D. Wu, *Org. Electron.* **2020**, *84*, 105759.
- [446] Y. Wang, J. Hao, Z. Huang, G. Zheng, K. Dai, C. Liu, C. Shen, *Carbon* **2018**, *126*, 360.
- [447] Y. R. Wang, J. M. Zheng, G. Y. Ren, P. H. Zhang, C. Xu, *Smart Mater. Struct.* **2011**, *20*, 045009.
- [448] T. Sharma, J. Langevine, S. Naik, K. Aroom, B. Gill, J. X. J. Zhang, *2013 Transducers & Eurosensors XXVII: The 17th International Conference on Solid-State Sensors, Actuators and Microsystems (TRANSDUCERS & EUROSENSORS XXVII)*, IEEE, Piscataway, NJ **2013**, p. 422.
- [449] S.-H. Park, H. B. Lee, S. Mo Yeon, J. Park, N. K. Lee, *ACS Appl. Mater. Interfaces* **2016**, *8*, 24773.
- [450] J. Jiang, S. Tu, R. Fu, J. Li, F. Hu, B. Yan, Y. Gu, S. Chen, *ACS Appl. Mater. Interfaces* **2020**, *12*, 33989.
- [451] F. Kibria, W. Rahman, S. N. Patra, *Nano Express* **2020**, *1*, 020027.
- [452] N. Liu, G. Fang, J. Wan, H. Zhou, H. Long, X. Zhao, *J. Mater. Chem.* **2011**, *21*, 18962.
- [453] X. Wang, B. Yang, J. Liu, Y. Zhu, C. Yang, Q. He, *Sci. Rep.* **2016**, *6*, 36409.
- [454] O. Y. Kweon, S. J. Lee, J. H. Oh, *NPG Asia Mater* **2018**, *10*, 540.
- [455] H.-Y. Mi, X. Jing, Q. Zheng, L. Fang, H.-X. Huang, L.-S. Turng, S. Gong, *Nano Energy* **2018**, *48*, 327.
- [456] Y. Zheng, L. Cheng, M. Yuan, Z. Wang, L. Zhang, Y. Qin, T. Jing, *Nanoscale* **2014**, *6*, 7842.
- [457] M. Tian, Y. Wang, L. Qu, S. Zhu, G. Han, X. Zhang, Q. Zhou, M. Du, S. Chi, *Synth. Met.* **2016**, *219*, 11.
- [458] S. M. Hosseini, A. A. Yousefi, *Org. Electron.* **2017**, *50*, 121.
- [459] C. M. Wu, M. H. Chou, *Compos. Sci. Technol.* **2016**, *127*, 127.
- [460] C. Merlini, G. M. O. Barra, T. Medeiros Araujo, A. Pegoretti, *RSC Adv.* **2014**, *4*, 15749.
- [461] J. Nunes-Pereira, V. Sencadas, V. Correia, J. G. Rocha, S. Lanceros-Méndez, *Sens. Actuators, A* **2013**, *196*, 55.
- [462] T. Xu, Y. Ding, Z. Wang, Y. Zhao, W. Wu, H. Fong, Z. Zhu, *J. Mater. Chem. C* **2017**, *5*, 10288.
- [463] W. Fu, Y. Dai, X. Meng, W. Xu, J. Zhou, Z. Liu, W. Lu, S. Wang, C. Huang, Y. Sun, *Nanotechnology* **2019**, *30*, 045602.
- [464] F. Fang, H. Wang, H. Wang, X. Gu, J. Zeng, Z. Wang, X. Chen, X. Chen, M. Chen, *Micromachines* **2021**, *12*, 252.
- [465] J. Huang, D. Li, M. Zhao, A. Mensah, P. Lv, X. Tian, F. Huang, H. Ke, Q. Wei, *Adv. Electron. Mater.* **2019**, *5*, 1900241.
- [466] G.-F. Yu, X. Yan, M. Yu, M.-Y. Jia, W. Pan, X.-X. He, W.-P. Han, Z.-M. Zhang, L.-M. Yu, Y.-Z. Long, *Nanoscale* **2016**, *8*, 2944.
- [467] T. Sharma, S. Naik, J. Langevine, B. Gill, J. X. J. Zhang, *IEEE Trans. Biomed. Eng.* **2015**, *62*, 188.
- [468] A. S. Motamedi, H. Mirzadeh, F. Hajiesmaeilbaigi, S. Bagheri-Khoulenjani, M. A. Shokrgozar, *J. Biomed. Mater. Res.* **2017**, *105*, 1984.
- [469] H.-G. Jeong, Y.-S. Han, K.-H. Jung, Y.-J. Kim, *Nanomaterials* **2019**, *9*, 184.
- [470] P. Hitscherich, S. Wu, R. Gordan, L.-H. Xie, T. Arinzech, E. J. Lee, *Biotechnol. Bioeng.* **2016**, *113*, 1577.
- [471] D. Mandal, S. Yoon, K. J. Kim, *Macromol. Rapid Commun.* **2011**, *32*, 831.
- [472] G. F. Zheng, X. Wang, W. W. Li, T. P. Lei, W. Tao, J. Du, Q. Y. Qiu, X. G. Chi, D. H. Sun, *2011 16th International Solid-State Sensors, Actuators and Microsystems Conference* **2011**, p. 2782.
- [473] Y. Jia, X. Yue, Y. Wang, C. Yan, G. Zheng, K. Dai, C. Liu, C. Shen, *Composites, Part B* **2020**, *183*, 107696.
- [474] L. T. Beringer, X. Xu, W. Shih, W.-H. Shih, R. Habas, C. L. Schauer, *Sens. Actuators, A* **2015**, *222*, 293.
- [475] H.-F. Guo, Z.-S. Li, S.-W. Dong, W.-J. Chen, L. Deng, Y.-F. Wang, D.-J. Ying, *Colloids Surf., B* **2012**, *96*, 29.
- [476] R. Augustine, P. Dan, A. Sosnik, N. Kalarikkal, N. Tran, B. Vincent, S. Thomas, P. Menu, D. Rouxel, *Nano Res.* **2017**, *10*, 3358.
- [477] S. H. Ji, J. H. Cho, Y. H. Jeong, J.-H. Paik, J. D. Yun, J. S. Yun, *Sens. Actuators, A* **2016**, *247*, 316.
- [478] Z. Lou, S. Chen, L. Wang, K. Jiang, G. Shen, *Nano Energy* **2016**, *23*, 7.
- [479] B. Li, J. Zheng, C. Xu, *Proc. SPIE* **2013**, *8793*, 879314.
- [480] C. Lee, D. Wood, D. Edmondson, D. Yao, A. E. Erickson, C. T. Tsao, R. A. Revia, H. Kim, M. Zhang, *Ceram. Int.* **2016**, *42*, 2734.
- [481] P. M. Martins, S. Ribeiro, C. Ribeiro, V. Sencadas, A. C. Gomes, F. M. Gama, S. Lanceros-Méndez, *RSC Adv.* **2013**, *3*, 17938.
- [482] K. Mondal, Md. A. Ali, V. V. Agrawal, B. D. Malhotra, A. Sharma, *ACS Appl. Mater. Interfaces* **2014**, *4*, 2516.
- [483] L. Shu, T. Xiaoming, F. D. Dagan, *IEEE Sens. J.* **2014**, *15*, 442.
- [484] V. Modafferi, G. Panzera, A. Donato, P. L. Antonucci, C. Cannilla, N. Donato, D. Spadaro, G. Neri, *Sens. Actuators, B* **2012**, *163*, 61.
- [485] G.-Y. Lee, H.-T. Lee, W. Ryu, S.-H. Ahn, J. Yang, *Smart Mater. Struct.* **2018**, *27*, 11LT01.
- [486] X. Lu, Q. Zhao, X. Liu, D. Wang, W. Zhang, C. Wang, Y. Wei, *Macromol. Rapid Commun.* **2006**, *27*, 430.
- [487] W. Shi, W. Lu, L. Jiang, *J. Colloid Interface Sci.* **2009**, *340*, 291.
- [488] D. H. Kang, N. K. Kim, H. W. Kang, *Nanotechnology* **2019**, *30*, 365303.
- [489] K. Chandra Sekhar Reddy, P. Sahatiya, I. Santos-Sauceda, O. Cortázar, R. Ramirez-Bon, *Appl. Surf. Sci.* **2020**, *513*, 145804.
- [490] H. Wu, Y. Sun, D. Lin, R. Zhang, C. Zhang, W. Pan, *Adv. Mater.* **2009**, *21*, 227.
- [491] B. Ding, J. Kim, Y. Miyazaki, S. Shiratori, *Sens. Actuators, B* **2004**, *101*, 373.
- [492] A. Rianjanu, R. Roto, T. Julian, S. Hidayat, A. Kusumaatmaja, E. Suyono, K. Triyana, *Sensors* **2018**, *18*, 1150.
- [493] M. M. Aria, A. Irajizad, F. R. Astaraei, S. P. Shariatpanahi, R. Sarvari, *Measurement* **2016**, *78*, 283.
- [494] X. Wang, B. Ding, M. Sun, J. Yu, G. Sun, *Sens. Actuators, B* **2010**, *144*, 11.
- [495] B. Ding, M. Wang, X. Wang, J. Yu, G. Sun, *Mater. Today* **2010**, *13*, 16.
- [496] X. He, R. Arsat, A. Z. Sadek, W. Wlodarski, K. Kalantar-Zadeh, J. Li, *Sens. Actuators, B* **2010**, *145*, 674.
- [497] R. Augustine, F. Sarry, N. Kalarikkal, S. Thomas, L. Badie, D. Rouxel, *Nano-Micro Lett.* **2016**, *8*, 282.
- [498] B. S. De Farias, T. R. Sant'anna Cadaval Junior, L. A. De Almeida Pinto, *Int. J. Biol. Macromol.* **2019**, *123*, 210.
- [499] M. Arkoun, F. Daigle, M.-C. Heuzey, A. Ajji, *Molecules* **2017**, *22*, 585.
- [500] B. Ghorani, N. Tucker, *Food Hydrocolloids* **2015**, *51*, 227.
- [501] S. Chen, R. Li, X. Li, J. Xie, *Adv. Drug Delivery Rev.* **2018**, *132*, 188.
- [502] W. E. Teo, S. Ramakrishna, *Nanotechnology* **2006**, *17*, R89.
- [503] A. Zhang, G. Zheng, C. M. Lieber, *MRS Bulletin* **2017**, *42*, 540.



**Saraswathi Kailasa** received her M.Sc. in nanotechnology and nanoelectronic devices from the University of Surrey, UK. Currently, she is working as a research fellow at the Centre for Nano Science and Technology, Institute of Science and Technology from JNT University Hyderabad. Her research interests are the synthesis of polymer nanocomposites with different techniques that are used for nanosensors, energy storage, organic electronics, etc., applications. She has published more than 18 papers in international journals and one book chapter.



**M. Sai Bhargava Reddy** is currently pursuing his Ph.D. in metallurgical and materials engineering at IIT Kharagpur. He received his M.Tech. degree in nanotechnology from the Institute of Science and Technology, Jawaharlal Nehru Technological University Hyderabad, India. His research interest is mainly focused on the synthesis, and characterization of different metal oxide nanoparticles, 2D materials, polymer nanocomposites, and carbon allotropes, such as carbon nanotubes, graphene, graphene oxide, for gas, VOCs, and electrochemical sensing applications. He has 13 publications in international journals and one book chapter to his credit.



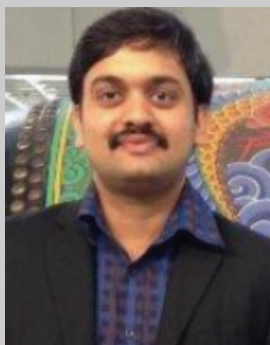
**Muni Raj Maurya** received his Ph.D. in engineering science (2020) from CSIR-National Physical Laboratory, New Delhi, India. He is currently a staff researcher at the Center for Advanced Materials, Qatar University. His research interests include investigation of the optical properties of nanocomposites semiconductor materials and the development of optically active nanostructures. His current research is mainly focused on nanomanufacturing, and device designs for sensor and nanophotonic applications.



**B. Geeta Rani** obtained her M.Tech. (Nano Technology) Degree in 2013 from JNT University Hyderabad, India. Currently, she is doing Ph.D. under the supervision of Dr. K. V. Rao from JNT University Hyderabad. Her research topic is the development of flexible chemical sensors by novel nanomaterials. Her current area of research is chemiresistive gas sensors for detection of explosive and poisonous gases. She has published more than 12 papers in international journals.



**K. Venkateswara Rao** has received his M.Sc. degree from University of Hyderabad, Hyderabad, Telangana State, India in 1997. He obtained his Ph.D. degree in 2008 from Department of Physics, University of Hyderabad. Currently he is professor of nanotechnology in the Centre for Nanoscience and Technology, JNT University Hyderabad. His current interest of research includes chemical and humidity sensors, solar cell applications, bio-sensors and seed germination etc. He has published more than 220 papers in international journals.



**Kishor Kumar Sadasivuni** is a scientist and has established an international reputation in the fields of nanocomposites composite materials, device designs, especially based on sensors, and high-performance nanocomposites with different industrial applications. In the past five years, he has published around 250 papers in international peer-reviewed journals. He is serving as a managing editor for the *Emergent Materials journal* (Springer) lead by the Qatar University. Dr. Kishor's achievements have been recognized by TRILA: Young Research Scholar of the Year 2017 and being listed in the Top 2% Global Scientists list in 2020 created by Stanford University.